Prepared for

NATIONAL AERONAUTICS AND SPACE ADMINISTRATION
Headquarters
Washington, D.C. 20546

by

Dr. F. F. Marmo, Project Director and
Principal Investigator

September 1966

EXPERIMENTAL AND THEORETICAL STUDIES
IN PLANETARY AERONOMY

Quarterly Progress Report

Covering the Period 1 July 1966
through 17 September 1966

Prepared under Contract No. NASW-1283

TABLE OF CONTENTS

I. INTRODUCTION

This is the Sixth Quarterly Progress Report which describes the technical progress from 1 July through 17 September 1966 under NASA Contract No. NASW-1283. Scientific investigations accomplished during the current reporting period resulted in the generation of the following papers submitted and/or accepted for publication in accredited scientific journals, books and/or GCA Technical Reports or presented at scientific meetings.

Technical Papers Submitted and/or Accepted for Publication

	Publication
a. Submitted	
Reactions of ^{1}D Oxygen Atoms III. Ozone Formation in the 1470Å Photolysis of O_2 (P. Warneck and J.O. Sullivan)	J. Chem. Phys.
Reactions of ^{1}D Oxygen Atoms IV. Reactions with N_2O, N_2 and CO_2 (P. Warneck and J.O. Sullivan)	J. Chem. Phys.
The Photoionization Cross Section of Atomic Hydrogen (R.B. Cairns and J.A.R. Samson)	Phys. Review
Ion Temperatures in the Topside Ionosphere (A. Dalgarno and J.C.G. Walker)	Planetary Space Sci.
b. Accepted	
Studies of Ion-Neutral Reactions by a Photoionization Mass Spectrometer Technique II. Charge Transfer Reactions of Argon Ions at Near Thermal Energies (P. Warneck)	J. Chem. Phys.
On the Quenching of 6300Å Airglow (P. Warneck and J.O. Sullivan)	Planetary Space Sci.

Atmospheric Ion-Molecule Reactions by a Photoionization Mass Spectrometric Technique (P. Warneck and F.F. Marmo) - INVITED PAPER presented at a Sumposium on the Physics and Chemistry of the Lower Atmosphere held at the University of Colorado in Boulder, Colorado, on 27-29 June 1966.

Collision Processes in Planetary Atmospheres (A. Dalgarno) - INVITED PAPER prepared for presentation* by A. Dalgarno at the International Astronomical Union Working Group on Collision Processes in Astrophysics held in Boulder, Colorado, on 11-15 July 1966.

Atom-Atom Collision Processes in Astrophysics (A. Dalgarno) - INVITED PAPER prepared for presentation* by A. Dalgarno at the International Astronomical Union Working Group on Collision Processes in Astrophysics held in Boulder, Colorado, on 11-15 July 1966.

Reactions of ^{1}D Oxygen Atoms (P. Warneck) - Presented at the American Chemical Society Meeting held in New York City on 12-14 September 1966.

In Section II, technical summaries are given on the work performed under the present contract. During the current reporting period, significant progress has been achieved in the following areas: (a) photochemistry of planetary atmospheres, (b) theoretical studies, (c) laboratory investigations in the VUV and the EUV spectral regions, and (d) planetary aeronomy.

Section III contains other pertinent information and reports miscellaneous information on the attendance and presentation of papers at scientific meetings.

---

*Unable to attend meeting because of airline strike.

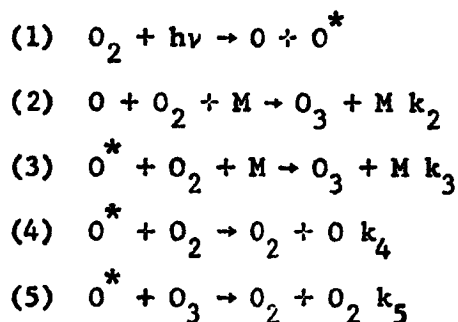## II. TECHNICAL SUMMARIES OF WORK PERFORMED DURING THIS QUARTER

A. PHOTOCHEMISTRY OF PLANETARY ATMOSPHERES

During this Quarter, the major emphasis under this phase of the program was directed towards completing the remaining requirements under the Statement of Work; specifically, Items A(2) and A(3). The former deals with the experimental determination of the rates of reactions $O(^1D) + N_2 \rightarrow O(^3P) + N_2$ and $O(^1D) + N_2 \rightarrow N_2O$ to establish the quenching efficiency of nitrogen whereas the latter involves the study of VUV photolyses of planetary gases to establish the role of minor constituents.

1. Reactions of $O(^1D)$ Oxygen Atoms with N_2, N_2O and CO_2

In a previous Quarterly Report, it was shown that the experimental determination of the rates of reactions $O(^1D) + N_2 \rightarrow O(^3P) + N_2$ and $O(^1D) + N_2 \rightarrow N_2O$ could be achieved without involving isotope measurements. In fact, these studies have now been accomplished by employing photolysis techniques described previously and directly applicable to determining the role of $O(^1D)$ with other molecules such as N_2O and CO_2. In fact, in this report a detailed account is given which summarizes the reactions of $O(^1D)$ oxygen atoms with N_2O, N_2, and CO_2. It turns out that only in this manner can the quenching efficiency and relative role of molecular nitrogen be evaluated. It will be shown that the reactions of (O^1D) with N_2O and CO_2 have similar rates whereas those involving N_2 are slower by at least one order of magnitude. In addition, all three reactions are slow in comparison to the reactions between $O(^1D)$ and ozone. A rather detailed report is given here so that a proper perspective can be obtained for the relative roles of N_2, CO_2 and N_2O in planetary atmospheres.

3

It has been previously shown[1] that the amount of ozone formation resulting from the 1470Å photolysis of oxygen in a flow system is a function of pressure and several other parameters. It was also shown that the variation of the ozone quantum yield originates from reactions of ^1D oxygen atoms, which at 1470Å, are generated simultaneously with ground state ^3P oxygen atoms (approximately in a 1:1 ratio) by the primary process of O_2 photodissociation. The experimental observations are in agreement with the reaction sequence.

$$(1) \quad O_2 + h\nu \rightarrow O + O^*$$
$$(2) \quad O + O_2 + M \rightarrow O_3 + M \quad k_2$$
$$(3) \quad O^* + O_2 + M \rightarrow O_3 + M \quad k_3$$
$$(4) \quad O^* + O_2 \rightarrow O_2 + O \quad k_4$$
$$(5) \quad O^* + O_3 \rightarrow O_2 + O_2 \quad k_5$$

where the asterisk indicates oxygen atoms in the metastable ^1D state. The ozone quantum yield is determined essentially by the balance of ozone formation via steps (2) through (4) and ozone consumption in step (5). The consumption of ozone by reaction with ^3P oxygen atoms can be neglected for the considered flow conditions.

On this basis, it appears that the ozone quantum yield can be utilized as an indicator of $O(^1D)$ reactivity toward other gases, admixed to the oxygen flow, provided that (a) they do not react appreciably with ^3P oxygen atoms and (b) they do not disturb the predominance

4

of the primary process (1). This possibility was investigated for mixtures of oxygen with nitrous oxide, nitrogen and carbon dioxide. The results and their interpretation are the subject of this paper. The quantitative evaluation of the data provides further information on the relative reactivity of ^1D oxygen atoms with these gases.

A detailed description of the flow apparatus has been given previously.[1,2] Briefly, a xenon source fitted with a BaF_2 window was used to generate 1470 Å radiation. Oxygen or mixtures of oxygen with N_2O, N_2 and CO_2 were irradiated in the flow system; and the amount of ozone formed in the turbulent reaction region near the window was determined as a function of pressure, utilizing the absorption of 2537 Å mercury line in a 40 cm long absorption tube as a measure of the ozone concentration. The ozone quantum yield is defined by $\varphi = [O_3] v/I$, where $[O_3]$ is the ozone concentration in the absorption tube, v is the gas flow rate in cc/sec, and I in photons/sec is the over-all intensity of the xenon source. The source intensity was determined actinometrically from the amount of ozone produced in a fast flow of pure oxygen at atmospheric pressure. It has been shown previously[1,3] that, under these conditions, the ozone quantum yield is only slightly lower than two.

The results of this investigation are presented in Figs. 1 and 2, where the ozone quantum yields are plotted as a function of pressure for
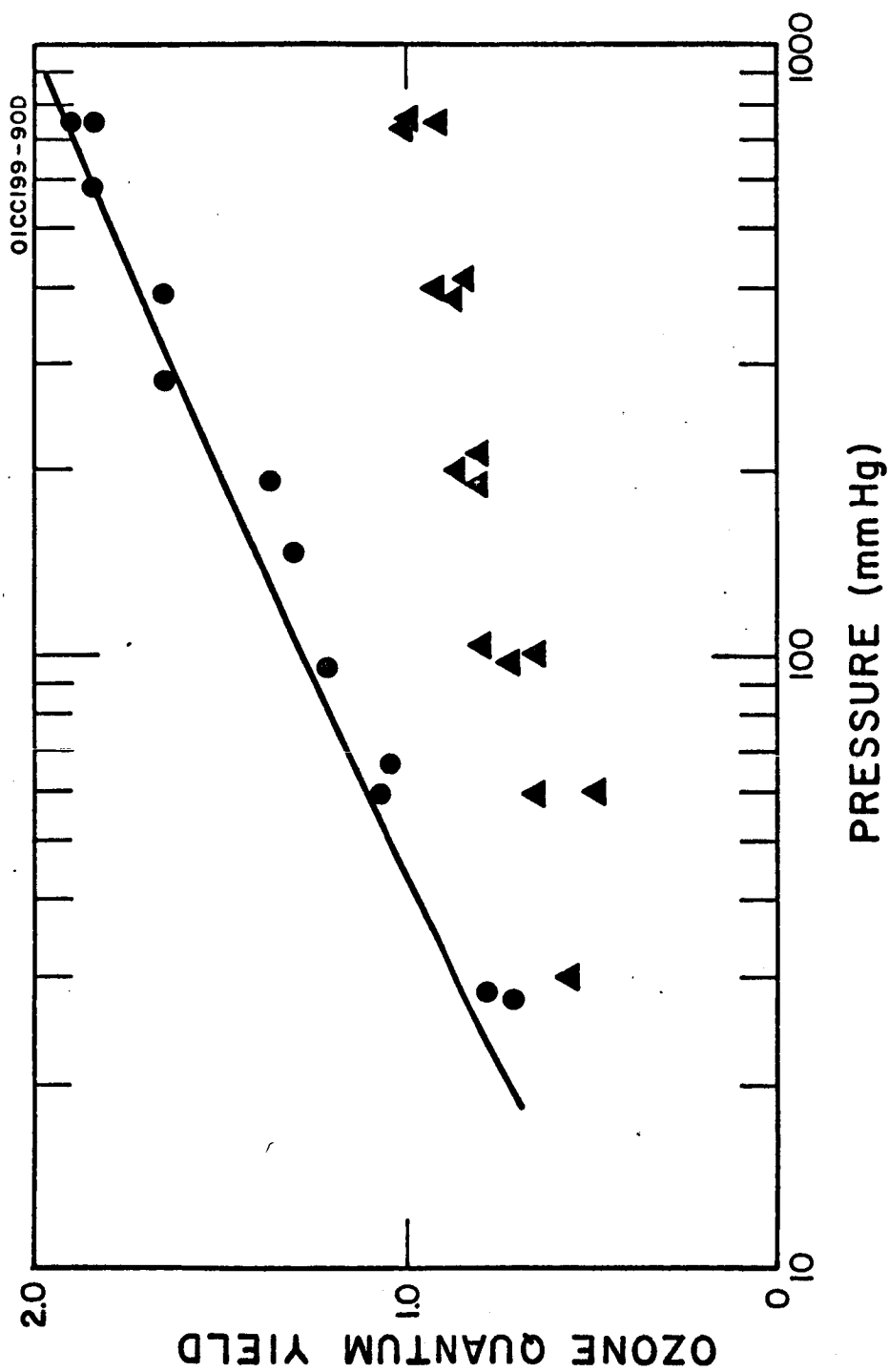
5

Figure 1. Ozone quantum yields as a function of pressure for a 4:1 mixture of oxygen with nitrogen oxide (▲); and a 1:1 mixture of oxygen with nitrogen (●). Ozone quantum yields in pure oxygen are indicated by the solid line.
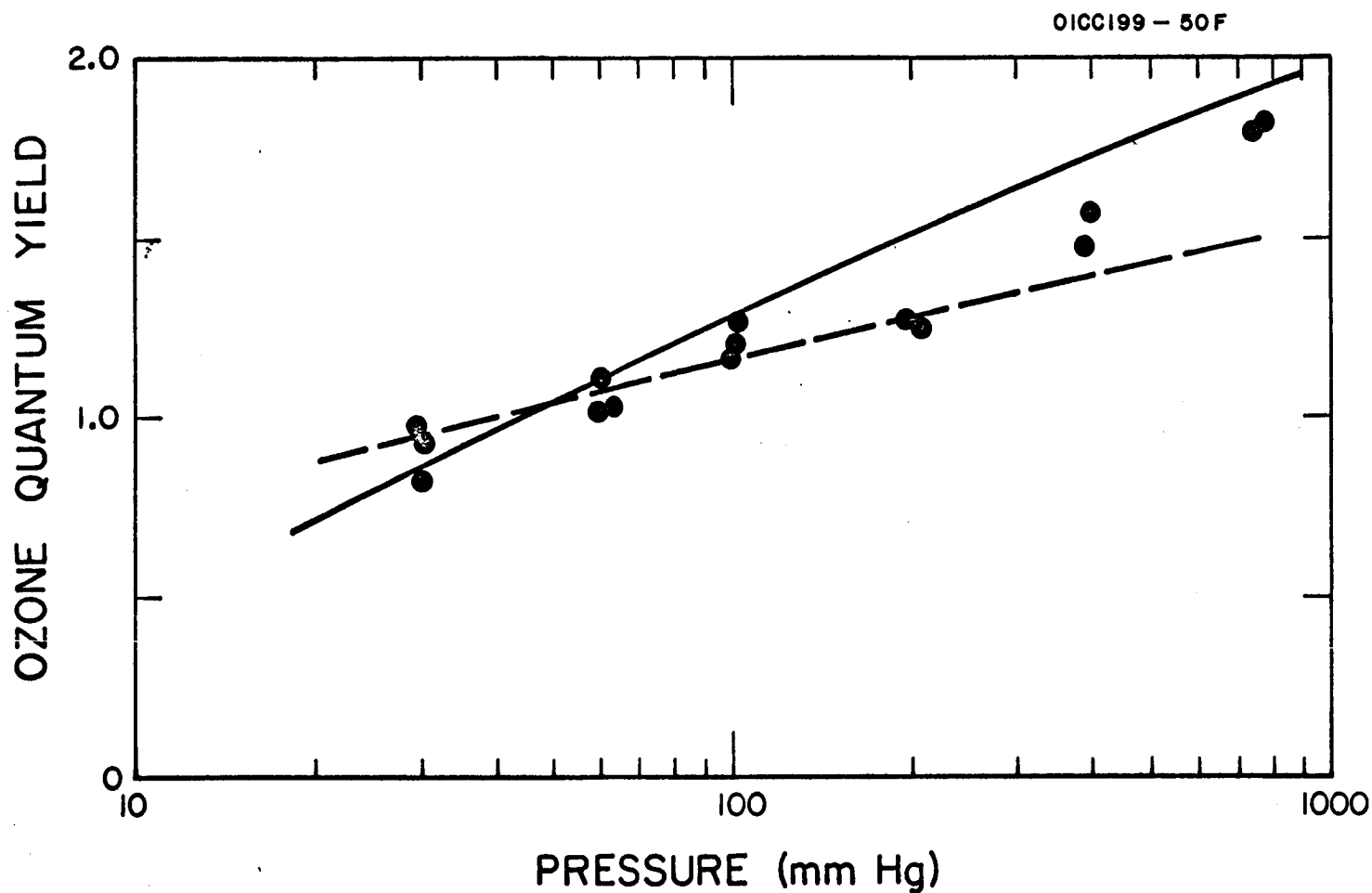
6

Figure 2. Ozone quantum yields as a function of pressure for a 1:1 mixture of oxygen with carbon dioxide. The solid line indicates ozone quantum yields in pure oxygen. The broken line indicates ozone quantum yields calculated on the basis of reactions 9a and 9b.

7

a 4:1 mixture of oxygen with nitrous oxide and for 1:1 mixtures of

oxygen with nitrogen and with carbon dioxide. For comparison, the

pressure dependence of the ozone quantum yield in pure oxygen deter-

mined previously is indicated in both figures by solid lines. According

to these data, the ozone quantum yield is reduced considerably upon the

admixture of N_2O, but the effect is less pronounced for CO_2 and hardly

noticeable for N_2. From the known absorption coefficients of these gases

at 1470 $\overset{o}{A}$, it can be shown that, for the indicated mixing ratios, oxygen

is still the predominant absorber, intercepting at least 90 percent of

the incident radiation, so that the effective primary process in these

mixtures is the same as that in pure oxygen. Since, in addition, none

of the added gases reacts appreciably with ^3P oxygen atoms, it seems rea-

sonable to attribute the observed changes in the ozone quantum yield, com-

pared with those observed in pure oxygen, to reactions of ^1D oxygen atoms

with the admixed gases. These reactions must occur in addition to the re-

actions with oxygen and ozone, reactions (3) through (5). The various

possibilities will be considered individually in the following discussion.

In the analysis of ozone quantum yields observed in pure oxygen, it

has been found convenient to treat the reaction region in the vicinity of

the window as a stirred reactor on account of the turbulence produced at

this location by the reversal of gas flow. In this manner, the ratios of

rate constants $k_3/k_5 = 2.1 \times 10^{-23}$ and $k_4/k_5 = 6.1 \times 10^{-4}$ have been evalu-

ated. The present results are again discussed on the basis of the stirred

reactor treatment, making use also of the previously determined rate constant ratios.

a. Nitrous Oxide

From work on the photolysis of N_2O in the 1850 Å wavelength region[4,5] and related experimental studies,[6,7] it has been established that ^1D oxygen atoms react with N_2O in two ways,

$$(6a) \quad O^* + N_2O \rightarrow N_2 + O_2$$
$$(6b) \quad O^* + N_2O \rightarrow 2\ NO\ ,$$
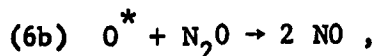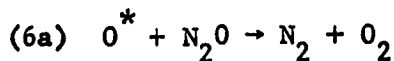
with the probability of the reaction entering either channel being approximately equal. In the present experiments, the ozone quantum yield is further affected by the subsequent reaction of nitric oxide with ozone

$$(7) \quad NO + O_3 \rightarrow NO_2 + O_2\ .$$
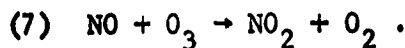
These reactions must be considered in addition to reactions (1) through (5). The pertinent stirred reactor equations read

$$\frac{v[O_3]}{R} = \frac{I}{R} + [O^*]\ (k_3[M] + k_4)\ [O_2] - k_5[O_3] - k_7[NO]\ [O_3]$$

$$\frac{v[O^*]}{R} = \frac{I}{R} - [O^*]\ (k_3[M] + k_4)\ [O_2] + k_5[O_3] + (k_{6a} + k_{6b})\ [N_2O]$$

$$\frac{v[NO]}{R} = 2\ k_{6b}[O^*]\ [N_2O] - k_7[NO]\ [O_3]$$

In these equations, v is the flow rate, R the reactor volume, I the integrated irradiation intensity, and the concentrations are indicated by brackets.

9

Further, it has been assumed that the efficiency of N_2O as a third body in reaction (3) is approximately the same as that for O_2 as the third body. This simplification is justified by the previous observation that reaction (3) serves mainly as a correction to reaction (4) and becomes significant only at higher pressures. Since R is of the order of 1 cc, it is found that $I/R \gg v[O^3]/R$. Similarly, with the known rate constant for reaction (7),[8-10] it is found that k_7 [NO] $[O_3] \gg v[NO]/R$, so that both the O^* atoms and NO are almost entirely consumed within the boundaries of the reactor. With these conditions, the above equations can be rearranged to yield

$$\text{(a)} \quad \frac{k_{6b}}{k_5} \frac{[N_2O]}{[O_2]} = \frac{(2 - \varphi) A - \varphi^2 I/[O_2]v}{(k_{6a}/k_{6b}) (\varphi - 1) + (1 + \varphi)}$$

where $\varphi = [O_3]v/I$ is the ozone quantum yield, and $A = (k_3[M] + k_4)/k_5$. Note that the reaction volume R has cancelled. Equation (a) has been applied to the data shown in Figure 1 to determine the rate constant ratios k_{6b}/k_5, and the results are listed in Table 1. Since the degree of partitioning between the two channels of reaction (6) is not precisely known, the calculations were performed for two cases, $k_{6a}/k_{6b} = 1$ and $k_{6a}/k_{6b} = 2$. The resulting k_{6b}/k_5 values are similar. The corresponding overall rate constant ratios are $(k_{6a} + k_{6b})/k_5 = 4.4 \times 10^{-3}$, respectively, and $(k_{6a}/k_{6b}/k_5 = 7.5 \times 10^{-3}$. By comparison with the previously established value for k_4/k_5 in pure oxygen, it is seen that the reaction of $O(^1D)$ with N_2O is by an order of magnitude faster than that with O_2, but that it is by two orders of magnitude slower than the reaction of $O(^1D)$ with ozone.

TABLE 1

Pressure (mm Hg)	$[O_2]/[N_2O]$	I/v 10^5 photons/cc	φ	$k_{6b}/k_5) \times 10^3$ (a)	(b)
31	4.44	1.19	0.55	1.75	3.26
60.9	7.00	1.14	0.69	2.90	3.74
61.2	3.55	1.11	0.49	2.89	5.90
61.7	5.66	1.16	0.67	2.38	3.18
99.2	4.81	1.17	0.74	2.05	2.49
99.3	6.81	1.23	0.81	2.14	2.38
100.1	4.44	1.19	0.68	2.22	2.88
196.5	4.60	1.12	0.82	2.04	2.27
199.0	4.47	1.05	0.83	2.02	2.46
201.7	4.32	1.27	0.81	1.95	2.90
398.6	4.62	1.27	0.94	2.05	2.12
400.0	4.56	1.32	0.89	2.15	2.31
401.0	4.23	1.47	0.85	2.27	2.49
760.0	4.00	1.01	0.98	2.30	2.31
761.2	4.00	1.09	1.00	2.16	2.16
763.0	4.20	1.06	1.01	2.20	2.23

(a) $k_{6a}/k_{6b} = 1$ average value $k_{6b}/k_5 = 2.2 \pm 0.2 \times 10^{-3}$

(b) $k_{6a}/k_{6b} = 2$ average value $k_{6b}/k_5 = 2.82 \pm 0.5 \times 10^{-3}$

b. Nitrogen

The interaction of ^1D oxygen atoms with nitrogen leads either to a deactivation of the singlet state or to the formation of nitrous oxide by attachment

$$(8a) \quad O^* + N_2 \rightarrow N_2 + O$$
$$(8b) \quad O^* + N_2 \rightarrow N_2O \; .$$
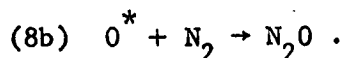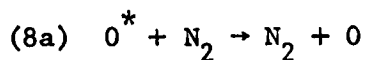
The generation of N_2O via reaction (8b) has been observed in several laboratory studies, i.e., in the gas phase by Groth and Schierholz[11] and more cently by Norrish and Wayne;[12] in liquid nitrogen by DeMore and Raper;[13] and in a solid nitrogen matrix by DeMore and Davidson.[14] The yield of N_2O in all of these cases was relatively low, indicating that reaction (8b) is either slow or that it is overshadowed by the deactivation of reaction (8). Indeed, the quantitative results of DeMore and Raper[13] show that for ^1D oxygen atoms reacting with liquid nitrogen, deactivation is 75 times more probable than N_2O formation.

The present results on ^1D oxygen atoms reacting in the gas phase can provide no quantitative information on the partitioning between reactions (8a) and (8b), but they show qualitatively that the deactivation reaction is predominant so that they substantiate the conclusions reached by DeMore and Raper.[13] To demonstrate this, the stirred reaction treatment given above is extended to include reactions (8). It is found that reactions (6) and consequently also reaction (7) are negligible in comparison to the removal of N_2O from the reaction space by the gas flow, so that the essential reactions are (1) through (5) and (8). From the

stirred reactor equations, one obtains the expression

$$\frac{k_{8a}}{k_5} \frac{[N_2]}{[O_2]} = \frac{\varphi^2 I/v(O_2) - (2 - \varphi)A}{(2 - \varphi) - (k_{8b}/k_{8a})(\varphi - 1)} \quad .$$

The numerator on the right-hand side of this equation is positive throughout the range of quantum yields observed in the experiments with nitrogen-oxygen mixtures. Since the left-hand side is positive by definition, it is apparent that the denominator on the right must also be positive. This requirement leads to the criterion that $k_{8b}/k_{8a} < (2 - \varphi)/(\varphi - 1)$. From the highest ozone quantum yield, $\varphi \approx 1.85$, observed in the nitrogen oxygen mixture near atmospheric pressure, one obtains $k_{8b}/k_{8a} < 0.17$. This upper limit value clearly indicates that N_2O formation by reaction of $O(^1D)$ with nitrogen is a minor reaction path and that the deactivation reaction (8a) predominates. For the determination of the rate constant ratio k_{8a}/k_5, it is convenient to neglect reaction (8b) altogether, setting $k_{8b}/k_{8a} = 0$. The values for k_{8a}/k_5 resulting from the experimental data are shown in Table 2. The results are reasonably consistent in view of the many parameters that enter into Eq. (b), and the absence of trends with pressure can be taken as further indication that deactivation predominates the interaction of $O(^1D)$ with nitrogen. The average rate constant ratio $k_{8a}/k_5 = 3.0 \times 10^{-4}$ is slightly smaller than the equivalent ratio involving deactivation by oxygen, $k_4/k_5 = 6.1 \times 10^{-4}$, determined previously from the ozone quantum yields in pure oxygen. The ratio k_4/k_{8a} is approximately two. This is in agreement with the conclusions by DeMore and Raper[15] that the rate constants for quenching of $O(^1D)$ by oxygen and nitrogen are of the same order of magnitude. The rates of both reactions are small when compared to that of $O(^1D)$ reacting with ozone.

TABLE 2

OZONE QUANTUM YIELDS AND RATE CONSTANT RATIOS FOR 1:1

Pressure (mm Hg)	$I/v \times 10$ photons/cc	φ	$(k_{8a}/k_5) \times 10^4$
760	0.83	1.85	3.92
28.5	1.04	0.68	1.53
29	0.66	0.78	0.63
60	0.86	1.08	3.78
69.5	0.96	1.03	2.64
100	0.83	1.21	2.43
150	0.97	1.33	3.40
195	0.93	1.36	1.40
290	1.04	1.65	8.20
400	1.08	1.64	2.67
595	1.05	1.75	2.55
760	0.92	1.83	3.10

average $k_{8a}/k_5 = 3.0 \pm 1.2 \times 10^{-4}$

c. Carbon Dioxide

The interpretation of the present results on the interaction of $O(^1D)$ with carbon dioxide is hampered by the lack of specific information concerning the involved reactions and their products. From the observation of an isotope exchange of excited oxygen atoms with (labeled) CO_2, it is known[16,17] that $O(^1D)$ reacts with carbon dioxide in a manner essentially different from that of simple deactivation; i.e., by formation of a CO_3 complex. The concept of a long-lived CO_3 intermediate was first suggested by Katakis and Taube[16] to explain the isotope effect, and it has subsequently been invoked in Part II of this series[18] to explain the observed oxygen deficiency in the vacuum ultraviolet photolysis of CO_2. More recently, the existence of CO_3 has been confirmed by Thompson and collaborators[19] using the matrix isolation method. Accordingly, the formation of CO_3 must be considered in the interpretation of the present results.

From a detailed study of the isotope effect, Yamazaki and Cvetanović[17] have found that the exchange reaction of $O(^1D)$ with CO_2 is almost as rapid as the reaction of $O(^1D)$ with N_2O, whereas the present data in Figs. 1 and 2 appear to indicate a greater effect for N_2O than CO_2. However, this behavior may be an apparent one owing to a balancing between two reactions involving $O(^1D)$ and CO_2; one diverting ^1D oxygen atoms from producing ozone and one enhancing ozone formation.

Two mechanisms that can produce this effect were considered, and these will be discussed separately.

The simplest pair of reactions which can explain the results in the 20 to 200 mm Hg pressure region is

$$9a \quad O^* + CO_2 \rightarrow CO_2 + O$$

$$9b \quad O^* + CO_2 \rightarrow CO_3 \; ,$$
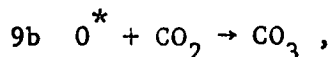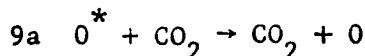
where reaction 9a is assured to involve oxygen atom interchange. When these reactions are taken together with reactions (1) through (5), the application of the stirred reactor equations yield the expression

$$(c) \quad \frac{k_{9a}}{k_5} \frac{[CO_2]}{[O_2]} = \frac{\varphi^2 I/v[O_2] - (2 - \varphi)A}{(2 - \varphi) - (k_{9b}/k_{9a})(\varphi - 1)} \; .$$

Here it is again assumed that the third body activity in reaction (3) is approximately equal for oxygen and carbon dioxide. Equation (c) then provides ratios of rate constants k_{9b}/k_5 as a function of pressure with k_{9b}/k_{9a} as a parameter. It is found that there exists a relatively narrow range, $1 < k_{9b}/k_{9a} < 2.5$, for which a reasonable pressure independence of k_{9a}/k_5 is achieved. Table 3 lists the rate constant ratios resulting for the choice of $k_{9b}/k_{9a} = 2.0$. From the average rate constant ratios for this case, $k_{9a}/k_5 = 8.0 \times 10^{-4}$, one obtains for the combined reactions of $O(^1D)$ with CO_2: $(k_{9a} + k_{9b})/k_5 = 2.4 \times 10^{-3}$. This rate constant ratio is of the same order of magnitude as that found above for the reaction of $O(^1D)$ with nitrous oxide. This agrees with the results of Yamazaki and Cvetanović, and thereby supports our assumption that the present results are due to a balancing of two reactions between $O(^1D)$ and carbon dioxide.

However, while reactions (9) can explain the experimental data in the 20 to 200 mm Hg pressure region, they do not provide for the sharp increase

TABLE 3

Pressure (mm Hg)	I/v 10^{15} photons/cc	φ	$(k_{9a}/k_5) \times 10^4$ (a)	$(k_{11}/k_5) \times 10^{22}$ (cc/molecule) (b)
29.9	0.93	0.98	18.00	4.4
30.0	0.96	0.81	3.32	---
30.3	0.82	0.94	6.52	11.4
59.8	0.89	1.13	9.50	12.1
60.1	1.14	1.03	6.80	7.8
60.9	1.14	1.03	6.40	7.3
100.0	1.02	1.20	8.65	7.5
100.3	1.29	1.20	8.85	7.5
101.3	1.07	1.10	10.46	11.9
200.1	1.30	1.28	6.82	6.3
201.6	1.33	1.26	8.85	4.0
396.4	1.60	1.48	---	4.9
401.7	1.46	1.57	---	7.2
760.0	1.39	1.81	---	11.8
760.0	1.09	1.82	---	12.1

(a) $k_{9b}/k_{9a} = 2$ average $k_{9a}/k_5 = 8.0 \pm 1.9 \times 10^{-4}$

(b) $k_{9b}/k_5 = 3 \times 10^{-3}$ average $k_{11}/k_5 = 8.3 \pm 2.3 \times 10^{-22}$ cc/molecule

in the ozone quantum yield at higher pressures. Using the values given

above for k_{9b}/k_{9a} and k_{9a}/k_5, ozone quantum yields were calculated from

Eq. (c) for the entire pressure region. The results are shown in Fig. 2

by the dashed line which demonstrates the discrepancy between calculated

and observed ozone quantum yields at pressures greater than 200 mm Hg.

In this pressure region, evidently, additional reactions are required

to interpret the data, and two such reactions have been considered:

$$(10) \quad CO_3 + O_2 \quad \rightarrow O_3 + CO_2$$
$$(11) \quad O + CO_2 + O_2 \rightarrow O_3 + CO_2 \ .$$
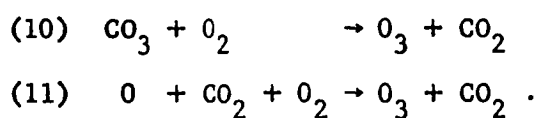
The first of these is a logical extension of the CO_3 concept, but it fails

to raise the ozone quantum yield sufficiently rapidly with increasing pres-

sure to represent the experimental data at the higher pressures satisfactorily.

Reaction (11) on the other hand can provide the required increase in the ozone

quantum yields if its rate is by an order of magnitude faster than that of

the equivalent reaction (3). This conclusion has two consequences: (a) it

invalidates one of the assumptions made in the above analysis of reactions

(9), and (b) it disturbs the balance between the two channels of reactions (9)

such that reaction (11) essentially replaces reaction (9a).

The resulting mechanism is different from the one discussed above and

consists of reaction (9b) and (11) occurring simultaneously with reaction (11)

through (5). The stirred reactor treatment yields the expression

$$(d) \quad \frac{k_{11}}{k_5} [CO_2] = \frac{\varphi^2 I/v[O_2]}{(2 - \varphi)} + \frac{k_{9b}}{k_5} \frac{(\varphi - 1)}{(2 - \varphi)} - \frac{k_4}{k_5}$$

for the ratios of rate constants k_{11}/k_5, where k_{9b}/k_5 must be considered an

adjustable parameter. A reasonable representation of the data is achieved

18

with $k_{9b}/k_5 = 3 \times 10^{-3}$, a value which about twice that found on the basis of the preceding reaction mechanism. Since reaction (9b) is now the only one leading to isotope exchange, it is apparent that the agreement with the results of Yamazaki and Cvetanović, which was noted above, is preserved. Values for k_{11}/k_5 obtained with $k_{9b}/k_5 = 3 \times 10^{-3}$ are entered in the last column of Table 3. The internal consistency of these data makes evident that the considered mechanism can explain the experimental observations throughout the entire investigated pressure region, in contradistinction to the first mechanism. The average k_{11}/k_5 value is $k_{11}/k_5 = 8.3 \pm 2.3 \times 10^{-22}$ cc/molecule. A comparison with the equivalent rate constant ratio for reaction (3), $k_3/k_5 = 2.1 \times 10^{-23}$ cc/molecule given previously, indicates that provided the interpretation is correct, reaction (11) is approximately 40 times faster than reaction (3). This large difference in third body activity probably has its origin in the reactivity of $O(^1D)$ toward CO_2 and the ensuing formation of a CO_3 intermediate.

The present investigation utilizes the 1470 Å photolysis of oxygen to generate ^1D oxygen atoms simultaneously with ^3P ground-state oxygen atoms, and the extent of $O(^1D)$ reactivity toward admixed N_2O, N_2 and CO_2 is assessed from the ozone quantum yields measured in a flow system. The results generally confirm previous data on these reactions. Specifically, it is found that the reactions of $O(^1D)$ with N_2O and CO_2 have similar rates. The reactions of $O(^1D)$ with N_2 and O_2 also have similar rates, but they are about an order of magnitude slower. All these reactions are slow compared to the reactions of ^1D oxygen atoms with ozone.

19

This material has been submitted for publication in the Jounral of Chemical Physics as a paper entitled "Reactions of (^{1}D) Oxygen Atoms IV. Reactions with N_2O, N_2 and CO_2" by P. Warneck and J. O. Sullivan. In addition, the results have been presented at the Americal Chemical Society Meeting held in New York City on 12-14 September 1966.

REFERENCES

1. J. O. Sullivan and P. Warneck, J. Chem. Phys. to be published.

2. P. Warneck, Disc. Faraday Soc. 37, 57 (1964).

3. W. E. Groth, Z. Phys. Chem. B37, 307 (1937).

4. M. Zelikoff and L. M. Aschenbrand, J. Chem. Phys. 22, 1685 (1954).

5. J. P. Doering and B. H. Mahan, J. Chem. Phys. 36, 1682 (1962).

6. H. Yamazaki and R. J. Cvetanovic, J. Chem. Phys. 34, 1902 (1963).

7. R. J. Cvetanovic, J. Chem. Phys. 43, 1850 (1965).

8. H. S. Johnston and H. J. Crosby, J. Chem. Phys. 19, 799 (1951).

9. H. W. Ford, G. J. Doyle and N. Endow, J. Chem. Phys. 26, 1337 (1957).

10. L. F. Phillip and H. I. Schiff, J. Chem. Phys. 36, 1509 (1962).

11. W. E. Groth and Schierholz, J. Chem. Phys.

12. R. G. W. Norrish and R. P. Wayne, Proc. Roy. Soc. A288, 200 (1965).

13. W. DeMore and O. F. Raper, J. Chem. Phys. 37, 2048 (1962).

14. W. DeMore and N. Davidson, J. Am. Chem. Soc. 81, 5869 (1959).

15. W. DeMore and O. F. Raper, Astrophys. J. 139, 1381 (1964).

16. D. Katakis and H. Tanbe, J. Chem. Phys. 36, 416 (1962).

17. H. Yamazaki and J. J. Cvetanovic, J. Chem. Phys. 40, 582 (1964).

18. P. Warneck, J. Chem. Phys. 41, 3435 (1964).

19. W. E. Thompson, private communication.

2. **The VUV Photolysis of Planetary Gases to Determine the Role of Minor Constituents**

During this Quarter, photolysis experiments were performed and analyzed in a manner designed to define the role of minor constituents.

The present experimental setup consisted of a 1/2-meter Seya monochromator with a photomultiplier detector and a 6-inch length photolysis cell attached to the entrance port of the monochromator. The light source employed was a hydrogen discharge which supplied sufficient radiation in a 1200 to 3000Å wavelength region. The entrance window of the absorption cell was lithium fluoride to permit wavelengths down to 1200Å, whereas the exit window was made of quartz which transmitted only those wavelengths >1550Å so that the appearance of second order spectra were avoided.

Experiments were performed on the photolysis of pure CO_2, on $H_2S + O_2$ and $C_2H_2 + O_2$ mixtures. Rather definite results were obtained for the case of CO_2, whereas rather indefinite results were obtained for the gas mixtures. This will become evident by the brief description which is given herein on the results obtained thus far.

For the case of CO_2, the photolysis was performed with wavelengths >1750Å where CO_2 is a strong absorber. The spectroscopic product analysis was achieved by employing the continuous emission from the hydrogen source for the required absorption studies. The following experimental procedure was employed. The hydrogen source was operated until its

intensity stabilized; this required about two hours of operation time. Simultaneously, the cell was evacuated and CO_2 was then admitted into the cell at pressures which ranged from 10 to 50 mm Hg. The corresponding initial (no photolysis) absorption spectra for these pressures were recorded. Thereafter, during photolysis, repeated recordings of the spectra were made for photolysis periods of one half, one and over three hours, respectively.

Briefly, the results are as follows: no change in the spectra were observed for the period investigated in the wavelength region 2000 to 3000Å. On this basis, it can be shown that the total ozone concentration was $<5 \times 10^{14}$ molecules per cc. On the other hand, in the 1600 to 1800Å region the observed absorption changed appreciably during the irradiation period. For this case, Figure 3 shows those spectra which were recorded under various conditions. I_o designates the initial spectrum obtained with an evacuated cell. The spectra designated as (1), (2) and (3) were obtained for times-of-photolysis of 0, 1/2 and 1 hour, respectively. Continued irradiation beyond one hour did not change the spectra noticeably, indicating that a steady state was established. In the absorption measurements,.a spectral resolution of 5Å was employed so that it is not surprising to note a lack of structure in the observed spectra. However, the known spacings of the O_2 and CO discrete absorption bands is much greater than 5Å so that these gases can be precluded as significant contributors to the observed absorption. A contribution due to ozone can also be precluded since its absorption intensity in the spectral
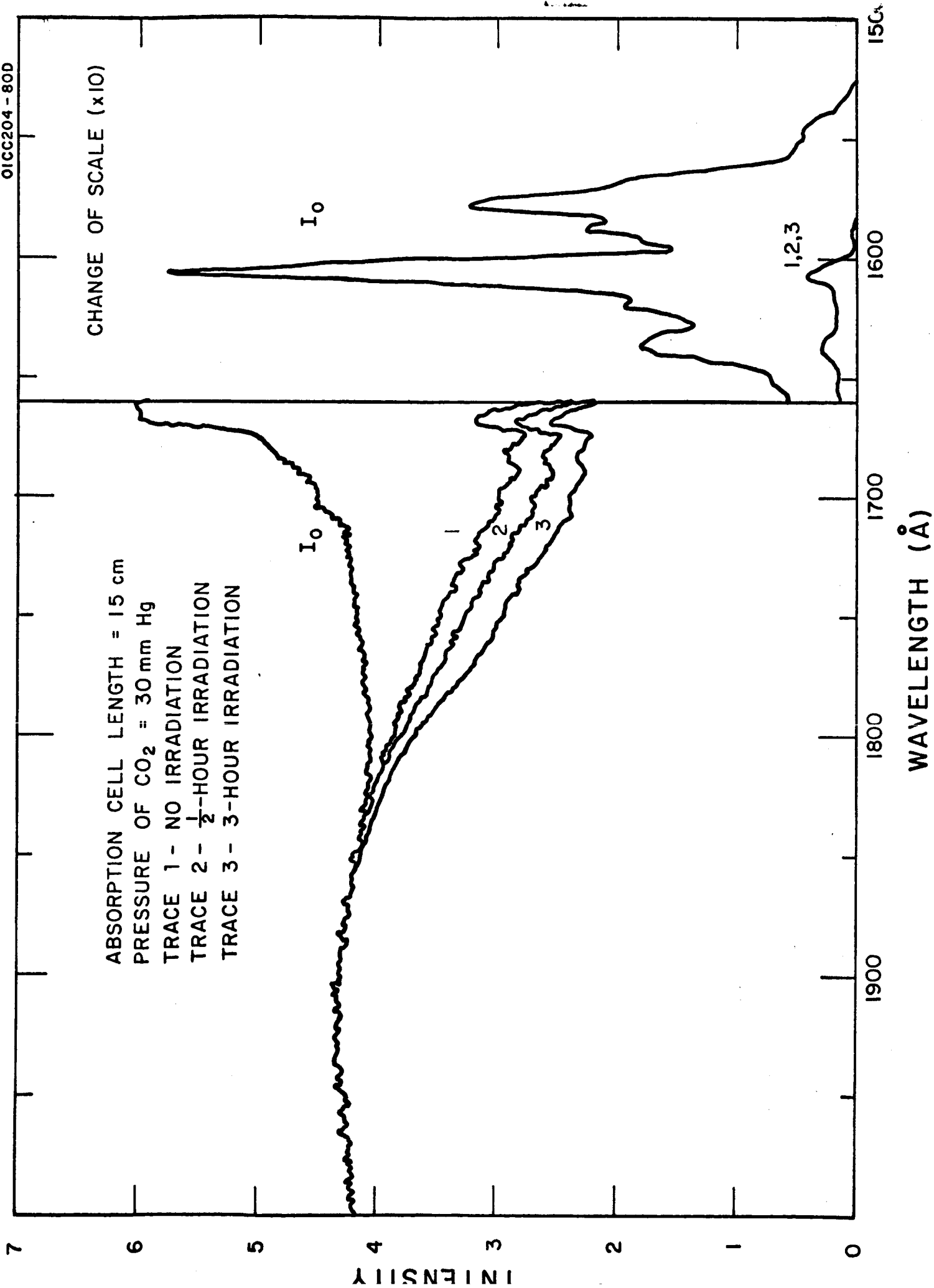
Figure 3

ABSORPTION CELL LENGTH = 15 cm
PRESSURE OF CO_2 = 30 mm Hg

TRACE 1 - NO IRRADIATION
TRACE 2 - $\frac{1}{2}$-HOUR IRRADIATION
TRACE 3 - 3-HOUR IRRADIATION

CHANGE OF SCALE (x10)

WAVELENGTH (Å)

INTENSITY

OICC204-80D

region is less than one-tenth of that in the 2500Å region where, as discussed above, no absorption was detected. In other words, an ozone concentration of less than 5×10^{14} molecules per cc could not possibly contribute any observable absorption. In addition, it should be noted that the observed change cannot be due to depletion of CO_2 since it corresponds to an increase in absorption rather than a decrease. Finally, auxiliary experiments were performed to establish that the observed absorption could not be due to outgassing or leaks in the system. Accordingly, it appears that the photolysis of CO_2 generates one or more as yet unidentified products. It would, indeed, be interesting to be able to establish that this product is CO_3 since it is of prime importance in solving some question on the incomplete reduction of the Martian atmosphere.

Since it was not possible to identify the photolysis product by absorption spectroscopy, it was decided to employ mass spectrometric techniques. In this manner, it was hoped to identify either CO_3 or some other product by mass analysis. The employed experimental setup combines a mass spectrometer with an arc liter-flask to which a vacuum ultraviolet light source is attached. The mass spectrometer is small 60-degree instrument operated with a permanent magnetic field; scanning was accomplished by variation of the acceleration voltage. A smooth capillary is used to direct the gas sample from the reaction vessel into the ion source of the spectrometer. The sample lost by the flow through the capillary is replaced by additional gas feed-in from a ballast volume. A hydrogen source is used for irradiation. The time variation of the product concentration, X, in the vessel under these conditions is governed by the equation

$$V \frac{dX}{dt} = P - XF$$

where V is the volume of the flask, P is the production rate, and F the flow rate into the spectrometer. The solution to this equation for the case that the product, X, is not initially present is

$$X = \frac{P}{F} [1 - \exp(-\frac{F}{V} t)]$$

indicating that the concentration approaches a steady state. For a flask volume of 1 liter and a flow rate of $I = 0.3$ cc/sec, the time until steady state is reached is approximately 7×10^3 sec or two hours, regardless of the productive rate of the product. However, the steady state concentration is proportional to P. It should therefore be possible to follow the evolution of a product with time in considerable detail.

In the experiments, CO_2 was photolyzed for about two hours and the spectrum scanned in 15-minute intervals. The evolution of oxygen was noted, but no other products were identified. Since the parent peak of CO at mass number 28 was overlapped by an ionized fragment from CO_2, the evolution of CO could not be assessed. In the mass 60 to 70 region, specifically no peak could be detected that might be associated with CO_3. However, in this range the mass spectrometer was not very sensitive due to the employed scanning mode. Magnetic scanning is definitely desirable to enhance the sensitivity in the higher mass range. In addition, it appears that stronger light sources, that is, xenon or krypton lamps will be beneficial for these experiments.

26

Additional photochemical systems were investigated in a pre-liminary fashion. These consisted of mixtures of oxygen with acetylene and hydrogen sulfide irradiated with light in the 1000Å region. The first required a 10:1 excess of oxygen; under these conditions the initial reaction is

$$O + C_2H_2 \rightarrow CO + CH_2$$

with the atomic oxygen being all consumed by acetylene. The ^1D oxygen atoms generated simultaneously with $O(^3P)$ may react differently, but so far no specific evidence in this respect has been obtained. The methylene radical evolving from the above reaction is in the triplet state and reacts rapidly with oxygen. The resulting products have not been defined as yet. One appears to be CO_2, but it is not known if this results directly from the interaction of CH_2 with oxygen or by subsequent reactions of an intermediate.

The photolysis of the $H_2S + O_2$ mixtures was also analyzed in a similar manner. It was found that the large rate of evolution of hydrogen makes its role important; but the present experimental set-up makes it difficult to study the low mass range simultaneously with the higher mass range. Additional optimization of the system is required, that is, perhaps the addition of magnetic scanning. It may also be noted that due to overlap of mass spectra of primary and product molecules difficulties exist in obtaining a sufficient amount of the desired informa-tion, particularly for minute amounts of minor product evolution.

For the gas analyses problems encountered, gas chromatography appears to be a more versatile and appropriate analytical tool. An appropriate gas chomatograph has been purchased on company funds in order to apply an improved analysis in future investigations in the identification of minor constituents in the photolysis of planetary gases.

B. THEORETICAL STUDIES

During the current Quarter, theoretical studies were performed and completed in three scientific areas: (1) Atom-atom collision processes in astrophysics, (2) Collision processes in planetary atmospheres, and (3) Ion temperatures in the topside ionosphere. The first two papers are reproduced here in their entirety since they were prepared for presentation at the International Astronomical Union Working Group on Collision Processes in Astrophysics and the plans for publication in an accredited journal are at present not fixed. On the other hand, a summary report is given for the third paper since it has been submitted for publication in Planetary and Space Science so that the detailed report will be available in that journal.

1. Atom-Atom Collision Processes in Astrophysics

Atom-atom collision processes which are relevant to astrophysical problems appear to occur either at thermal energies or at very high energies. Low energy collisions require special considerations but, with the exception of rearrangement processes, high energy collisions can be described by the Born approximation. It follows that proton impact cross sections for excitation and ionization of the target species are comparable to, but larger than, those for electron impact for equal <u>velocities</u> of the proton and the electron. Excitation and ionization by heavy particles other than bare nuclei is complicated by the possibility of excitation and ionization of the incident heavy particle, and collisions in which the incident particle and the target particle both undergo transitions may be more probable at high energies that collisions in which only one of the colliding pair undergoes a transition. However, high energy neutral particles are rarely of interest in astrophysics since they are readily ionized and the reverse process of charge transfer or electron capture is improbable. Although the high energy behavior of the cross section for charge transfer

$$X^+ + Y \rightarrow X + Y^+$$
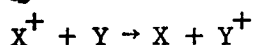
is still obscure (see Bransden 1966 for a detailed review), it is clear that the cross section ultimately decreases rapidly. The expected rapid decrease may not emerge from laboratory investigations since capture of inner shell electrons is important up to very high energies (Mapleton 1966).

Except for bare nuclei, heavy particles can induce transitions involving a change of spin multiplicity. In such transitions the core of the heavy particle behaves as a spectator in the high velocity limit and the active electron may be regarded as a free electron. Explicit calculations for the reaction

$$H + He \ (1^1S) \ \rightarrow \ H + He \ (2^3S)$$
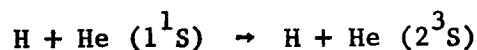
have been carried out by Bates and Crothers (1966).

Comprehensive accounts of atom-atom collisions are given in "Atomic and Molecular Processes" edited by Bates (1962), and a collection of more recent papers and reviews comprises "Atomic Collision Processes" edited by McDowell (1964).

High Energy Collisions

Because of the occurrence of cosmic rays, high energy collisions of protons and of neutral hydrogen atoms with hydrogen and possibly helium assume a special importance, and we present a brief discussion of the available data.

Comprehensive data are available only within the Born approximation. Calculations on a few processes hvae been performed using more refined approximations which are useful in assessing the accuracy and the range of velocity of the Born approximation results (Bates 1959, 1961, Mittleman 1961, Bates and Williams 1964, Coleman and McDowell 1965, Lovell and McElroy 1965, Ingber 1965, Fulton and Mittleman 1965, Cheshire 1965, Coleman and McDowell 1966, Wilets and Gallaher 1966).

Excitation and Ionization of H by H^+

Bates and Griffing (1953) (see also Bates 1958) have presented the results of Born approximation calculations of cross sections $Q(n_i \ell_i; n_f \ell_f)$ for the excitation processes

$$H^+ + H(1s) \rightarrow H^+ + H(2s,2p,3s,3p,3d) \qquad (1)$$
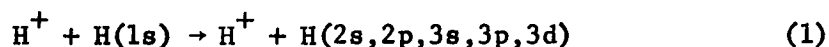
and the ionization process

$$H^+ + H \rightarrow H^+ + H^+ + e. \qquad (2)$$

(See also Peach 1965). For the ionization process, they present the velocity distributions of the ejected electron. The ionization cross section agrees closely with the measurements of Gilbody and Ireland (1964) above 40 keV but lie above the measurements of Fite, Stebbings, Hummer and Brackman 1960) below 40 keV. The cross section for excitation into the 2p state is about twice that measured by Stebbings, Young, and Ehrhardt (1965) between 5 and 30 keV but falls below it for energies below 3 keV.

At high energies E measured in keV,

$$Q(1s;2s) \sim \frac{11.1}{E} \left(1 - \frac{7.8}{E}\right) \pi A_o^2$$

and

$$Q(1s;2p) \sim \frac{128}{E} \left(\log E - 1.185 + \frac{4.1}{E}\right) \pi A_o^2.$$

Thus excitation of p states dominates in the asymptotic region. Cross sections for other values of n_i, ℓ_i, n_f and ℓ_f may be derived from electron impact cross sections (Bates and Griffing 1953, Carew and Milford 1963). May (1965a) has obtained a simple formula for excitation into all the sub-states corresponding to a particular value of n when n is large. He shows that

$$Q(1s; \Sigma_\ell n_\ell) = \frac{I(E)}{n^3} \left(1 + 0(n-2)\right) \pi A_o^2 \tag{3}$$

where $I(E)$ is given in Table 4. Cross sections for excitation into all the discrete levels $\sum_{n\ell} Q(1s;n\ell)$ have been calculated by Butler and Parcell (1965) and their results are reproduced in Table 5.

Cross sections for transitions in which the target atom is excited have been computed by Carew and Milford (1963) who give results for the target atom in states with principal quantum number n_i = 2,3,4,5 and 10 for transitions such that $n_f - n_i$ = 1 or 2. With decreasing threshold energy, the cross section maximum increases to lower energy and as n_i increases, proton impact becomes more efficient than electron impact in causing transitions in the thermal energy range.

32

TABLE 4

VALUES OF THE FUNCTION I(E) APPEARING IN EQUATION (3)

Impact Energy E (keV)	I(E)
1.6	0.58
3.1	2.5
6.3	6.1
12.5	8.9
25	8.5
50	6.5
100	4.4
200	2.8

TABLE 5

CROSS SECTIONS Q IN UNITS OF πa_o^2

Impact Energy (keV)	$\sum_\ell Q(1s,2e)$ $+ Q(1s,3e)$	$\sum_{n\ell} Q(1s;n\ell)$
6.24	2.26	2.53
7.71	2.49	2.83
9.76	2.67	3.04
12.74	2.74	3.12
17.35	2.75	3.15
25.0	2.58	2.95
39.0	2.24	2.57
69.4	1.72	1.95
156.1	1.08	1.23
277.6	0.74	0.83
624.5	0.41	0.44

34

Excitation and Ionization of H by H

Bates and Griffing (1954, 1955) (see also Bates 1958) have presented the results of Born approximation calculations of cross sections $Q(1s - n_1 \ell_1; 1s - n_2\,_2)$ for the excitation processes

$$H(1s) + H(1s) \rightarrow H(n_1\ell_1) + H(n_2\,_2) \tag{4}$$

and for the ionization processes

$$H(1s) + H(1s) \rightarrow H(n_1\ell_1) + H^+ + e \tag{5}$$

$$H(1s) + H(1s) \rightarrow H^+ + e + H^+ + e \ . \tag{6}$$
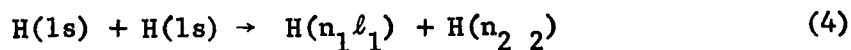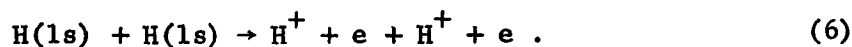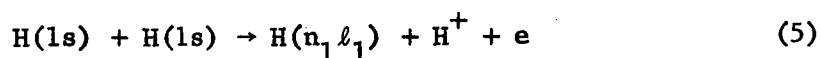
At high impact energies, E(keV),

$$Q(1s\text{-}2s; 1s\text{-}\Sigma) \sim \frac{4.3}{E} \ \pi a o^2 \tag{7}$$

$$Q(1s\text{-}2p; 1s\text{-}\Sigma) \sim \frac{21}{E} \ \pi a_o^2 \tag{8}$$

where Σ is the sum of all possible final states, including the continuum. For ionization at high energies,

$$Q(1s - C; 1s - \Sigma) \sim \frac{128}{E} \ \pi a o^2 \ .$$

Collisions in which the incident atom remains in the 1s state contribute only about 13% of the total.

May (1965b) has derived further asymptotic formulae for $Q(1s - \sum_e n\ell; 1s - 1s)$ and $Q(1s\ell \cdot \sum_e n\ell; 1s - \Sigma)$, showing that for large n they decrease as n^{-3}.

Bates and Griffing (1955) have obtained the velocity distributions
of the electrons ejected in ionizing collisions of stationary hydrogen
atoms by hydrogen atom impact. To compute the velocity distributions of
electrons ejected from the moving projectile atom, it is necessary to
calculate also the angular distributions of the ejected electrons, and
this calculation has been carried out by Dalgarno and Griffing (1958).

Collisions in which the target atom is excited have been investi-
gated by Bouthilette, Healey and Milford (1964) and collisions in which
both the projectile and the target atoms are excited by Pomilla and
Milford (1966).

The charge transfer process

$$H + H \rightarrow H^+ + H^-$$
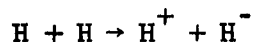
has been investigated by Mapleton (1965).

Charge Transfer of H^+ in H

Cross sections for electron capture by protons from atomic hydrogen

$$H^+ + H(1s) \rightarrow H(he) + H^+$$
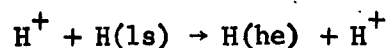
have been computed using the Brinkman-Kraner form of the Born approximation
for final states up to 4f by Bates and Dalgarno (1953) and their work has
been extended to higher states of excitation and to capture from excited
atoms by Butler and Johnston (1964), by May (1964), by Hiskes (1965) and
by May and Hodge (1965). The accuracy of the absolute cross sections is

36

open to question but the relative values for capture into different excited states appear to be satisfactory for impact energies above 40 keV (cf Hiskes 1965). For large values of n, the cross sections decrease as n^{-3}.

Comparisons of different first order approximations (cf Bates 1962) have been made by Bates and Dalgarno (1952), Jackson and Schiff (1953), Bessel and Gerjuoy (1960), McCarroll (1961), and Mapleton (1962).

The cross section for capture into the 2p state is about twice that measured by Stebbings, Young, Oxley and Ehrhardt (1965) between 5 and 30 keV but falls below it for energies below 3 keV.

Stopping Power of H^+ in H

The efficiency with which a beam of protons is slowed down in a gas of ground state hydrogen atoms has been examined in detail by Dalgarno and Griffing (1955) using the Born approximation to the cross sections for the various processes. The mean energy expended in producing an ion pair in hydrogen gas has also been calculated as a function of impact energy (Dalgarno and Griffing 1958). The neutralization of the ion beam appears to extend the range of impact energies over which the beam energy per ion pair is essentially constant at a value of about 32 eV.

Stopping Power of H^+ in an H^+, e Plasma

The energy loss of fast protons in an ionized plasma has been calculated by Hayakawa and Kitao (1956) and by Butler and Buckingham (1962). The pressure of free electrons in a gas increases markedly the rate of energy loss.
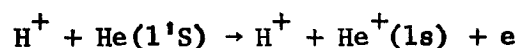
Excitation and Ionization of He by H^+ and H

Theoretical calculations of the excitation and ionization of He are much less comprehensive than for H. The following processes have been studied:
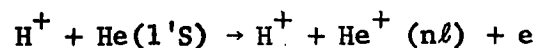
$$H^+ + He(1'S) \rightarrow H^+ + He(1s2p'P)$$
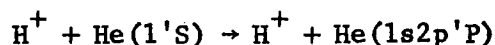
(Moiseiwich and Stewart 1954, Bell 1961, Bell and Skinner 1962)

$$H^+ + He(1'S) \rightarrow H^+ + He(1s3p'P)$$

(Bell 1961, Bell and Skinner 1962)

$$H^+ + He(1'S) \rightarrow H^+ + He^+(1s) + e$$
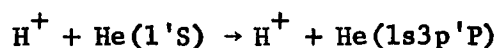
(Mapleton 1958, Peach 1965)

$$H^+ + He(1'S) \rightarrow H^+ + He^+(n\ell) + e$$

(Dalgarno and McDowell 1955, Mapleton 1958)

$$H + He(1'S) \rightarrow H(\Sigma) + He(1s2p'P)$$
$$H + He(2^3S) \rightarrow H(\Sigma) + He(1s2p^3P)$$
$$H + He(2^3S) \rightarrow H(\Sigma) + He(1s3p^3P)$$
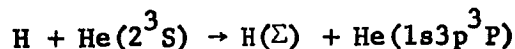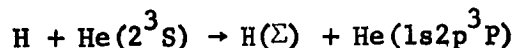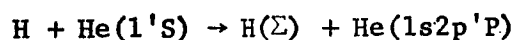
(Adler and Moiseiwich 1957),

$$H + He(1'S) \rightarrow H^+ + e + He(\Sigma)$$
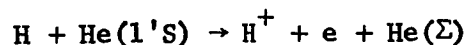
(Bates and Williams 1957)

The predicted ionization cross sections agree well with the measurements of Hooper, Harmer, Martin and McDaniel (1962) at impact energies above 400 keV but be above the experimental cross sections (Federenko, Afrosimov, Il'in and Solov'ev 1960 Hooper et al. 1962) at lower energies.

38

Charge Transfer of H^+ in He

Mapleton (1961,1963) has used the Born approximation to calculate cross section for electron capture by protons from helium,

$$H^+ + He(1'S) \rightarrow H(\ell e) + He^+(n'\ell')$$
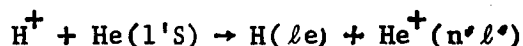
for various excited states of the end products. The total charge transfer cross section is in good agreement with the measured cross section (Stier and Barrett 1956, Barrett and Reynolds 1958), above 40 keV and the cross section for capture into the 3s state of atomic hydrogen is in good agreement with that measured by Hughes, Dawson, Doughty, Kay and Stiger (1966) above 100 keV, but lies above it at lower energies. Hughes et al. also obtained evidence suggesting that the cross sections for capture into the nth state of hydrogen decrease as n^{-3} for impact energies above about 20 keV. The theoretical cross sections for capture into the 2s states and 2p states of hydrogen lie well above those measured by Pretzer, Van Zyl and Geballe (1964), by ColliCristofori Frigerio and Sona (1962) and by Jaecks, Van Zyl and Geballe (1965) at energies below 20 keV.

The electron capture process for the case when the hydrogen atom and helium ion are produced in their ground states has been studied using higher order approximations by Bransden and Cheshire (1963), by Green, Stanley and Chang (1965) and by Bransden and Sin Fai Laim (1966).

Low Energy Collisions

Excitation by Proton Impact

The cross section for direct excitation by electron impact is broadly similar to that by proton impact if the electron and proton have the same

39

velocity. The electron impact excitation cross section rises rapidly from threshold to a maximum, which occurs at an impact velocity corresponding to about twice the threshold energy, and then decreases asymptotically as $E^{-1} \ln E$ for optically allowed transitions or as E^{-1} for optically forbidden transitions. Thus electron impact excitation is usually more efficient than proton impact excitation except when the threshold energy is only a small fraction of the thermal energy of the plasma.

An example of an excitation process for which proton impact is more efficient than electron impact is the 2s-2p transition in atomic hydrogen

$$H^+ + H(2s_{\frac{1}{2}}) \rightarrow H^+ + H(2p_{\frac{1}{2}}, \, 2p_{3/2}).$$
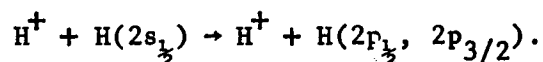
The threshold energies are respectively 0.0354 cm^{-1} and 0.327 cm^{-1}. The reaction is important in reducing the intensity of the two-quantum emission from H(2s).

The cross section has been calculated by Seaton (1955) using a partial wave analysis in which he ensured that no partial wave violated the conservation laws. The derived rate coefficients at $10,000^{\circ}$K and at $20,000^{\circ}$K are reproduced in Table 6. They are an order of magnitude larger than those for electrons. The charge transfer process

$$H^+ + H(2s_{\frac{1}{2}}) \rightarrow H(2p_{\frac{1}{2}}, 2p_{3/2}) + H^+$$
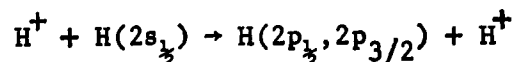
is negligible compared to the direct reaction (Boyd and Dalgarno 1958).

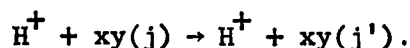Collisions which lead merely to a redistribution of angular momentum

$$H^+ + H(n\ell) \rightarrow H^+ + H(n\ell')$$
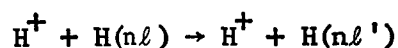
will usually proceed very rapidly.

TABLE 6

RATE COEFFICIENT k FOR $H^+ + H(2s) \rightarrow H^+ + H(2p_j)$

$T \; ^\circ K$		10,000	20,000
$k(cm^3 sec^{-1})$	$j = \frac{1}{2}$	2.5×10^{-4}	2.1×10^{-4}
	$j = \frac{3}{2}$	2.2×10^{-4}	2.2×10^{-4}

Similar reactions which may be of astrophysical importance are the proton impact excitation of molecular rotations

$$H^+ + xy(j) \rightarrow H^+ + xy(j').$$

The particular case

$$H^+ + CN(j=0) \rightarrow H^+ + CN(j=1)$$
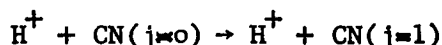
has been investigated by Thaddeus and Clauser (1966) in connection with the cosmic microwave radiation at $\lambda = 2.63$ mm (see also Field and Hitchcock 1966). Their calculations appear to be based upon an approximation analogous to the Bethe form of the Born approximation (cf. Seaton 1962). There occurs a strong long-range interaction between the proton and the permanent dipole moment of CN and the derived cross section for 1 eV protons is about 10^{-12} cm^2. Thaddeus and Clauser suggest that the process may be important in HII regions.

Because of the strong coupling between different rotational levels during the collision, the cross sections for exciting higher rotational levels will be of comparable magnitude.

Charge Transfer

The symmetrical resonance charge transfer process

$$H^+ + H \rightarrow H + H^+$$
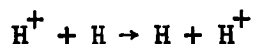
does not involve an electronic transition and its cross section can be predicted reliably. At 1 eV the cross section is about 4×10^{-15} cm^2 decreasing slowly with increasing energy (Dalgarno and Yadav 1953, Ferguson 1961, Peek 1966).

42

Resonance charge transfer significantly modifies the diffusion of H^+ in H. Values of the ion diffusion coefficient have been calculated by Dalgarno (1961) and they are reproduced in Table 7.

Asymmetric charge transfer processes

$$H^+ + X \rightarrow H + X^+$$

involve an electronic transition and they will, in most cases, proceed very slowly at thermal energies. Exceptions occur and one such is

$$H^+ + O(^3P) \rightarrow H + O^+(^4S)$$
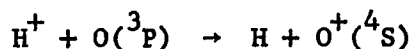
which is accidentally resonant. Chamberlain (1956) has suggested that the reaction may affect the ratio of the O to O^+ densities in the Cassiopeia radio source.

There is no satisfactory theory of asymmetric charge transfer reactions but an approximate analysis by Rapp (1963) of the measurements at high energies by Fite, Smith and Stebbings (1962) shows that it behaves like a symmetric charge transfer reaction down to very low energies. The predicted cross section at 1 eV is 2×10^{-15} cm^2, a value consistent with the cross section of 8×10^{-15} cm^2 at $1000^\circ K$ derived by Hanson, Patterson and Degaonkor (1963) from upper atmosphere data.

Radiative Charge Transfer

Radiative charge transfer processes in which a photon is emitted may proceed more rapidly than ordinary charge transfer at thermal energies.

43

TABLE 7

DIFFUSION COEFFICIENT D^+ OF H^+ IN H

$T\ ^{\circ}K$	1000	2000	5000	10,000	20,000	50,000
$D^+n(H) \times 10^{17}$	1.7	2.6	4.6	7.1	11.0	20.0

Calculations have been carried out for two simple cases using a theory in which the probability of a transition of the quasi-molecule formed by the colliding pair is integrated along the classical path (Bates 1951). The reactions which have been investigated are

$$He^{++} + H \rightarrow He^{+} + H^{+} + h\nu$$
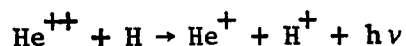
(Arthurs and Hyslop 1957) and

$$He^{++} + He \rightarrow He^{+} + He^{+} + h\nu$$
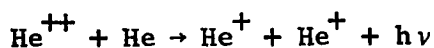
(Allison and Dalgarno 1965). The first reaction has a rate coefficient of 1.5×10^{-13} $cm^3 sec^{-1}$ at $20,000^{\circ}K$ and the second a rate coefficient of 4×10^{-15} $cm^3 sec^{-1}$.

Radiative Association

Radiative association

$$X + Y \rightarrow XY + h\nu$$

provides a mechanism for the formation of molecules in gases at low densities. It may be described by a theory analogous to that appropriate to radiative charge transfer. Bates (1951) has computed the rate coefficient for

$$H^{+} + H \rightarrow H_2^{+} + h\nu$$
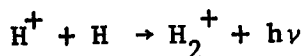
obtaining a value of 5×10^{-18} $cm^3 sec^{-1}$ at $1000^{\circ}K$ increasing to 4×10^{-16} $cm^3 sec^{-1}$ at $20,000^{\circ}K$. Bates also tabulates the rate coefficient for the free-free transition

$$H^{+} + H \rightarrow H^{+} + H + h\nu$$

45

For the reactions

$$C + H \rightarrow CH + h\nu$$

$$C^+ + H \rightarrow CH^+ + h\nu$$
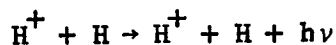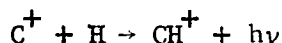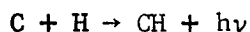
Bates (1951) has given tentative estimates of 2×10^{-18} $cm^3 sec^{-1}$ but he
notes that the rate coefficient of the former may be 6×10^{-18} $cm^3 sec^{-1}$
if the carbon atoms are all in the ^3P_o state and that the rate coefficient
of the latter may vanish if the carbon ions are all in the $^2P_{\frac{1}{2}}$ state.

The rate of formation of HeH^+ has not been calculated though the
molecule undoubtedly exists (Michels 1966, Harris 1966).

The free-bound absorption

$$H + H + h\nu \rightarrow H_2'$$
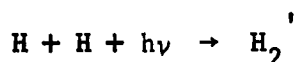
has been investigated by Erkovich (1960), Soshnikov (1964) and Soloman (1964)
for the transition $(1s\ \sigma\ 2p\sigma\ ^3\Sigma_u^+ - 1s\sigma\ 2s\sigma\ ^3\Sigma_g^+)$. The process does not
seem to be a significant source of absorption.

The radiative association of two hydrogen atoms

$$H + H \rightarrow H_2 + h\nu$$
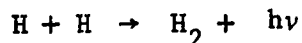
is a very slow process since the stabilizing transition is highly forbidden.
Malville (1964) has given an estimate of 4×10^{-27} $cm^3 sec^{-1}$ at $100^{\circ}K$ for its
rate coefficient.

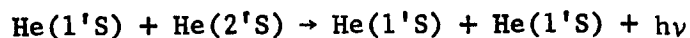Collision-Induced Radiative Deactivation

Allison and Dalgarno (1963) have calculated the rate coefficient for

$$H^+ + He(2'S) \rightarrow H^+ + He(1'S) + h\nu.$$
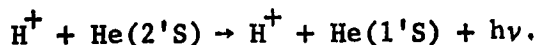
Because of the large polarizability of He(2'S), the reaction proceeds quite rapidly with a rate coefficient of 10^{-11} cm^3sec^{-1} at $20,000^{\circ}K$.

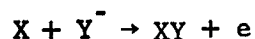A similar study of the reaction

$$He(1'S) + He(2'S) \rightarrow He(1'S) + He(1'S) + h\nu$$

has been completed by Allison, Browne and Dalgarno (1966) who obtain a rate coefficient of 3×10^{-14} cm^3sec^{-1} at $20,000^{\circ}K$.

Associative Detachment

Associative detachment

$$X + Y^- \rightarrow XY + e$$

is an efficient mechanism for the destruction of negative ions. It may be regarded as proceeding through the formation of a quasi-molecule XY^- which can undergo autodetachment. Since the mean time for autodetachment is usually much less than the mean time the nuclei remain in the autodetaching region, the probability of autodetachment is high. This simple picture led Dalgarno (1961) to advocate a rate coefficient of up to 10^{-10} cm^3sec^{-1} for

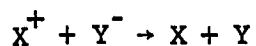$$H + H^- \rightarrow H_2 + e .$$
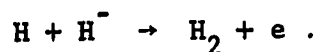
Developments in the theory of resonating states should yield a more precise estimate (see in particular Bardsley, Herzenberg and Mandl 1966).

The process is also of interest in that it leads to a production of hydrogen molecules (McDowell 1961).

Mutual Neutralization

Mutual neutralization

$$X^+ + Y^- \rightarrow X + Y$$

usually proceeds rapidly at thermal energies because of the long range attraction in the initial channel and because intersecting potential energy surfaces are available connecting the initial and final channels. (Bates and Massey 1954, Bates and Boyd 1956). The case

$$H^+ + H^- \rightarrow H + H$$
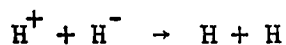
has been studied in detail by Bates and Lewis (1955) who have shown that the rate coefficient may be as large as 10^{-7} cm^3 sec^{-1} and varies approximately as $T^{-\frac{1}{2}}$.

Penning Ionization

Thermal ionization

$$X + Y \rightarrow X + Y^+ + e$$
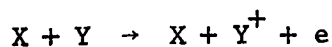
can also occur efficiently in many instances because of the existence of intersecting potential energy surfaces (Bates and Massey 1954). The process is analogous to associative detachment in that a radiationless transition (autoionization) occurs. The rate coefficients for

$$He(2'S) + H \rightarrow He(1'S) + H^+ + e$$

and

$$He(2^3S) + H \rightarrow He(1'S) + H^+ + e$$
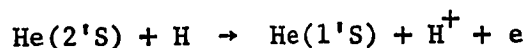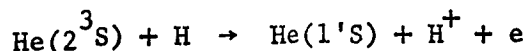
may approach values near 10^{-11} cm^3 sec^{-1}.

The colliding systems may become bound forming HeH$^+$, a process known as associative ionization.

Excitation by Neutral Hydrogen Atom Impact

The excitation of rotational levels of molecular hydrogen by the impact of hydrogen atoms is an important cooling mechanism in interstellar space. Cross sections for

$$H + H_2 (j = 0) \rightarrow H + H_2(j = 2)$$

have been calculated by Takayanagi and Nishimura (1960) using an approximate version of the distorted wave method. The distorted wave method has been applied without further approximation by Dalgarno, Henry and Roberts (1966) with results in close agreement with the earlier calculations. Their cooling rates are reproduced in Table 8.

Recently Allison and Dalgarno (1967) have solved the set of coupled equations that describes the collision, obtaining cross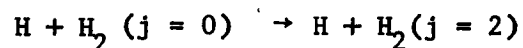 sections which are somewhat lower at high temperatures than those derived from the distorted wave approximation. However, the major uncertainty in the predicted cooling rates lies in the interaction potential between H and H_2.

Takayanagi and Nishimura (1960) and Dalgarno, Henry and Roberts (1966) have also tabulated excitation rates for other rotational transitions in H_2 and in D_2

The excitation of H_2 by H_2

$$H_2(j = 0) + H_2(j' = 0) \rightarrow H_2(j) + H_2(j')$$

50
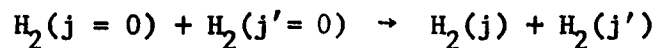
TABLE 8

RATE COEFFICIENT $H-H_2(j-j)$ $(cm^3 \ sec^{-1})$

T^oK	0-2	1-3	2-4
20	3.4(-23)		
30	2.8(-19)	7.2(-25)	
40	2.8(-17)	1.3(-21)	
50	4.4(-16)	1.3(-19)	4.3(-23)
60	2.9(-15)	2.7(-18)	3.1(-21)
80	3.2(-14)	1.3(-16)	6.8(-19)
100	1.4(-13)	1.5(-15)	1.9(-17)
200	3.8(-12)	2.6(-13)	2.1(-14)
300	1.4(-11)	1.9(-12)	2.9(-13)
500	5.3(-11)	1.3(-11)	3.4(-12)
1000	2.2(-10)	7.8(-11)	3.4(-11)
2000	7.1(-10)	3.1(-10)	1.7(-10)
3000	1.4(-9)	6.4(-10)	3.7(-10)
4000	2.2(-9)	1.0(-9)	6.2(-10)
5000	3.1(-9)	1.5(-9)	9.2(-10)

is less important. The most accurate cross sections are those computed by Davison (1962,1964).

Takayanagi and Nishimura (1960) have roughly estimated the rate co-efficient for excitation of the 0-1 rotational transition in CH, CN and OH to be 3.5×10^{-10} cm^3 sec^{-1}, corresponding to a cross section of about 10^{-15} cm^2.

Spin-Change Processes

Purcell and Field (1956) draw attention to the role of the spin-change process

$$H(F = 0) + H \rightarrow H(F = 1) + H$$

in controlling the spin population of atomic hydrogen and gave a rough estimate of its cross section. The process has been further studied by Dalgarno (1962) and by Dalgarno and Henry (1964) using a theory which assumes the collision to be elastic and which ignores the effect of molecular rotation during the collision. The derived cross sections, averaged over a Maxwellian velocity distribution, oscillate about a value of 8×10^{-15} cm^2 for $T < 100°K$ and decrease slowly at higher temperatures.

A similar process

$$O(3P_J) + H \rightarrow O(3P_{J'}) + H$$
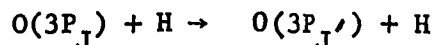
was advanced by Burgess, Field and Michie (1960) as a possible cooling mechanism in interstellar space and Dalgarno and Rudge (1964) proposed

the additional mechanisms

$$C^+(^2P_J) + H \rightarrow C^+(^2P_J) + H$$

$$Si^+(^2P_J) + H \rightarrow Si^+(^2P_J) + H$$
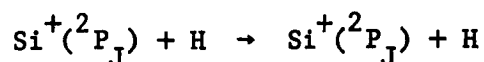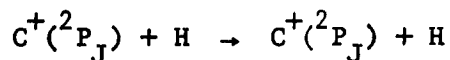
giving a rough estimate of the cross section. Smith (1966b) has computed the corresponding cooling rates and he concludes that the O - H reaction is more efficient than the C^+ - H and Si^+ - H reactions (despite the long-range attraction) and that below $300^{\circ}K$ the O - H reaction is a more efficient cooling mechanism than excitation of the rotational levels of H_2 by hydrogen atom impact.

The theoretical description used by Smith is an extension of that presented by Dalgarno and Rudge (1965) for collision-induced changes in the hyperfine structure of alkali metal vapors and it may not be adequate for collision-induced changes in fine structure (cf. Nikitin 1965, Callaway and Bauer 1965).

Quenching Collisions

The quenching of radiation through the destruction process

$$X + Na(^2P_{1/2}) \rightarrow X + Na(^2S_{1/2})$$
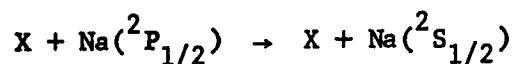
has been studied theoretically by Nikitin and Bykhovskii (1964) but the lack of adequate wave functions for the quasi-molecule XNa has prevented qualitative predictions. For inert gas atoms, the measured cross sections

53

are about 10^{-16} cm^2. Larger cross sections occur when X is a diatomic molecule. (cf. Starr and Shaw 1966)

Chemical Reactions

Herzberg (1955) has listed a number of exothermic reactions which produce molecular hydrogen:

$$CH^+ + H \rightarrow H_2 + C^+,$$

$$CH + H \rightarrow H_2 + C,$$

$$NH + H \rightarrow H_2 + N,$$

$$OH + H \rightarrow H_2 + O ,$$
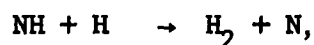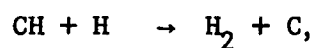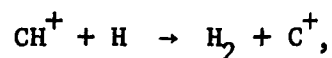
and Stecher and Williams (1966) have listed other exothermic reactions which produce CH, OH, NH, CN, CO and N_2. It is conventional practice to adopt the Arrhenius form for the rate coefficients

$$K = A \exp(-E/kT)$$

and to assume that the activation energy E is given by

$$A = 0.055D$$

where D is the dissociation energy of the initial molecule. (Polayni 1962)

Transport Properties

The thermal conductivity and the viscosity of atomic hydrogen have been calculated to high accuracy by Dalgarno and Smith (1962) at high temperatures and by Buckingham, Fox and Gal (1965) at low temperatures . The diffusion coefficient of protons in atomic hydrogen gas is given in Table 7. Formulas for the transport coefficients appropriate to a fully ionized plasma have been derived by Spitzer (1956) (see Devoto 1966).

REFERENCES

J. Adler and B. L. Moiseiwitsch 1957 Proc. Phys. Soc. A70, 117.

A. C. Allison and A. Dalgarno 1967 Proc. Phys. Soc. in press.

D. C. Allison and A. Dalgarno 1963 Proc. Phys. Soc. 81, 23.

D. C. Allison and A. Dalgarno 1965 Proc. Phys. Soc. 85, 845.

D. C. Allison, J. C. Browne and A. Dalgarno 1966 Proc. Phys. Soc. in press.

A. M. Arthurs and J. Hyslop 1957 Proc. Phys. Soc. A70, 849.

J. N. Bardsley, A. Herzenberg and F. Mandl 1966 in press.

C. F. Barnett and H. K. Reynolds 1958 Phys. Rev. 109, 355.

R. H. Bassel and E. Gerjuoy 1960 Phys. Rev. 117, 749.

D. R. Bates 1951 Mon. Not. Roy. Astron. Soc. 111, 303.

D. R. Bates 1958 Proc. Roy. Soc. A245, 299.

D. R. Bates 1959 Proc. Phys. Soc. A73, 227.

D. R. Bates 1961 Proc. Phys. Soc. A77, 59.

D. R. Bates 1962 Atomic and Molecular Processes (Academic Press).

D. R. Bates and T. J. M. Boyd 1956 Proc. Phys. Soc. A69, 910.

D. R. Bates and D. S. F. Crothers 1966 in press.

D. R. Bates and A. Dalgarno 1952 Proc. Phys. Soc. A65, 919.

D. R. Bates and A. Dalgarno 1953 Proc. Phys. Soc. A66, 972.

D. R. Bates and G. W. Griffing 1953 Proc. Phys. Soc. A66, 961.

D. R. Bates and G. W. Griffing 1954 Proc. Phys. Soc. A67, 663.

D. R. Bates and G. W. Griffing 1955 Proc. Phys. Soc. A68, 90.

D. R. Bates and J. T. Lewis 1955 Proc. Phys. Soc. A68, 173.

D. R. Bates and H. S. W. Massey 1954 Phil. Mag. 45, 111.

REFERENCES

(Continued)

D. R. Bates and A. Williams 1957 Proc. Phys. Soc. A70, 117.

D. R. Bates and D. A. Williams 1964 Proc. Phys. Soc. 83, 425.

R. J. Bell 1961 Proc. Phys. Soc. 78, 903.

R. J. Bell and B. G. Spinner 1962 Proc. Phys. Soc. 80, 404.

D. B. Bouthilette, J. A. Healey and S. N. Milford 1964 Atomic Collision Processes (North-Holland) p. 1081.

T. J. M. Boyd and A. Dalgarno 1958 Proc. Phys. Soc. 72, 694.

B. H. Bransden 1966 Adv. Atom. Mol. Phys. 1, 85.

B. H. Bransden and I. Cheshire 1963 Proc. Phys. Soc. 81, 820.

B. H. Bransden and L. T. Sin Fie Lam 1966 Proc. Phys. 87, 653.

A. Burgess, G. B. Field and R. W. Michie 1960 Astrophys. J. 131, 529.

R. A. Buckingham, J. W. Fox and E. Gal 1965 Proc. Roy. Soc. A 284, 237.

S. T. Butler and M. J. Buckingham 1962 Phys. Rev. 126, 1.

S. T. Butler and I. D. S. Johnston 1964 Nucl. Fusion 4, 196.

J. W. Chamberlain 1956 Astrophys. J. 124, 390.

J. Callaway and E. Bauer 1965 Phys. Rev. 140, A1072.

J. Carew and S. N. Milford 1963 Astrophys. J. 138, 772.

I. Cheshire 1965 Phys. Rev. 138, A992.

J. P. Coleman and M. R. C. McDowell 1965 Proc. Phys. Soc. 85, 1097.

J. P. Coleman and M. R. C. McDowell 1966 Proc. Phys. Soc. 87, 879.

L. Colli, F. Cristofori, G. E. Frigerio and P. G. Sona 1962 Phys. Rev. Letts. 3, 1962.

A. Dalgarno 1961a Annales de Geophys. 17, 16.

A. Dalgarno 1961b Proc. Roy. Soc. A262, 132.

REFERENCES

(Continued)

A. Dalgarno and G. W. Griffing 1955 Proc. Roy. Soc. A232, 423.

A. Dalgarno and G. W. Griffing 1958 Proc. Roy. Soc. A248, 415.

A. Dalgarno and R. J. W. Henry 1964 Proc. Phys. Soc. 83, 157.

A. Dalgarno, R. J.W. Henry and C. S. Roberts 1966 Proc. Phys. Soc. 88, 611.

A. Dalgarno and M. R. C. McDowell 1955 The Airglow and the Aurorae.

A. Dalgarno and M. J. Rudge 1964 Astrophys. J. 140, 800.

A. Dalgarno and M. J. Rudge 1965 Proc. Roy. Soc. A286, 519.

A. Dalgarno and F. J. Smith 1962 Proc. Roy. Soc. A267, 417.

A. Dalgarno and H. N. Yadav 1953 Proc. Phys. Soc. A66, 173.

W. D. Davison 1962 Disc. Faraday Soc. 33, 71.

W. D. Davison 1964 Proc. Roy. Soc. A280, 227.

R. S. Devoto 1966 Phys. Fluids 9, 1230.

C. Erkovich 1960 Optics and Spectr. 8, 162.

N. V. Federenko, V. V.Afrosimov, R. N. Il'in and E. S. Solov'ev 1960
Ionization Phenomena in Gases IV (North-Holland) p. 47.
P. M.Stier and C. F. Barnett 1956 Phys. Rev. 103, 896.

A. F. Ferguson 1961 Proc. Roy. Soc. A246, 540.

G. B. Field and J. L. Hitchcock 1966 Phys. Rev. Letts. 16, 817.

W. L. Fite, R. F. Stebbings, D. G. Hummer and R. T. Brackman 1960
Phys. Rev. 119, 663.

W. L. Fite, A. C. H. Smith and R. F. Stebbings 1962 Proc. Roy. Soc.
A268, 527.

M. J. Fulton and M. H. Mittleman 1965 Annales Phys. (N.Y.) 33, 65.

H. B. Gilbody and J. V. Ireland 1964 Proc. Roy.Soc. A277, 137.

T. A. Green, H. E. Stanley and Y. C. Chang 1965 Helv. Phys. Acta. 38, 109.

W. B. Hanson, T. L. W. Patterson, and S. S. J. Degaonkar 1963 J. Geophys.
Res. 68, 6213.

REFERENCES

(Continued)

F. E. Harris 1966 J. Chem. Phys. 44, 3636.

S. Hayakawa and K. Kitao 1956 Prog. Theor. Phys. 16, 139.

G. Herzberg 1955 Mem. Soc. R. Sci. Liege (4), 15, 291.

J. R. Hiskes 1965 Phys. Rev. 137, A361.

J. W. Hooper, D. S. Harm, D. W. Martin and E. W. McDaniel 1962 Phys. Rev. 125, 2000.

R. H. Hughes, H. R. Dawson, B. M. Doughty, D. B. Kay and C. A. Stigers 1966 Phys. Rev. 146, 53.

L. Ingber 1965 Phys. Rev. 139, A35.

J. D. Jackson and H. I. Schiff 1953 Phys. Rev. 89, 359.

D. Jaecks, B. Ban Zyl and R. Geballe 1965 Phys. Rev. 137, A340.

S. E. Lovell and M. B. McElroy 1965 Proc. Roy. Soc. A283, 100.

R. W. McCarroll 1961 Proc. Roy. Soc. A246, 547.

M. R. C. McDowell 1964 Atomic Collision Processes (North-Holland).

M. R. C. McDowell 1961 Observatory 81, 240.

J. M. Malville 1964 Astrophys. J. 139, 198.

R. A. Mapleton 1961 Phys. Rev. 122, 528.

R. A. Mapleton 1958 Phys. Rev. 109, 1166.

R. A. Mapleton 1962 Phys. Rev. 126, 1477.

R. A. Mapleton 1963 Phys. Rev. 130, 1839.

R. A. Mapleton 1965 Proc. Phys. Soc. 85, 841.

R. A. Mapleton 1966 Phys. Rev. 145, 25.

R. M. May 1964 Nucl. Fusion 4, 207.

R. M. May 1965a Phys. Letts. 14, 98.

REFERENCES

(Continued)

R. M. May 1965b Phys. Letts. $\underline{14}$, 198.

R. M. May and J. G. Lodge 1965 Phys. Rev. $\underline{137}$, A699.

H. H. Michels 1966 J. Chem. Phys. $\underline{44}$, 3834.

M. H. Mittleman 1961 Phys. Rev. $\underline{122}$, 499.

B. L. Moiseiwitsch and A. L. Stewart 1954 Proc. Phys. Soc. $\underline{A67}$, 1069.

E. E. Nikitin 1965 J. Chem. Phys. $\underline{43}$, 744.

E. E. Nikitin and V. K. Bykhovskii 1964 Optics and Spectr. $\underline{17}$, 444.

J. M. Peek 1966 Phys. Rev. $\underline{143}$, 33.

G. Peach 1965 Proc. Phys. Soc. $\underline{85}$, 709.

J. C. Polanyi 1962 Atomic and Molecular Processes (Academic Press) p. 807.

F. R. Pomilla and S. N. Milford 1966 Astrophys. J. $\underline{144}$, 1174.

D. Pretzer, B. Van Zyl and R. Geballe 1964 Atomic Collision. Processes (Academic Press) p. 618.

E. M. Purcell and G. B. Field 1956 Astrophys. J. $\underline{124}$, 542.

D. Rapp 1963 J. Geophys. Res. $\underline{68}$, 1773.

M. J. Seaton 1955 Proc. Phys. Soc. $\underline{A68}$, 457.

M. J. Seaton 1962 Atomic and Molecular Processes (Academic Press) p. 374.

F. J. Smith 1963 Planet. Spac. Sci. $\underline{11}$, 126.

F. J. Smith 1966a Planet. Spac. Sci. in press.

F. J. Smith 1966b Planet. Spac. Sci. in press.

P. M. Solomon 1964 Astrophys. J. $\underline{139}$, 999.

L. Spitzer 1956 Physics of fully ionized gases (Interscience).

REFERENCES
(Continued)

W. L. Starr and T. M. Shaw 1966 J. Chem. Phys. $\underline{44}$, 4181.

T. P. Stecher and D. A. Williams 1966 in press.

R. F. Stebbings, R. A. Young, C. L. Oxley and H. Ehrhardt 1965 Phys. Rev. $\underline{138}$, A1312.

K. Takayanagi and S. Nishimura 1960 Publ. Astron. Soc. Japan $\underline{12}$, 77.

P. Thaddeus and J. F. Clauser 1966 Phys. Rev. Letts. $\underline{16}$, 819.

L. Wilets and D. F. Gallaher 1966 Phys. Rev. $\underline{147}$, 13.

## 2. Collision Processes in Planetary Atmospheres

The interpretation of phenomena occurring in the atmospheres of
the planets requires a knowledge of the rates of a large variety of
atomic collision processes. In this summary, we select some of the
more significant problems posed by our present understanding of the
atmospheres of the planets Earth and Mars.

Substantial progress has been made during the last decade in the
laboratory determination of the rates of the thermal chemical reactions
which determine the structure of the atmosphere and ionosphere of the
planet Earth and comprehensive reviews have appeared of the laboratory
measurements of reactions involving oxygen and nitrogen (Schiff 1964)
and involving hydrogen (Kaufman 1964). Most of the measurements refer
to a narrow temperature region about room temperature and efforts to
extend the temperature range to that occurring in the atmosphere (150°K -
3000°K) are necessary. The role of metastable species in affecting the
chemistry of the atmosphere has not been seriously explored yet, largely
because there are few measurements of reactions in which the states of
the reacting species are identified.

Hunt (1966) has recently extended the original work of Bates and
Nicolet (1950) on the photochemistry of an oxygen-hydrogen atmosphere
and he has investigated in detail the diurnal variation of the ozone
concentration. Hunt's papers include a list of reaction rates. Of
special interest is his demonstration that the metastable ^{1}D atom of

oxygen may play a significant role, despite its low concentrations. Its importance appears to stem from the reaction

$$O(^1D) + H_2O \rightarrow OH + OH$$
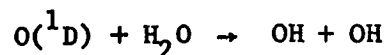
which leads to a source of free hydrogen atoms in the stratosphere. A major uncertainty in the calculation is the efficiency of deactivation of the metastable $O(^1D)$ atoms. The ^1D level is the upper level of the red line of atomic oxygen, the emission of which has been observed in the night and day airglows. The observed dayglow intensities are unexpectedly weak, since there are several large sources of $O(^1D)$ atoms such as photodissociation in the Schumann-Runge continuum of molecular oxygen, recombination of positive ions O_2^+ (but probably not NO^+ (Dalgarno and Walker 1964)) and collisional excitation by the impact of non-thermal photoelectrons. The dayglow intensities apparently require a rate coefficient of 7×10^{-11} cm^3 sec^{-1} for deactivation by collisions with the major constituent N_2:

$$O(^1D) + N_2 \rightarrow O(^3P) + N_2. \tag{1}$$
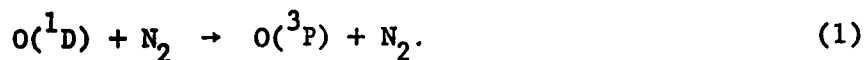
The reaction scheme used by Hunt, with which he is able to reproduce the measured ozone profile, is based on a rate for (1) smaller by about two orders of magnitude.

The presence of $O(^1D)$ atoms in the atmosphere may have important consequences on the nitrogen oxide chemistry also, but the rates of the possible reactions of $O(^1D)$ atoms with the various nitrogen oxides (which are largely unknown) are necessary before a realistic analysis can be carried out.

The metastable species of molecular oxygen may also affect the hydrogen - oxygen chemistry and the nitrogen oxides chemistry. O_2 molecules in the $^1\Delta_g$ state are produced by a number of processes, the most abundant of which may be photodissociation in the Hartley continuum of ozone. The metastable molecules have been detected in the twilight and day airglow (Gattinger and Vallance Jones 1966). The production and loss mechanisms have been studied by Gattinger and Vallance Jones (1966) and by Schiff and Megill (1964), who draw attention to the possible effect of the reaction

$$O_2(^1\Delta_g) + O_3 \rightarrow O_2 + O_2 + O$$
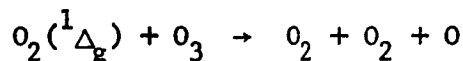
on the ozone chemistry. Hunt (1966) has presented a list of some of the reactions involving $O_2(^1\Delta_g)$ and $O_2(^1\Sigma_g^+)$ but the identification of the important reactions is tentative and the rate coefficients are very uncertain. Recent laboratory work on $O_2(^1\Delta_g)$ has been reported by Badger, Wright and Whitlock (1965).

The twilight emission of the 0-1 O_2 band of the $^1\Delta_g - 3\Sigma_g^-$ system is much weaker than predicted and the theory does not explain the seasonal, annual or evening-morning variations (Gattinger and Vallance Jones 1966).

The chemistry of the metastable $^1\Delta_g$ states of O_2 requires clarification in connection with a suggestion by Megill and Hasted (1965) that the detachment reaction

$$O_2(^1\Delta_g) + O_2 \rightarrow O_2 + O_2 + e$$
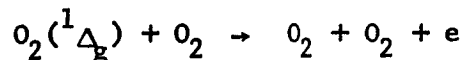
may be significant in the D-region during a polar cap absorption event and possibly also in the undisturbed D-region.

Associative detachment

$$O + O_2^- \rightarrow O_3 + e$$

may also be significant. The early theoretical suggestion that the rate coefficients may be as high as 10^{-10} cm^3 sec^{-1} has been confirmed by laboratory measurements of Ferguson, Fehsenfeld and Schmeltekopf (1966) who find that many associative detachment processes proceed with rates of about 10^{-10} cm^3 sec^{-1}.

Analysis of D-region phenomena suggest that in practice detachment does not occur rapidly and it appears necessary to transform O_2^- into a different negative ion which cannot participate in an apparent associative detachment process. A partial list of the relevant chemical reactions can be obtained from papers by Dalgarno (1961), Whitten and Popoff (1962) and Branscomb (1964).

It is now established that nitric oxide is an important constituent of the upper atmosphere, its ionization by solar Lyman-alpha being the principal source of electrons in the quiet upper D-region. Barth (1966) has detected NO by its fluorescence in the dayglow and he has determined a total abundance of 1.1×10^{14} cm^{-2} below 85 km. The production of NO has been studied most recently by Nicolet (1965) and by Wagner (1966) who give a list of the reactions involved in the nitrogen oxides chemistry

65

together with estimates of the rate coefficients. Further laboratory study of the reaction

$$N + O_2 \rightarrow NO + O$$

would be valuable. It is sensitive to temperature and the conventional method of extrapolating the data to higher and lower temperatures may be misleading. Another source of NO is provided by the ionic reaction

$$O_2^+ + N_2 \rightarrow NO^+ + NO. \tag{2}$$

Upper limits to its rate coefficient have been derived from laboratory measurements (Galli, Giardini-Guidoni and Volpi 1963, Ferguson, Fehsenfeld, Golden and Schmeltekopf 1965) but its actual value at D-region temperatures is unknown. Reaction (2) is also an important reaction in the chemistry of the ionic species, a subject which has been discussed most recently by Donahue (1966) who gives an extensive list of the chemical reactions affecting the major ions O^+, O_2^+, N_2^+ and NO^+. Most of the relevant rate coefficients have been measured and reported in a series of papers, summarized by Ferguson _et al_. (1965) and Golden _et al_.(1966) but usually only at room temperature. There is reasonable agreement between the theoretical and observed ion concentrations above 90 km (cf. Donahue 1966) but the position below 90 km is obscure. According to Donahue (1966), it is difficult to reconcile the reaction scheme selected for the E and F regions with the large O_2^+ concentrations detected in the D-region by Narcisi and Bailey (1965). It may be noted that the metastable O_2^+ (4π), which is produced in the atmosphere, (Dalgarno and

66

McElroy 1965), has been omitted from consideration. Little is known of the reactions responsible for the removal; they have been discussed briefly by Hunter and McElroy (1966) who have given a valuable, general review of deactivation processes in the atmosphere (see also Young and Black 1966). Reactions involving the metastable $O^+(^2D)$ ion may also affect the ionic chemistry (Dalgarno and McElroy 1966).

A number of problems involving the identification of the reactions responsible are posed by the mass spectrometer measurements of Narcisi and Bailey (1965) (see also Narcisi 1966) who discovered that complex ions, consisting possibly of water vapor clusters, are the dominant ionic species in the lower D-region.

However, the most serious difficulty in interpreting ion composition in the ionosphere is probably that presented by the observed high abundance of positive helium ions in the topside ionosphere. The rate coefficients measured for

$$He^+ + N_2 \rightarrow He + N_2^+ \quad (or \ N + N^+)$$
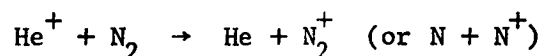
(cf. Ferguson et al. 1965, Fehsenfeld et al. 1966) is apparently much too large (cf. Bauer 1966). Either there is an abundant source of He^+ as yet unrecognized or the measured rate coefficient is not applicable in ionospheric conditions. Stebbings et al. (1965) has suggested that the degree of vibrational excitation may be relevant, but further study is necessary. The process is also of interest in connection with the

escape of neutral helium from the atmosphere and with the production at high altitudes of N_2^+ and N^+ ions.

The degree of vibrational excitation of the atmospheric molecules merits further study especially since Ferguson, Fehsenfeld and Schmeltekopf (1966) have recently demonstrated in the laboratory that the rate of

$$O^+ + N_2 \rightarrow NO^+ + N$$

increases rapidly with increasing vibrational temperature. This may be the explanation of the decrease in electron density in the vicinity of red arcs and during disturbed conditions. The vibrationally excited molecules can be produced by electron impact and possibly by the $O(^1D)$ deactivation process (1).

It has been suggested (Potter and Del Duca 1960) that vibrational excitation may be the energy source for excitation of the Na D lines according to

$$Na + N_2^* \rightarrow Na(^2P) + N_2$$
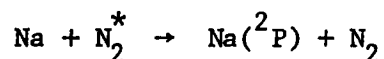
and Hunter (1965) has obtained evidence that this reaction occurs in low altitude aurora. Recent laboratory work is described by Starr and Shaw (1966).

Experimental studies of vibrational excitation and de-excitation processes and of the effect of vibrational excitation on reaction rates would be of value. Bates (1955) has argued that the atom - atom interchange process

$$O + O_2^* \rightarrow O_2 + O$$

may be an efficient mechanism for deactivating O_2^*. If it is not, a substantial population of O_2^* will occur in the atmosphere through production processes such as fluorescence in the discrete Schumann-Runge system. Apart from its effects on the atmospheric chemistry, O_2^* can be ionized by solar radiation at longer wavelengths and the absorption of Lyman-alpha may be modified by its presence.

All of the reactions discussed so far are thermal collision processes. The non-thermal heavy particle collision processes which are of interest involve fast protons and the hydrogen atoms which result from electron capture by the protons in collisions with the atmospheric particles. The atmosphere is bombarded by protons during many auroras and in particular during polar cap auroras. Little information is available on the cross sections for the various possible processes beyond that given in Chamberlain's book (Chamberlain 1961), which discusses in detail the collision processes which occur (see also Prag, Morse and McNeal 1966).

The position is similar in the case of electron impact. Electron impact excitation and ionization studies have a new importance since photoelectrons contribute substantially to excitation of the dayglow, the successful observation of which (cf. Wallace and McElroy 1966) provides a valuable additional means of investigating atmospheric properties.

Electron collision processes determine also the electron and ion temperatures in the ionosphere. Most of the important processes are known to sufficient accuracy (cf. Dalgarno, McElroy and Walker 1966) with the exception of vibrational and rotational excitation of molecular oxygen. Recent work on the cooling of electrons colliding with O_2 is described in papers by Geltman and Takayanagi (1966), Mentzoni and Rao (1965), and Sampson and Mjolness (1966).

The success of the Mariner IV occultation experiment (Kliore et al. 1965) presents a number of problems of interpretation. The rates of reactions involving CO_2 and its dissociation and ionization products are vital to a proper understanding of the structure of the Martian atmosphere. The ambient temperature may be very low and it is desirable to attempt measurements down to temperatures as low as $50^\circ K$. The reaction

$$O^+ + CO_2 \rightarrow O_2^+ + CO$$
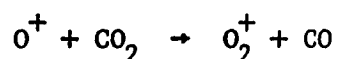
is important for the Martian ionosphere. Its rate coefficient has been measured at room temperature (Fehsenfled, Ferguson and Schmeltekof 1966, Paulson, Mosher and Dale 1966), but not at $80^\circ K$, the temperature suggested by Johnson (1965) and by Fjeldbo, Fjeldbo and Eshleman (1966) as appropriate to the atmosphere at 120 km. Chamberlain and McElroy (1966) argue that such low temperatures do not occur. Their argument rests on the assumption that CO_2^+ recombines rapidly with electrons and a measurement of the rate of dissociative recombination of CO_2^+ together with an identification of its end products is needed.

In discussing radiation losses, Chamberlain and McElroy (1966) assume that the rate coefficient for vibrational deactivation of CO_2 varies with temperature T as exp $(-82.8T^{-1/3})$. The formula reproduces the high temperature data adequately but it is uncertain whether or not it remains appropriate over the possible range of Martian temperatures.

Because of the low densities prevailing in the Martian atmosphere, two-body collision processes assume a greater importance than in the terrestrial atmosphere, and radiative association, about which little quantitative information is available, may be the major recombination mechanism.

Of the other planets, there has been some discussion of the upper atmospheres of Venus (cf. Shimizu 1963) and of Jupiter (cf. Gross and Rasool 1964). Reactions involving the dissociation and ionization products of CO_2 and N_2 are significant for Venus and of H_2 and He for Jupiter. Of particular relevance to a prediction of the composition of the ionosphere on Jupiter are the rates of the reactions

$$He^+ + H_2 \rightarrow HeH^+ + H$$
$$\rightarrow He + H_2^+$$
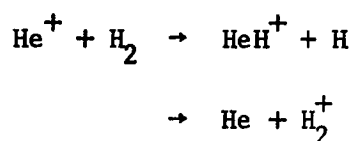
which, though slow (Fehsenfeld et al. 1966), are probably responsible for the removal of He^+ ions.

REFERENCES

R. M. Badger, A. C. Wright and R. F. Whitlock 1965 J. Chem. Phys. 43, 4345.

C. Barth 1966 Annales de Geophys. 22, 198.

D. R. Bates 1955 J. Atmos. Terr. Phys. 6, 171.

S. Bauer 1966 Annales de Geophys. 22, 247.

L. M. Branscomb 1964 Annales de Geophys. 20, 49.

J. W. Chamberlain 1961 Physics of the Aurora and Airglow (Academic Press).

J. W. Chamberlain and M. B. McElroy 1966 and Science 152, 21.

A. Dalgarno 1961 Annales de Geophys. 17, 16.

A. Dalgarno and M. B. McElroy 1965 Planet. Spa. Sci. 13, 947.

A. Dalgarno and M. B. McElroy 1966 Planet. Spa. Sci. (in press).

A. Dalgarno and M. B. McElroy and J. C. G. Walker 1966 Planet. Spac. Sci. (in press).

A. Dalgarno and J. C. G. Walker 1964 J. Atmos. Sci. 21, 463.

T. M. Donahue 1966 Planet. Spa. Sci. 14, 33 and J. Geophys. Res. 71, in press.

F. C. Fehsenfeld, E. E. Ferguson and A. L. Schmeltekopf 1966 J. Chem. Phys. 44, 3022.

F. C. Fehsenfeld, A. L. Schmeltekopf, P. D. Goldan, H. I. Schiff and E. E. Ferguson 1966 J. Chem. Phys. 44, 4087.

E. E. Ferguson, F. C. Fehsenfeld, P. D. Goldan and A. L. Schmeltekopf 1965 J. Geophys. Res. 70, 4323.

E. E. Ferguson, F. C. Fehsenfeld and A. L. Schmeltekopf 1966 private communication.

G. Fjeldbo, W. C. Fjeldbo and V. R. Eshleman 1966 J. Geophys. Res. 71, 2307.

A. Galli, A. Giardini - Guidoni and G. G. Volpi 1963 J. Chem. Phys. 38, 518.

R. L. Gattinger and A. Vallance Jones 1966 Planet. Spa. Sci. 14, 1.

S. Geltman and K. Takayanagi 1966 Phys. Rev. 143, 25.

P. D. Goldan, A. L. Schmeltekopf, F. C. Fehsenfeld, H. I. Schiff and E. E. Ferguson 1966 J. Chem. Phys. 44, 4095.

REFERENCES

(Continued)

S. H. Gross and S. I. Rasool 1964 Icarus 3, 311.

B. G. Hunt 1966 J. Geophys. Res. 71, 1385.

D. M. Hunten 1965 J. Atmos. Terr. Phys. 27, 503.

D. M. Hunten and M. B. McElroy 1966 Revs. Geophys. (in press).

F. S. Johnson 1965 Science 150, 1445.

F. Kaufman 1964 Annales de Geophys. 20, 106.

A. Kliore, D. L. Cain, G. S. Levy, V. R. Eshleman and G. Fjeldbo
1965 Science 149, 1243.

L. R. Megill and J. B. Hasted 1965 Planet. Spa. Sci. 13, 339.

M. H. Mentzoni and R. V. N. Rao 1965 Phys. Rev. Letts. 14, 779.

R. S. Narcis   1966 Annales de Geophys. 22, 224.

R. S. Narcis   and A. D. Bailey 1965 J. Geophys. Res. 70, 3687.

M. Nicolet 1965 J. Geophys. Res. 70, 679 and 691.

J. F. Paulson, R. L. Mosher and F. Dale 1966 J. Chem. Phys. 44, 3025.

A. E. Potter and B. S. Del Duca 1960 J. Geophys. Res. 65, 3915.

A. B. Prag, F. A. Morse and R. J. McNeal 1966 J. Geophys. Res. 71, 3141.

D. H. Sampson and R. C. Mjolness 1966 Phys. Rev. 144, 116.

H. I. Schiff 1964 Annales de Geophys. 20, 115.

H. I. Schiff and R. L. Megill 1964 J. Geophys. Res. 69, 5120.

M. Shimizu 1963 Planet. Spa. Sci. 11, 269.

W. L. Starr and T. M. Shaw 1966 J. Chem. Phys. 44, 4181.

R. F. Stebbings, J. A. Rutherford and B. R. Turner 1965 Planet. Spa. Sci.
13, 1125

L. Wallace and M. B. McElroy 1966 Planet. Spa. Sci. (in press).

REFERENCES

(Continued)

Chr. - Uhr. Wagner 1966 J. Atmos. Terr. Phys. $\underline{28}$, 607.

R. C. Whitten and I. G. Popoff 1962 J. Atmos. Sci. $\underline{21}$, 1.7.

R. A. Young and G. Black 1966 J. Chem. Phys. $\underline{44}$, 3741.

3. Ion Temperatures in the Topside Ionosphere

Analysis of backscatter observations (cf. Evans, 1965) has established that the positive ion temperature in the ionosphere exceeds the neutral particle temperature at altitudes above 300 km during the daytime and the results are in general accord with theoretical predictions which assume that the ions are heated by collisions with the hot ambient electrons and cooled by collisions with the neutral particles (Hanson 1963, Dalgarno 1963, Dalgarno, McElroy and Walker 1966). Since the efficiency of the heating and cooling mechanisms depends upon the ionic species involved, the different positive ions may have different temperatures.

We adopt the electron temperature and neutral particle distribution appropriate to noon in April 1963 (Dalgarno, McElroy and Walker, 1966), and use the ion distributions of Johnson (1966). The distributions are listed in Table 9.

The ions X^+ are heated by the electrons at the rates

$$Q(e,X^+) = \frac{8 \times 10^{-6} \, n_e \, n(X^+) \left\{ T_e - T(X^+) \right\}}{m(X^+) \, T_e^{3/2}} \quad \text{eV cm}^{-3} \text{ sec}^{-1} \quad (1)$$

where $m(X^+)$ is the mass of X^+ in units of the proton mass, $T(X^+)$ and $n(X^+)$ are the temperature and density of X^+ and T_e and n_e are the electron temperature and density (cf. Spitzer, 1956). Expressions for the cooling of O^+, He^+ and H^+ by ordinary elastic collisions with the neutral constituents have been given by Brace, Spencer and

TABLE 9
ALTITUDE DEPENDENCE OF DENSITY AND TEMPERATURE

Altitude km	T_n °K	n(O) cm^{-3}	n(He) cm^{-3}	n(H) cm^{-3}	n(O$^+$) cm^{-3}	n(He$^+$) cm^{-3}	n(H$^+$) cm^{-3}	n_e cm^{-3}	T_e °K
300	917	4.7(8)*	6.8(6)	6.8(4)	3.2(5)	1.0(2)	5.0(2)	3.2(5)	2617
400	917	7.2(7)	4.3(6)	6.1(4)	1.6(5)	4.5(2)	1.3(3)	1.6(5)	2617
500	917	1.2(7)	2.7(6)	5.4(4)	8.4(4)	6.5(2)	1.8(3)	8.6(4)	2617
600	917	2.1(6)	1.8(6)	4.9(4)	4.8(4)	7.0(2)	2.0(3)	5.1(4)	2617
700	917	3.7(5)	1.1(6)	4.4(4)	2.7(4)	7.0(2)	2.7(3)	3.0(4)	2617
800	917	7.0(4)	7.6(5)	3.9(4)	1.6(4)	7.5(2)	3.5(3)	2.0(4)	2617
900	917	1.4(4)	5.0(5)	3.5(4)	1.0(4)	8.5(2)	6.1(3)	1.7(4)	2617
1000	917	2.8(3)	3.4(5)	3.2(4)	4.0(3)	9.5(2)	7.0(3)	1.2(4)	2617

* $4.7(8) \equiv 4.7 \times 10^8$

Dalgarno (1965). Additional cooling occurs through resonance charge transfer processes

$$X^+ + X \rightarrow X + X^+$$

If we assume that resonance charge transfer merely transfers an electron without altering the velocity vectors, the cooling rates of O^+, He^+ and H^+ are given approximately by

$$L_n(O^+) = n(O^+) \left\{ 18 \times 10^{-14} \, n(O) + 6 \times 10^{-15} \, n(He) \right.$$
$$\left. + 2 \times 10^{-15} \, n(H) \right\} \left\{ T(O^+) - T_n \right\} \text{ eV cm}^{-3} \text{ sec}^{-1}$$

$$L_n(He^+) = n(He^+) \left\{ 6 \times 10^{-14} \, n(O) + 4 \times 10^{-13} \, n(He) \right.$$
$$\left. + 1 \times 10^{-14} \, n(H) \right\} \left\{ T(He^+) - T_n \right\} \text{ eV cm}^{-3} \text{ sec}^{-1} \qquad (2)$$

$$L_n(H^+) = n(H^+) \left\{ 3 \times 10^{-14} \, n(O) + 5 \times 10^{-14} \, n(He) \right.$$
$$\left. + 8 \times 10^{-13} \, n(H) \right\} \left\{ T(H^+) - T_n \right\} \text{ eV cm}^{-3} \text{ sec}^{-1}$$
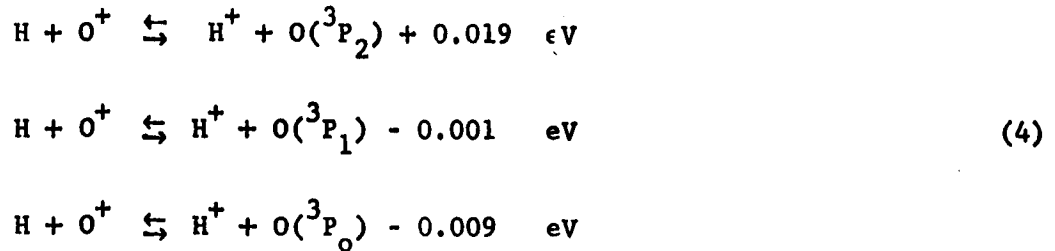
where $n(X)$ is the number density of X and T_n is the neutral particle temperature.

Substantial differences between the ion temperatures result from equating (1) and (2). However, because of the long-range Coulomb interaction, the ion temperatures are closely coupled to each other. The rate at which ions X^+ lose energy to ions Y^+ is given by Spitzer (1956) as

$$Q(X^+,Y^+) = 3.3 \times 10^{-4} \, n(X^+) \, n(Y^+) \left\{ T(X^+) - T(Y^+) \right\} \frac{1}{m(X^+) \, m(Y^+)}$$
$$\times \left\{ \frac{T(X^+)}{m(X^+)} + \frac{T(Y^+)}{m(Y^+)} \right\}^{-3/2} \text{ eV cm}^{-3} \text{ sec}^{-1} \qquad (3)$$

assuming that the ions have Maxwellian velocity distributions characterized by temperatures $T(X^+)$ and $T(Y^+)$.

Consideration must also be given to the role of the near-resonance reactions

$$H + O^+ \leftrightarrows H^+ + O(^3P_2) + 0.019 \quad eV$$

$$H + O^+ \leftrightarrows H^+ + O(^3P_1) - 0.001 \quad eV \tag{4}$$

$$H + O^+ \leftrightarrows H^+ + O(^3P_0) - 0.009 \quad eV$$

in which one ion is transformed into another. The reactions appear to behave like symmetrical resonance charge transfer processes (Rapp 1963). Thus, the cross sections vary only slowly with energy so that the reactions which remove ions do not significantly affect the ion temperature.

The fraction of O^+ ions in the ionosphere which are produced by (4) is negligible and so accordingly is the heat source, but (4) is an important source of H^+ ions. The initial temperature of the protons produced by (4) is given by

$$T'(H^+) = \frac{m(H) \; m(O) + m(O^+) \; m(H^+)}{\left\{ m(H) + m(O^+) \right\}^2} T(O^+) + \frac{m(H) \; m(H^+) + m(O^+) \; m(O)}{\left\{ m(H) + m(O^+) \right\}^2} T(H)$$

$$+ \frac{2m(O) \; \varepsilon}{3k \left\{ m(H^+) + m(O) \right\}}$$

where ε is the energy defect and k is Boltzmann's constant (Burgers, 1961). Substituting approximate values of the parameters yields an initial temperature $T'(H^+)$ between $1200^\circ K$ and $900^\circ K$, only slightly above the neutral particle temperature. The H^+ temperature obtained when (4) is ignored is about $1600^\circ K$ so that (4) is a source of cold protons which are heated mainly by collisions with the ambient thermal

78

proton gas. Adopting the rate coefficient 4×10^{-10} cm^3 sec^{-1} for

(4) (Hanson, Patterson and Degaonkar, 1963), it is clear that the

heat loss associated with (4) is negligible compared to $L_n(H^+)$.

Equating the heating and cooling rates of the ions, O^+, He^+

and H^+ leads to a set of coupled equations for the ion temperatures

which may be solved iteratively. The resulting ion temperature pro-

files are illustrated in Figure 4. Because of the high efficiency of

energy exchange in ion-ion collisions, the $H^+ - O^+$ temperature dif-

ference does not exceed $200^{\circ}K$, and the $He^+ - O^+$ temperature difference

does not exceed $20^{\circ}K$. In most circumstances it will suffice to charac-

terize the ionic distribution by a single ion temperature.

The flow of heat from electrons to neutrals at 700 km is shown in

Figure 5. At this altitude the H^+ and O^+ ions are of approximately

equal importance. At lower altitudes the heat flows principally to O^+

and then to O, and H^+ loses most of its heat to O^+. At higher alti-

tudes heat flows principally to H^+ and then to H and He, and O^+

receives most of its heat from H^+. The role of He^+ is negligible at
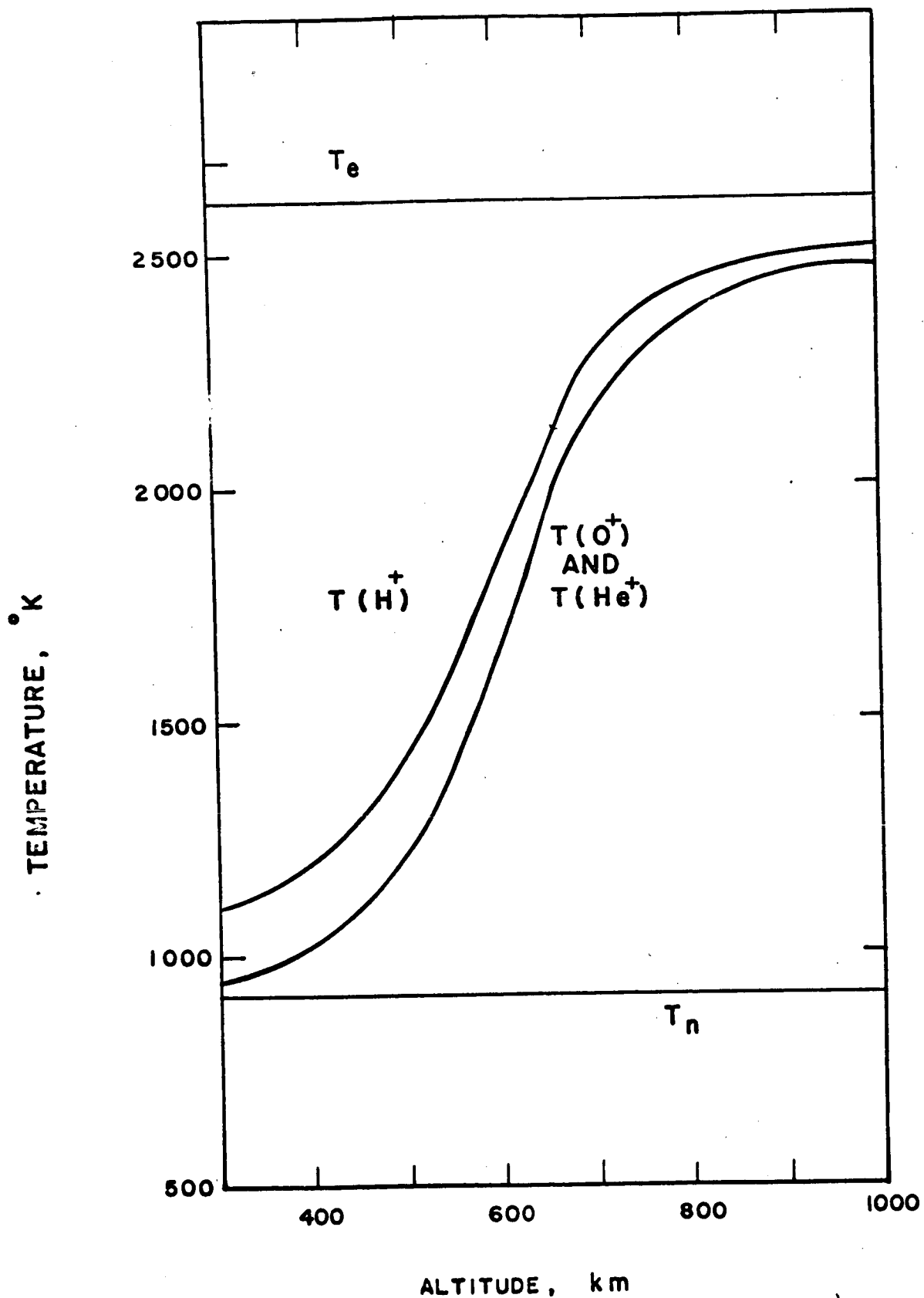
all altitudes.

Figure 4. Electron temperature, T_e, ion temperatures, $T(X^+)$ and neutral temperature, T_n, as a function of altitude.
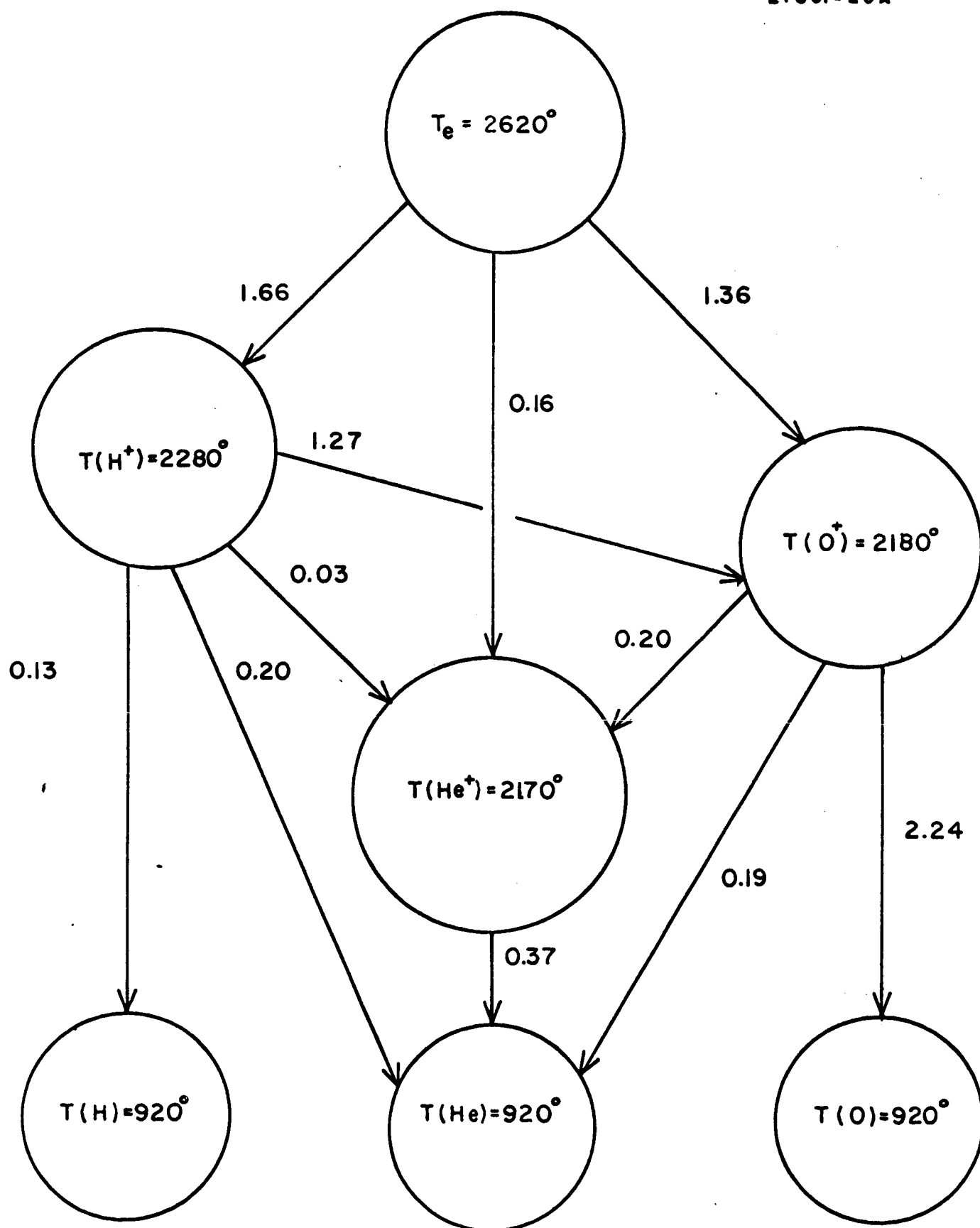
80

Figure 5. Flow of heat from electrons to neutrals at 700 km. The units are eV cm^{-3} sec^{-1}.

REFERENCES

Brace, L. H., Spencer, N. W. and Dalgarno, A., Planet Space Sci. $\underline{13}$, 647 (1965).

Burgers, J. M., in <u>Physical Chemistry in Aerodynamics and Space Flight</u> (Editors, A. L. Myerson and A. C. Harrison), p. 4. Pergamon Press, New York (1961).

Dalgarno, A., GCA Technical Report No. 63-11-N, GCA Corporation, Bedford, Mass. (1963).

Dalgarno, A., McElroy, M. B. and Walker, J.C.G. (1966). (in press)

Evans, J. V., Planet Space Sci. $\underline{13}$, 1031 (1965).

Hanson, W. B., Space Research $\underline{3}$, 282 (1963).

Hanson, W. B., Patterson, T.N.L., and Degaonkar, S. S., J. Geophys. Res. $\underline{68}$, 62-3 (1963).

Johnson, C. Y., J. Geophys. Res. $\underline{71}$, 330 (1966).

Rapp, D., J. Geophys. Res. $\underline{68}$, 1773 (1963).

Spitzer, L., <u>Physics of Fully Ionized Gases</u>. Interscience Publishers, Inc., New York (1956).

C. EXPERIMENTAL INVESTIGATIONS IN THE VUV AND EUV SPECTRAL REGIONS

During this quarter, the VUV and EUV laboratory effort has been directed toward two scientific areas:

1. The determination of photoionization cross sections of atomic hydrogen in the spectral region 912 to 300 Å.

2. Laboratory investigations on determining the electron energy spectrum due to the EUV and VUV photoionization of planetary gases.

1. Photoionization Cross Sections of H for $\lambda\lambda$ 912 to 500 Å

During this reporting period, the photoionization cross section measurements of H for $\lambda\lambda$ 912 to 500 Å have been completed. The data has been reduced, analyzed and interpreted. The details are available in a forth coming publication, so that only a brief technical summary is given below.

The photoionization cross section of H has been calculated[1-7] as a function of wavelength, λ, but laboratory measurements have been performed only at one wavelength, 850.6Å.[8-9] The present work is concerned with the first measurements on the cross sections as a function of wavelength throughout the spectral region 912 to 800Å.

The difficulties encountered in producing a sufficient amount of H and on quantitatively measuring the H-content have been discussed in previous quarterly reports. It was shown that this aspect of the

problem can be largely by-passed by employing a technique developed in
this laboratory which normalizes the photoionization cross section of H
at a single wavelength with the known cross section values of H_2 in
such a manner as to extract the σ-values for H at those wavelengths
where σ-values for H_2 are available. However, a practical limitation
of this technique is that its application is restricted to cases in which
the H_2 and H sample gases must be in their respective $1\Sigma_g^+$ and $1^2S_{1/2}$
(ground) states.

Under the conditions cited, it can be shown that the follow-
ing equation applies:

$$\sigma_{(H,\lambda)} = \frac{\ell n \dfrac{I_{(\lambda)}}{I'_{(\lambda)}}}{\ell n \dfrac{I_{(850.6)}}{I'_{(850.6)}}} \left[\sigma_{(H,850.6)} - \frac{1}{2} \sigma_{(H_2,850.6)} \right] + \frac{1}{2} \sigma_{(H_2,\lambda)}. \tag{1}$$

All quantities on the right-hand side can be measured and hence, $\sigma(H,\lambda)$,
the photoionization cross section for H, can be experimentally determined.
It is the application of this new formulation which has made it possible
to obtain the present $\sigma(H,\lambda)$-values.

The experimental apparatus employed is shown in Figure 6 .
Molecular hydrogen, 99.5 percent pure, was introduced directly into the
system through a flow meter and a needle valve. Hydroged atoms were
produced in an electrodeless microwave discharge maintained in a 1.0 cm id
Vycor tube using a Burdick Model MW-1 100W Mc/sec diathermy unit and an

84

MONOCHROMATIC RADIATION

MICROWAVE CAVITY

FLOW METER

He

H₂

Aℓ DETECTOR
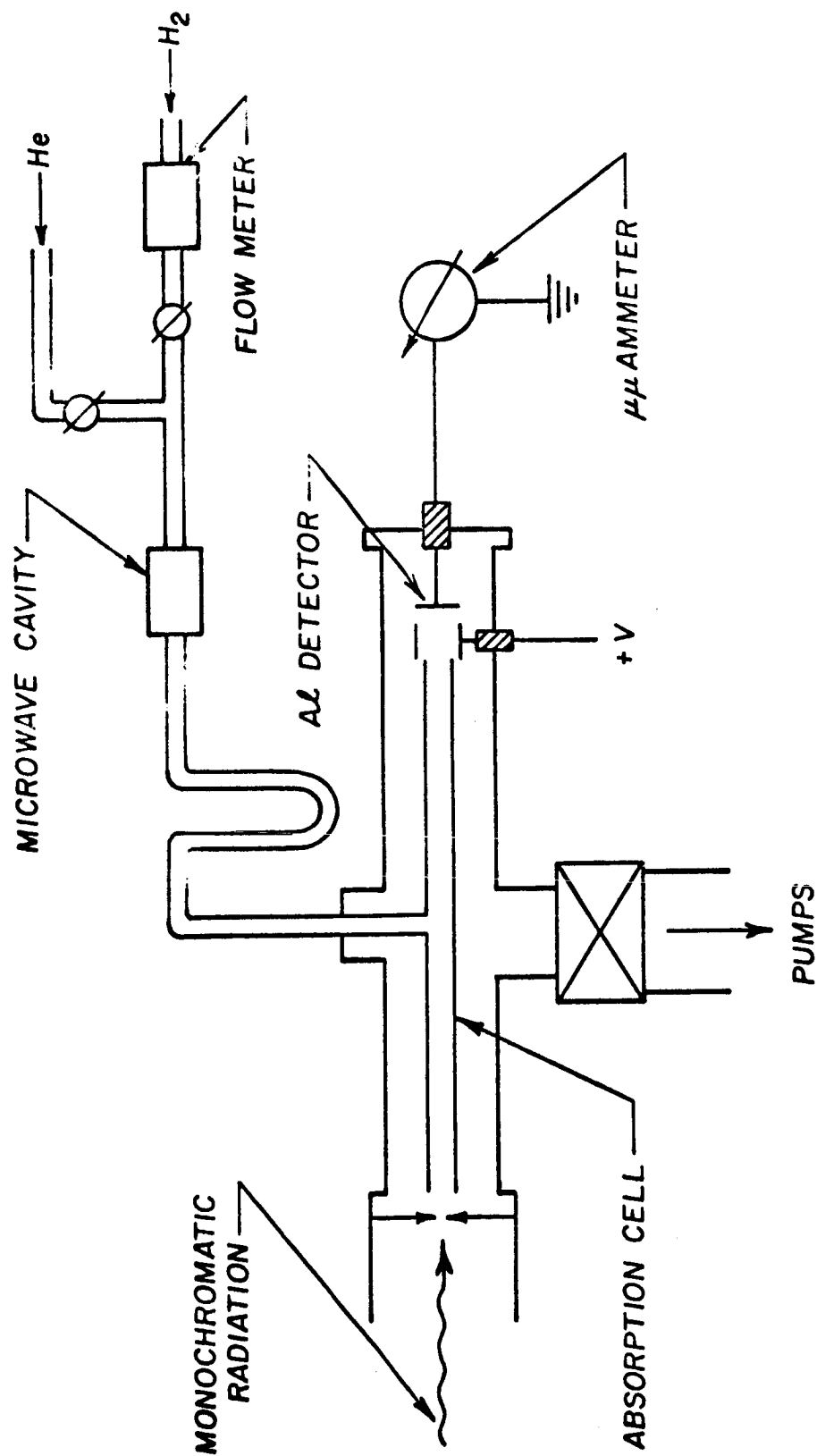
μμ AMMETER

+ V

ABSORPTION CELL

PUMPS

Figure 6. Schematic diagram of absorption cell, photon detector and gas inlet system.

"Evenson" cavity manufactured by the Ophthos Instrument Company. The discharge was cooled nearly to room temperature by a flow of cold air. The products of the gas discharge passed through a U bend and a 78.5 cm long 1.5 cm id Pyrex absorption cell before being pumped from the system. The absorption cell was mounted such that one end was about 0.5 cm from the exit slit of a McPherson 1/2-m Seya monochromator. A monochromatic photon beam (wavelength bandpass 3.5 $\overset{o}{A}$) passed axially through the cell and was detected using an aluminum photoelectric detector. The photoelectric current from the detector was measured with a Keithley Model 417 picoammeter. The radiation sources were a high voltage repetitive condensed spark discharge in argon and a hydrogen dc discharge. Both sources produced a many lined spectrum. The pressure in the entire system when evacuated was less than 5×10^{-5} torr. There was no detectable change i in the flow rate of the gas entering the system when the discharge was switched on, a change of 0.5 percent would have been observed.

During the performance of the experiment, it became evident that excited species to the ground state H and H_2 were present. To ascertain the error in the absorption cross section measurements due to these species, subsidiary experiments were performed. These consisted of measuring the photoionization current and searching for appropriate signature ionization thresholds for excited species. The observed magnitude of photoionization currents was sufficiently small to eliminate the possibility of a large number of electrically excited metastable states. It became obvious, however, that there were considerable numbers of vibrational excited molecules which virtually precluded accurate

86

measurements at wavelengths shorter than about 800 $\overset{\circ}{A}$. In brief, then, these subsidiary experiments indicated that the present technique was capable of measuring absolute cross sections from threshold to at least 850 $\overset{\circ}{A}$ and probably down to 800 $\overset{\circ}{A}$.

The final data is shown in Figure 7. The various displays are due to the fact that measurements were taken over the range from above threshold to 800 $\overset{\circ}{A}$ with a variety of gas mixtures and pressures. The mixtures ranged from 100 percent H_2 to 90 percent H + 10 percent H_2. The various pressures investigated were adjusted to yield photoionization currents which could be reliably measured. In any case, comparison of these data with theory (solid curve in Figure 7) indicate that excellent agreement exists for $\lambda\lambda$ from threshold to about 840 $\overset{\circ}{A}$. At shorter wavelength the agreement becomes less satisfactory due to the presence of the vibrational excited molecules.

This material has been prepared as a paper submitted for publication in Physical Reviews.

2. **Laboratory Studies on the Electron Energy Spectrum Due to EUV and VUV Photoionization of Planetary Gases**

During this quarter, considerable progress has been achieved in the experimental determination of the electron energy spectrum due to EUV and VUV photoionization of several planetary gases, including O_2, N_2, CO and CO_2. A rather detailed discussion of the techniques employed are included here since this is a continuing task so that it is desirable to set up continuity for future reports on this phase of the program.
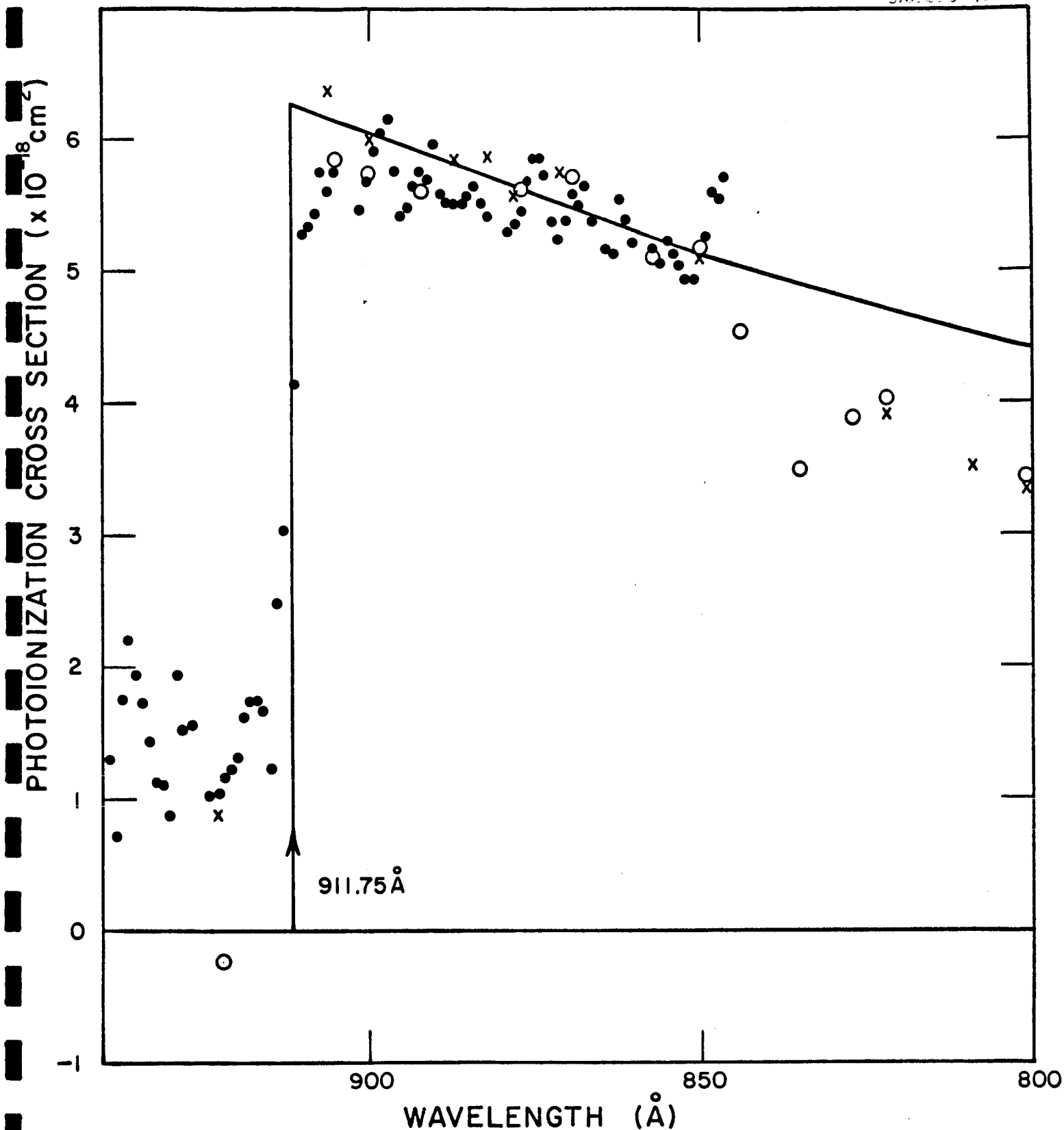
Figure 7. The photoionization cross section of atomic hydrogen calculated using Equation (5). The symbols ●, X and O denote three sets of data, the first two of which were obtained with H_2 alone flowing into the system. The third set (O) was calculated from data obtained with a H_2-He mixture flowing into the system. The percentage experimental error at wavelengths longer than the ionization threshold, 912Å, was large since, in this region, there was little change in absorption when the gas was discharged. In the region 912 to 850Å, the estimated experimental error was $\pm$ 10 percent. The solid line represents the theoretical cross section.

When radiation of a given wavelength is absorbed by a gas, the residual molecules are left in particular states of excitation. The probability of a molecule being excited to a given state j is denoted by the specific cross section for the process σ_j. The total absorption cross section σ is, therefore,

$$\sigma = \sum_j \sigma_j \tag{1}$$

If the radiation is sufficiently energetic, there is a finite probability that some of the molecules will be ionized and left in various degrees of excitation. That is, in Equation (1), some of the σ_j may refer to the cross sections for the production if ions while others simply refer to the excitation of neutral molecules. Let σ_e refer to the total absorption cross section for simple excitation of neutral molecules and let the σ_j refer to the specific cross sections for ionization, thus Equation (1) becomes

$$\sigma = \sigma_e + \sum_j \sigma_j. \tag{2}$$

In the following we are interested in determining the probability that the absorbed radiation will leave a molecular ion in a specific state of excitation. That is, we are interested in determining the specific photoionization cross sections σ_j. These cross sections can be found by measuring the current i_j of photoelectrons of specific kinetic energies. The kinetic energy of the electrons specifies the state in which the molecular ion is left. It can be shown that

$$\sigma_j = (i_j/i) \, \gamma \sigma \tag{3}$$

89

and

$$\sigma_e = \sigma(1 - \gamma), \qquad (4)$$

where $\underline{i}$ is the total electron current, i_j is the current due to electrons ejected from the state j, and γ is the photoionization efficiency defined as the total number of ions formed per photon absorbed by the gas.

Proof:

From the Lambert-Beer law, the number of photons absorbed ΔI_j in a specific process is proportional (a) to the intensity I of the incident radiation at the point of absorption, (b) to the number $\underline{n}$ of absorbing particles, and (c) to the pathlength Δx traversed by the photons. The proportionality constant σ_j is the specific absorption cross section. Thus,

$$\Delta I_j = (In\Delta x)\sigma_j. \qquad (5)$$

The total amount of radiation absorbed by all processes in the pathlength Δx is

$$\Delta I = (In\Delta x)\sigma. \qquad (6)$$

Eliminating $(In\Delta x)$ in Equation (5),

$$\Delta I_j = \Delta I \frac{\sigma_j}{\sigma}. \qquad (7)$$

From the definition of the photoionization efficiency,

$$\gamma_j = \frac{i_j/e}{\Delta I_j} \qquad (8)$$

90

and

$$\gamma = \frac{i/e}{\Delta i} , \qquad (9)$$

but since the state j is a state of the ion, γ_j is unity, therefore,

$$i_j = e\Delta I_j. \qquad (10)$$

Substituting ΔI_j from Equation (7) into Equation (10),

$$i_j = e\Delta I(\sigma_j/\sigma); \qquad (11)$$

and substituting ΔI from Equation (9) in Equation (11)

$$\sigma_j = (i_j/i)\gamma\sigma.$$

Further, summing up the separate i_j in Equation (11),

$$i = \sum_j i_j = \frac{e\Delta I}{\sigma} \sum_j \sigma_j,$$

but $i = \gamma e\Delta I$ from Equation (9)

$$\therefore \sum_j \sigma_j = \gamma\sigma. \qquad (12)$$

From Equation (2), $\sigma = \sigma_e + \sum_j \sigma_j$, therefore, Equation (12) becomes

$$\sigma_e = \sigma(1 - \gamma).$$

Thus, the specific absorption cross sections can be determined from Equations (3) and (4) provided the total absorption cross section and the photoionization yield are known along with the ratio of the number of electrons of specific energy j to the total number of electrons ejected. Values of γ and σ have been measured for most gases at many wavelengths. The present program has been involved with the determination of the ratio (i_j/i).

91

To determine the ratio (i_j/i), a spherical electron energy analyzer has been constructed and tested. The analyzer has been described in previous quarterly reports, however, for convenience, the basic construction is reproduced in Figure 8. Previous tests of the analyzer have proved its effectiveness in determining the gross features of the kinetic energy spectrum. To improve resolution, the analyzer must (a) be operated at extremely low pressure, (b) the ionization must occur in as small a volume as possible, (c) the wavelength bandpass of the monochromator must be as narrow as possible (see Table 10), and (d) the effects of the Earth's magnetic field must be counteracted.

Since the implementation of items (a), (b), and (c) reduces the electron current, it is necessary to devise an efficient system for collecting the photoelectrons. Various electron focusing systems are described below. Item (d) has been implemented by constructing a Helmholtz coil which provides a uniform magnetic field capable of annuling the Earth's field within the volume of the analyzer. Within the limits of the presently available gauss meter, Bell, Inc. No. 240 Incremental Gauss meter, the residual field has been reduced to zero ± 0.005 gauss. A photograph of the monochromator, analyzer, and Helmholtz coil is shown in Figure 9.

For maximum sensitivity, all of the electrons leaving the analyzer must be collected. However, due to the finite area of the electron multiplier cathode (Figure 8), this is not possible. It is essential, therefore, to use some type of electron focusing system. A study of different focusing systems is currently underway, and some preliminary results are shown in Figures 10 to 13.
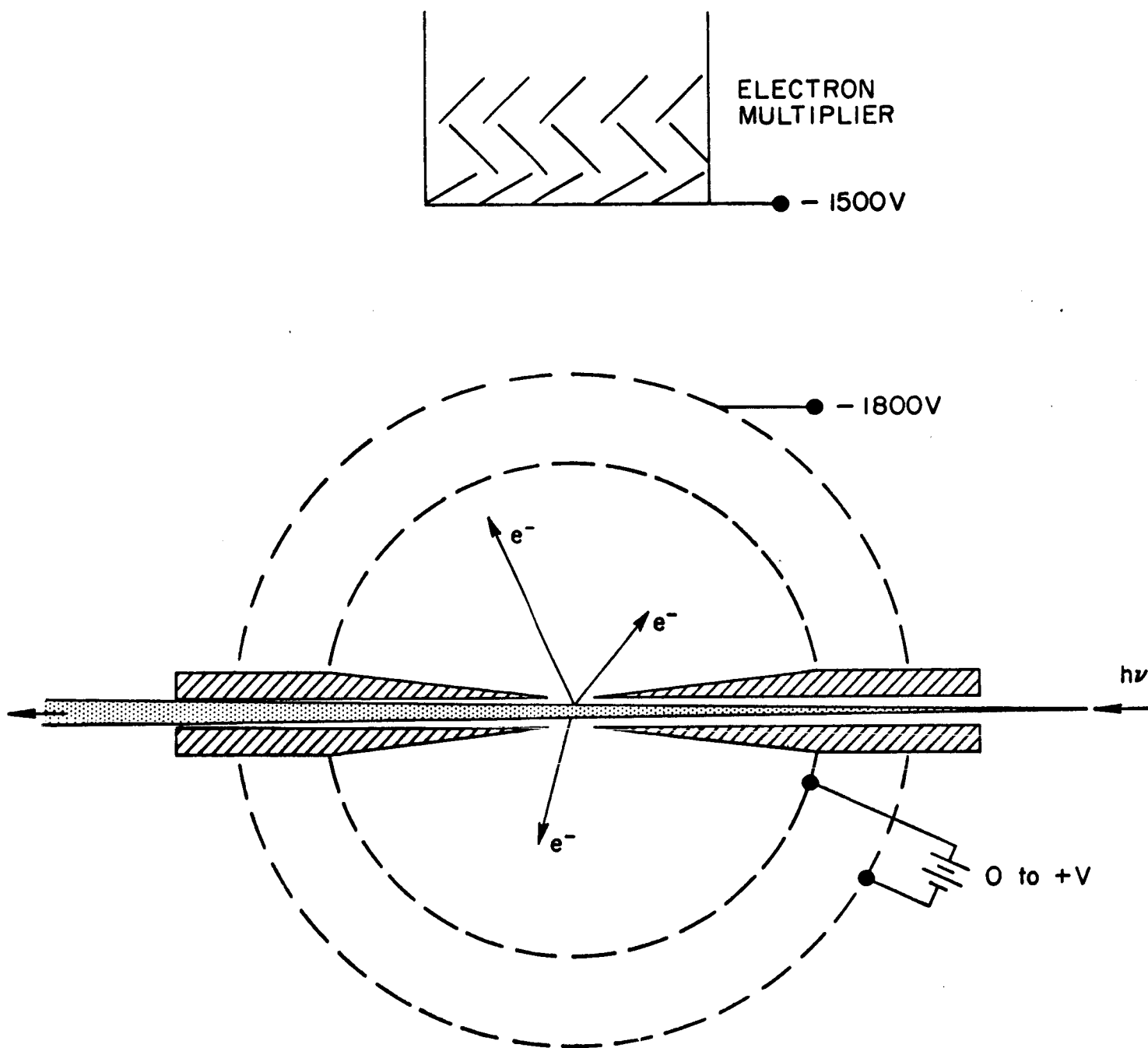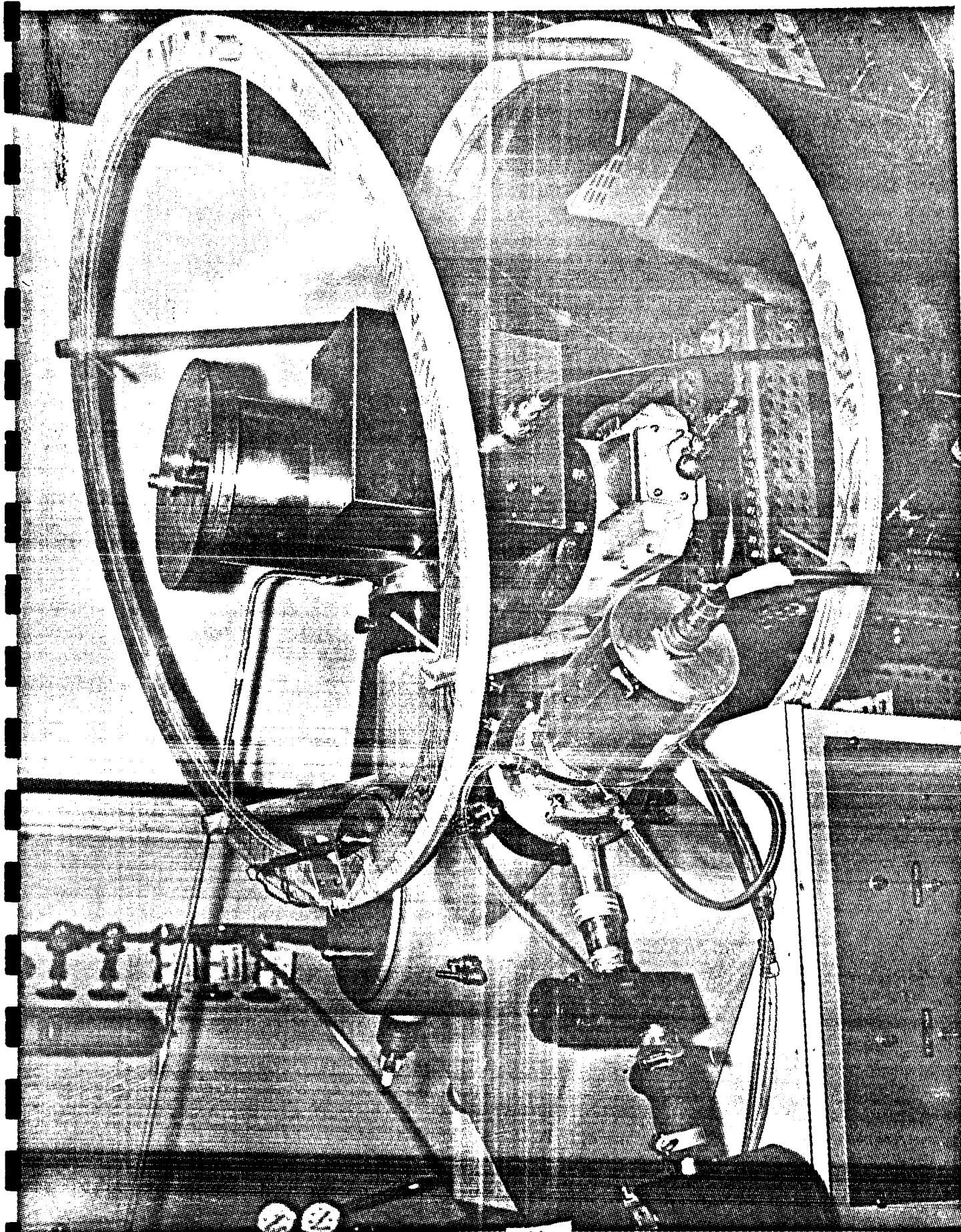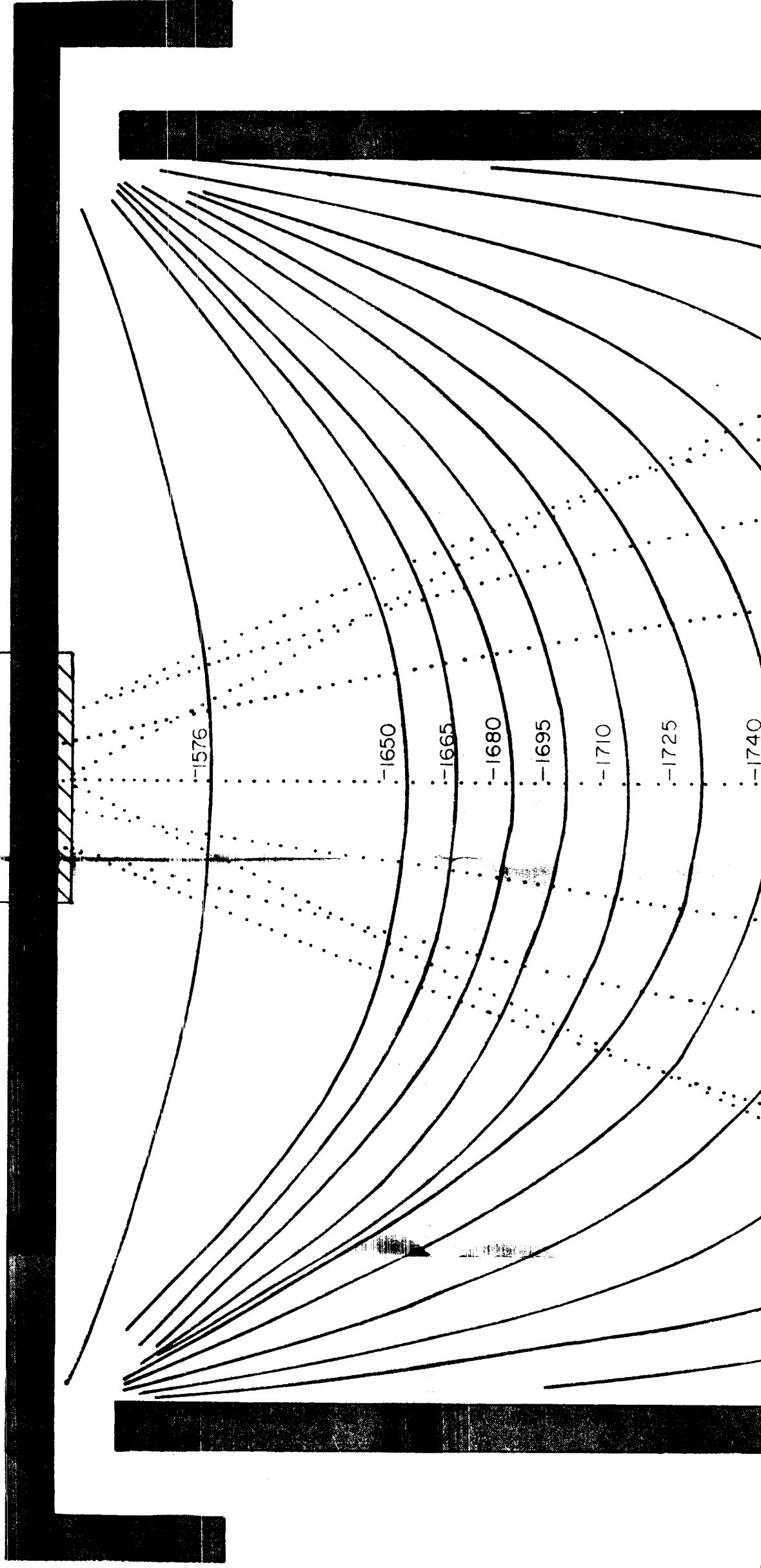
92

Figure 8

Figure 9. View of Seya monochromator, helmholtz coil, and analyzer housing.

94

OICC204—30E

ELECTRON
MULTIPLIER
−1500

−1576

−1650

−1665
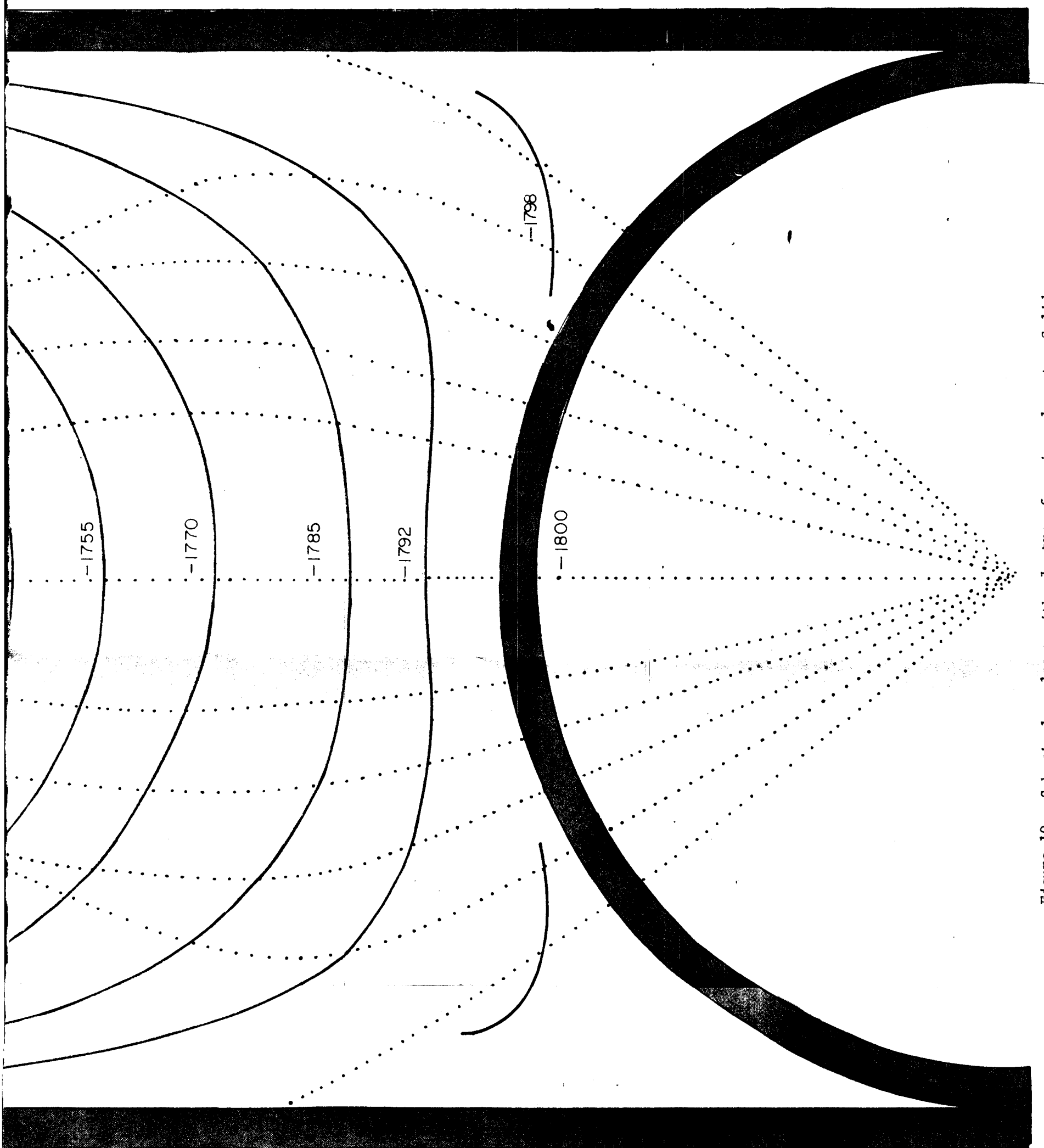
−1680

−1695

−1710

−1725

−1740

Figure 10. Spherical analyzer with electron focusing element. Solid curves represent equi-potential lines, dotted curves represent the actual electron trajectories for electrons with zero initial velocity.

-1798

-1755

-1770

-1785

-1792

-1800

ELECTRON
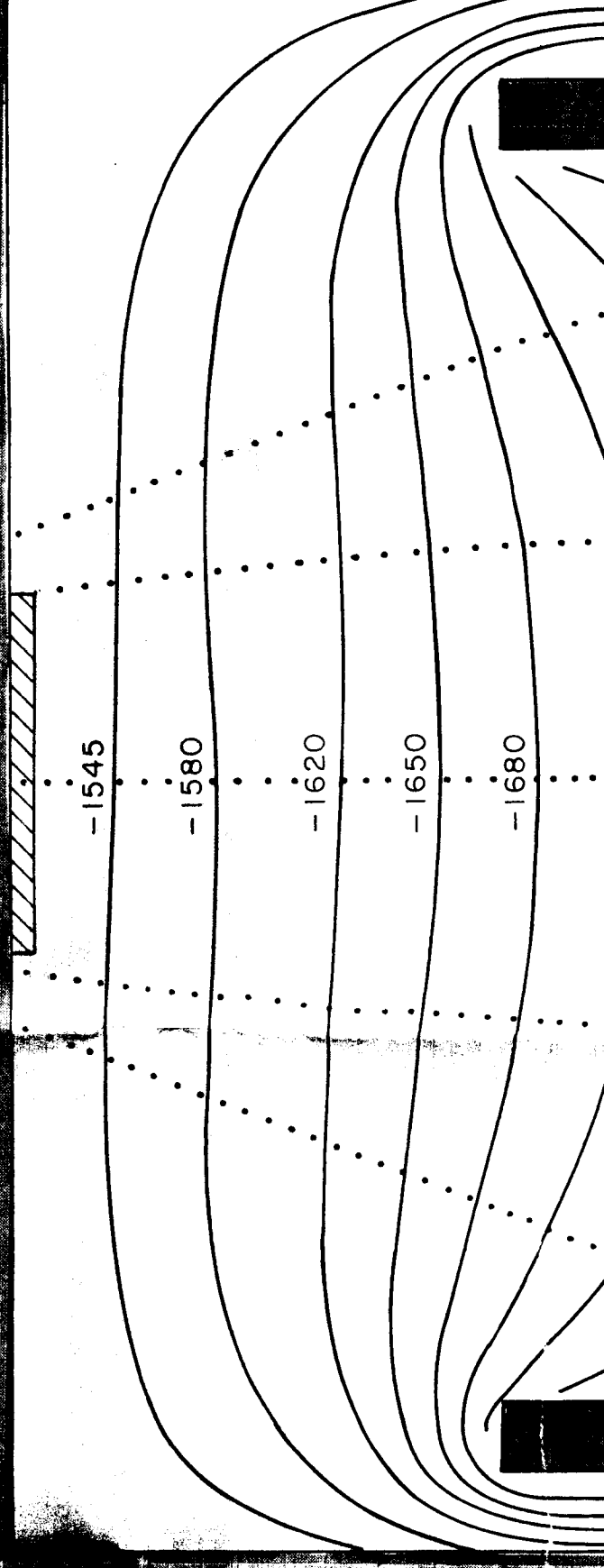MULTIPLIER

−1500

−1545

−1580

−1620

−1650

−1680

Figure 11. Spherical analyzer with electron focusing element. Solid curves represent equi-potential lines, dotted curves represent the actual electron trajectories for electrons with zero initial velocity.

−150

−151
−153
−154
−156
−157
−159
−160
−162
−163
−165
−166
−168
−169
−171
−172
−174
−175
−177
−179

−180

−1792

Figure 12. Spherical analyzer with
represent equi-potential
electron trajectories fo

RON
LIER

O

5
0.
5
0
5
0
5
0
5
0
5
0
5
0
5
0
5
40
55
70
35

0.
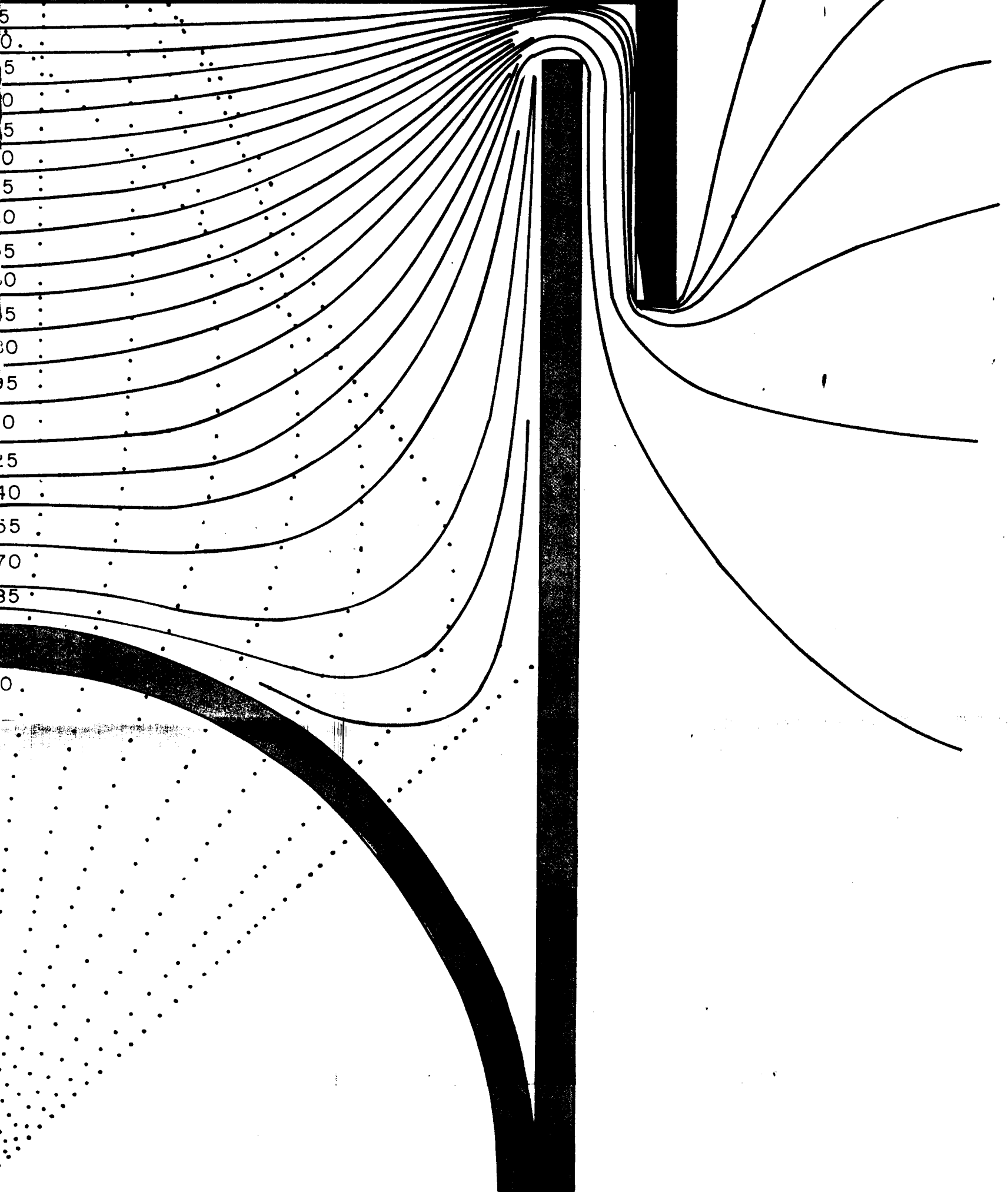
electron focusing element. Solid curves
lines, dotted curves represent the actual
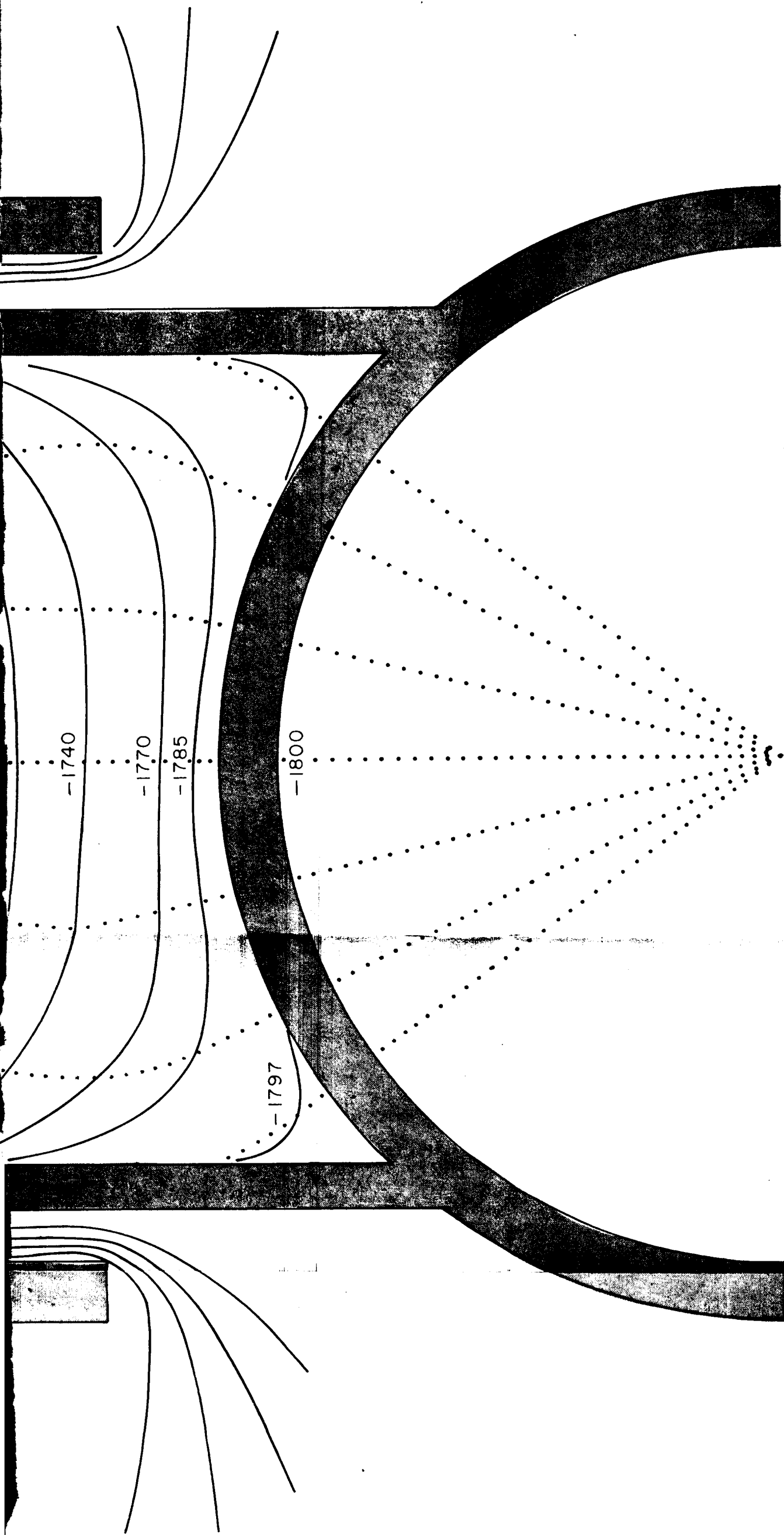r electrons with zero initial velocity.

Figure 13. Spherical analyzer with electron focusing element. Solid curves represent equi-potential lines, dotted curves represent the actual electron trajectories for electrons with zero initial velocity.

ELECTRON
MULTIPLIER

-1500

-1575

-1650

-1725

-1740

OICC204-60D

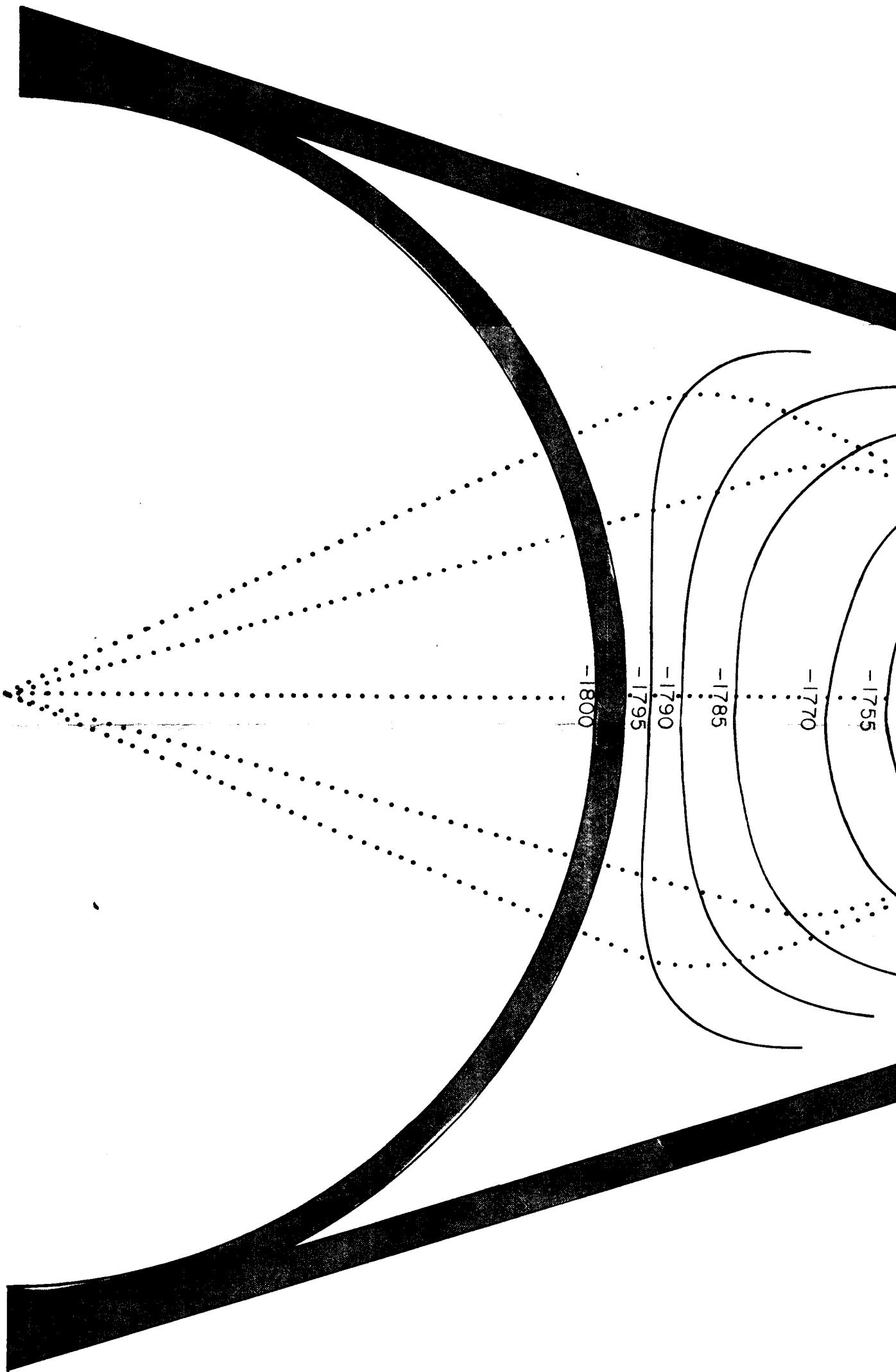Using a system similar to that shown in Figure 8, preliminary measurements have been made at 584 Å in O_2, N_2, CO, and CO_2. Typical results for N_2 and CO_2 are shown in Figures 14 and 15. The improved resolution of the present data can be seen in Figure 14, which shows the vibrational structure of the $A^2\Pi_u$ state of the molecular nitrogen ion. These states are separated by approximately 0.22 eV, thus the present energy resolution of the analyzer is about 3.7 percent for electrons of 6 eV energy.

The values of the photoionization cross section σ_j are listed in Table 11 for O_2, N_2, CO, and CO_2 at 584 Å. Since the photoionization yield for these gases is 100 percent at 584 Å, then $\sigma_e = 0$. The data in Table 11 thus provides, for the first time, a complete quantitative picture of the absorption process at 584 Å.

TABLE 10

Energy Resolution Determined by Monochromator Bandpass
in Units of eV/Å

$\lambda(\text{Å})$	$\Delta E(\text{eV/Å})$	$\Delta E(\text{eV per 5 Å bandpass})$
300	0.137	0.685
350	.101	.505
400	.077	.385
450	.061	.305
500	.050	.250 .
550	.041	.205
600	.034	.170
650	.029	.145
700	.025	.125
750	.022	.110
800	.019	.095
850	.017	.085
900	.015	.075
950	.014	.070
1000	.012	.060
1050	.011	.055
1100	.010	.050
1150	.009	.045
1200	.0086 ·	.043
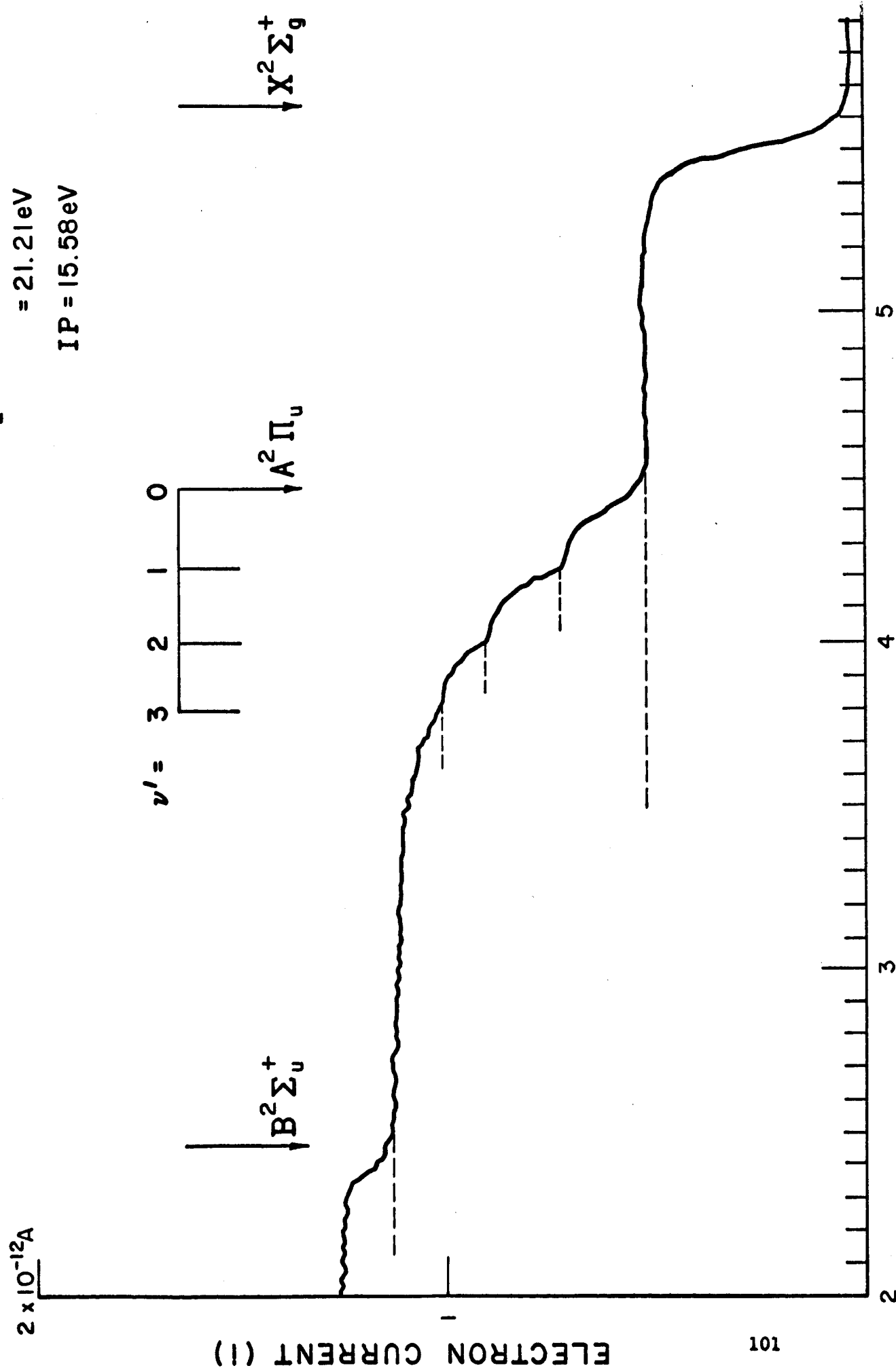
Figure 14. Electron energy groups in N_2 revealing vibrational structure in the $A^2\Pi_u$ state of the ion.

Figure 15. Electron energy groups in CO_2. The electronic state of the ion are clearly visible.

102

TABLE 11

The Specific Photoionization Cross Sections σ_j for Various Gases at 584 Å
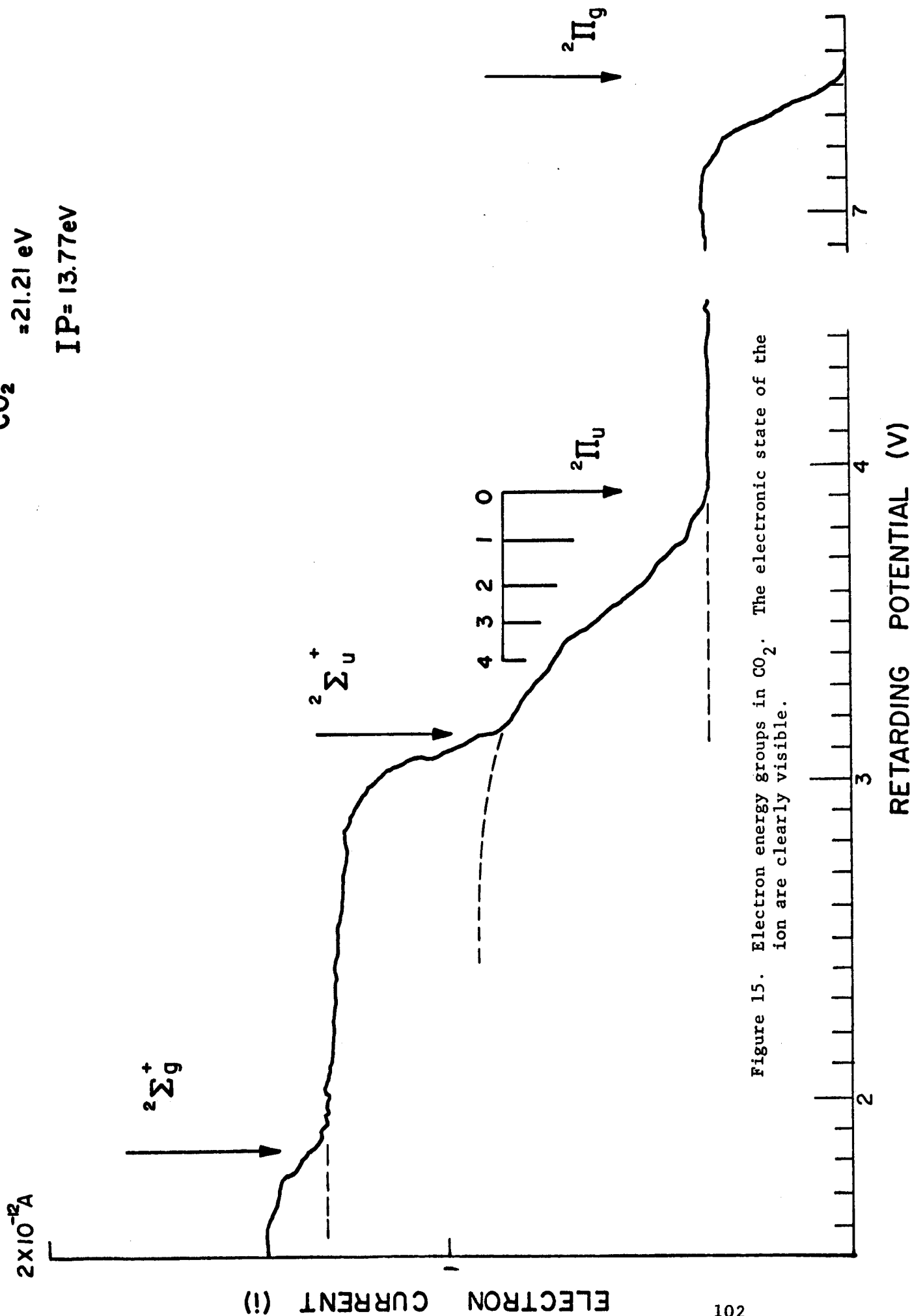
Gas and Transition	(i_j/i)	Total Photoionization Cross Section $\sigma\gamma$ (cm^2)	Specific Photoionization Cross Section $\sigma\gamma$ (cm^2)	Ionization Potential (eV)	(Å)
O_2 $X^3\Sigma_g^- \rightarrow X^2\Pi_g$	0.16	23×10^{-18}	3.7×10^{-18}	12.063	1027.8
$a^4\Pi_u$ $\Big\}$ $A^2\Pi_g$ $\Big\}$	0.30		6.9×10^{-18}	16.107 16.812	769.740 737.474
$b^4\Sigma_g^-$	0.24		5.5×10^{-18}	18.173	682.217
$^2\Sigma_g^-$	0.30		6.9×10^{-18}	20.308	610.493
N_2 $X^1\Sigma_g \rightarrow X^2\Sigma_g^+$	0.39	23×10^{-18}	9.0×10^{-18}	15.580	795.755
$A^2\Pi_u$	0.49		11.2×10^{-18}	16.704	742.225
$B^2\Sigma_u^+$	0.12		2.8×10^{-18}	18.750	661.231
CO $X^1\Sigma^+ \rightarrow X^2\Sigma^+$	0.31	22×10^{-18}	6.8×10^{-18}	14.013	884.73
$A^2\Pi_i$	0.45		9.9×10^{-18}	16.536	749.74
$B^2\Sigma^+$	0.24		5.3×10^{-18}	19.674	630.15
CO_2 $^1\Sigma_g^+ \rightarrow ^2\Pi_g$	0.26	34×10^{-18}	8.8×10^{-18}	13.769	900.414
$^2\Pi_u$	0.40		13.6×10^{-18}	17.312	716.158
$^2\Sigma_u^+$	0.26		8.8×10^{-18}	18.076	685.871
$^2\Sigma_g^+$	0.08		2.7×10^{-18}	19.392	639.345

REFERENCES

1. Y. Suguira, J. Phys. Radium $\underline{8}$, 113 (1927).

2. J. A. Gaunt, Phil. Trans. Roy. Soc. $\underline{A229}$, 163 (1930).

3. D. H. Menzel and L. Pekeris, Mon. Not. Roy. Astron. Soc. $\underline{96}$, 77 (1935).

4. A. Burgess, Mon. Not. Roy. Astron. Soc. $\underline{118}$, 477 (1958).

5. B. H. Armstrong and H. P. Kelly, J. Opt. Soc. Am. $\underline{49}$, 949 (1959).

6. P. O. M. Olsson, Ark. Fys. $\underline{15}$, 131,159,289 (1959).

7. D. R. Bates, Atomic and Molecular Processes (Academic Press, New York, 1963), pp. 79-99.

8. J. D. E. Beynon, Nature $\underline{207}$, 405 (1965).

9. J. D. E. Beynon and R. B. Cairns, Proc. Phys. Soc. $\underline{86}$, 1343 (1965).

D. PLANETARY AERONOMY

During the current Quarter, the planetary aeronomy effort has been concentrated on the role of meteoric debris in the earth's atmosphere, thus completing all items under the program Work Statement. Concerning the current meteoric investigation, a rocket experiment is suggested wherein the atmospheric residency of debris materials can be observed simultaneously using a quadrupole mass spectrometer in conjunction with an optical probe (e.g., a Fastie-Ebert spectrometer or a number of selected photometers). A detailed account of the work accomplished thus far is reported here since the study is incomplete and therefore not amenable to publication in the open literature.

1. The Role of Meteoric Debris in the Earth Atmosphere:
   Simultaneous Observation of Meteoric Debris by Employing a
   Rocket-Borne Mass Spectrometric and Optical Probe

Recently, identification and measurement of a considerable number of ambient ion species has been performed by both Narcisi and Bailey[1] and Istomin[2] using mass spectrometric techniques. Certain measurement ambiguities exist due to absolute instrumental calibration and the difficulty of precise mass identification of certain constituents. The results of the present investigation indicate that several meteoric debris species including the aforementioned and others may be observed with extremely high sensitivity by solar resonance scattering. Thus, the use of an appropriate optical instrument, such as a Fastie-Ebert spectrometer or a properly designed photometer, in addition to a quadrupole mass spectrometer would result in the simultaneous measurement of

105

a number of species by the two techniques. Additionally, measurements could be obtained on a number of neutral species not presently observable by mass spectrometric techniques. The incorporation of the optical capability additionally serves to reduce the above-cited experimental ambiguities by acting as an absolute calibration source for the mass spectrometer and by providing specific spectral species mass identification criteria for the observed atoms or ions. Thus, the additional and confirmatory optical measurements will provide more satisfactory data upon which to evaluate the role of interplanetary debris in the earth's atmosphere, especially where the ionic and neutral states of an individual species can be measured simultaneously.

In the present analysis, expected signal intensities from solar-illuminated debris species are calculated on the basis of the reported number density distributions obtained from rocket-borne mass spectrometric[1,2] and ground-based twilight measurements.[3,4] These signal intensities are then compared to the Rayleigh scattered background level to demonstrate the feasibility of the suggested experiment. Finally, assuming equivalent column count residency of selected neutral constituents (to their observed ionic counterparts), the high probability of performing the indicated resonance scattering observations is demonstrated.

a. Signal Characteristics

In the earth's atmosphere, trace materials of possible meteoric origin have been detected and measured by two methods of interest here. These involve ion density measurements employing a quadrupole mass

106

spectrometer wherein Narcisi and Bailey[1] have reported observations of Mg^+, Na^+ and Ca^+, while Istomin[2] has reported Mg^+, Ca^+, Si^+ and Fe^+. The density profiles and integrated vertical column counts are presented in Figures 16 and 17, respectively. As a partial confirmation of the above results, Vallance Jones[3] has reported a column count of Ca^+ of about 4.5×10^8 cm^{-2} by twilight resonance scatter observations from a ground-based photometric site. Additionally, neutral Na, K and Li twilight photometric measurements have been summarized by Vallance Jones.[4] These density distributions and corresponding integrated column counts are also reproduced in Figures 16 and 17. To obtain estimates of the overhead signal intensities I_S, as a function of altitude, due to the solar resonance scatter from these observed values it is necessary to obtain the product of the appropriate solar resonance efficiency per atom or ion, $P(\frac{photon}{sec\ atom})$ and the total column counts, N_T, i.e., $I_S = PN_T$.

The solar resonance efficiency per atom P is defined by

$$P = \phi_\lambda \alpha \qquad (1)$$

where ϕ_λ is the incident solar flux and α is given by

$$\alpha = \frac{\pi e^2}{mc} \frac{gf}{g_1} \lambda_o^2 \qquad (2)$$

where   e = the unit charge

   m = electron mass

   gf = the oscillator strength of the particular transition (for the present purpose, the statistical weight of the upper state is incorporated in this value)

   g_1 = the statistical weight of the ground level

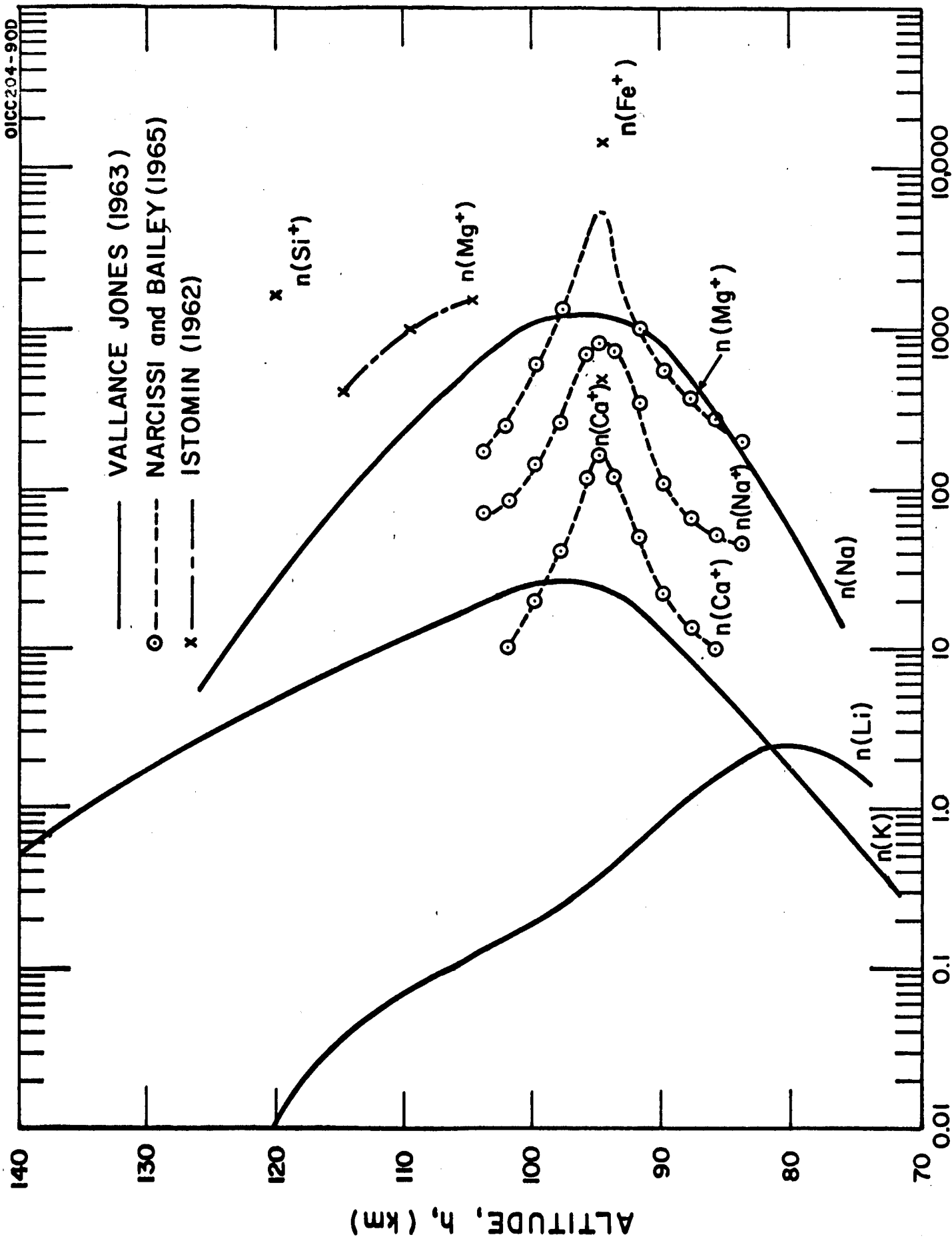 λ_o = the wavelength of the resonance line.

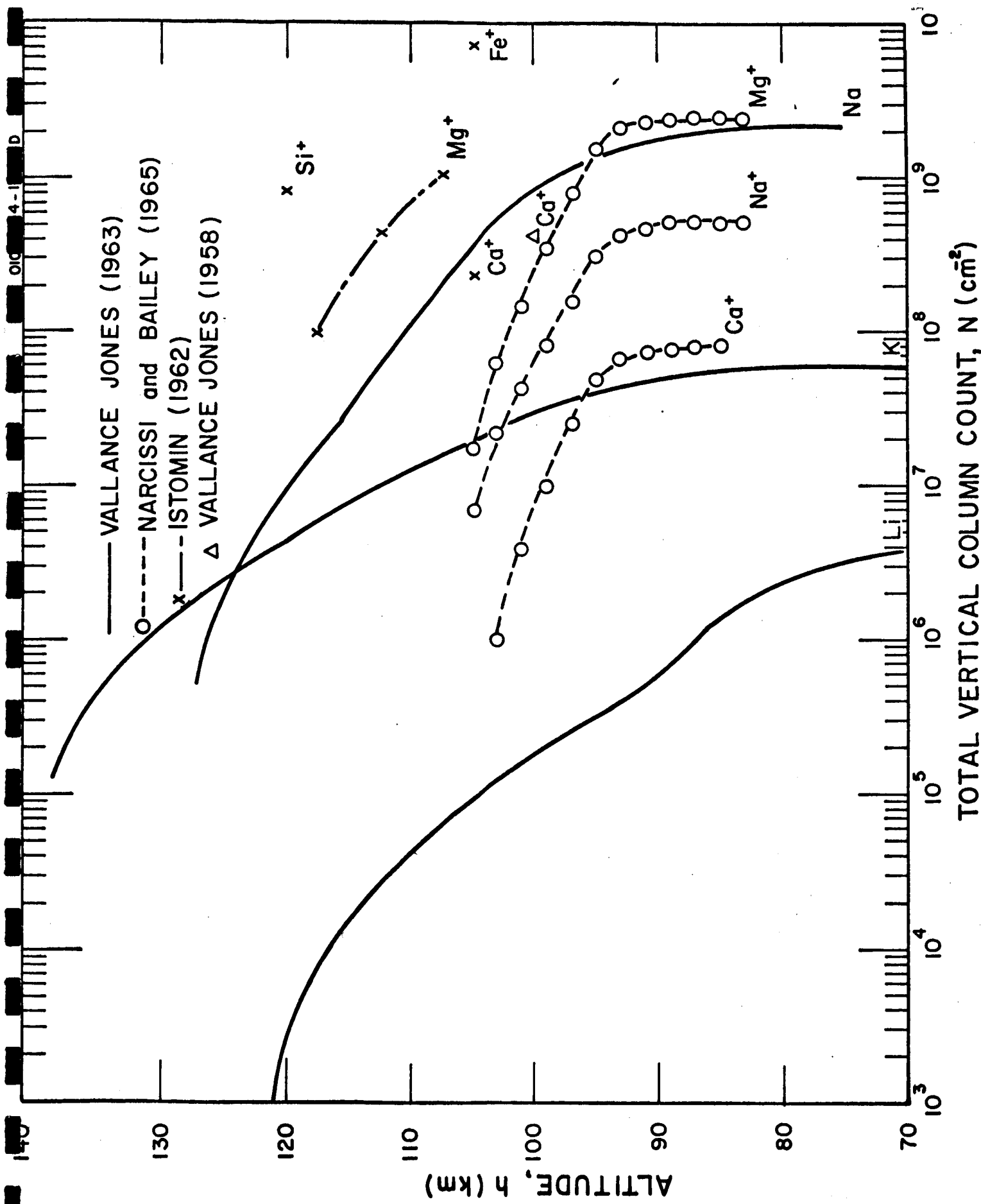Figure 16. Observed number densities of debris species as a function of altitude.

Figure 17. Vertical column counts of debris species as a function of altitude.

The P-values for all of the observed neutral and ionic species and their neutral and/or ionic species counterparts have been previously calculated by Marmo and Engelman.[5] In Equation (1), no account has been taken for the increased illumination of the species due to earth and atmospheric albedo radiation.[6]

The resultant overhead signal strengths, I_S are presented in Figure 18 for all of the observed species having available resonance lines. The summarized data indicate that the expected signal strength values are essentially constant to about 95 km and decrease as expected, at higher altitudes.

b. Rayleigh Scattered Background Intensities

In the signal rocket experiment discussed above, it is evident that the indicated measurements must be performed against the ambient Rayleigh scattered background, defined by

$$I_B (\lambda,\psi) = P(\psi) \, \phi_\lambda \, \sigma_\lambda \, n_o \, H \qquad (3)$$

where: $P(\psi)$ = Rayleigh scattering phase function = $\frac{3}{4} (1 + \cos^2 \psi)$

ϕ_λ = solar photon flux (photons cm^{-2} sec^{-1} $\overset{o}{A}^{-1}$)

σ_λ = Rayleigh scattering cross section (cm^{-2})

n_o = column count of ambient atmospheric constituents.

The evaluation of background profile with altitude assists in the selection of an optimum probe level. In order to consider a representative case, in Equation (3), a geometrical configuration has been assumed involving a solar zenith angle of 45° and a 0° instrumental zenith angle.
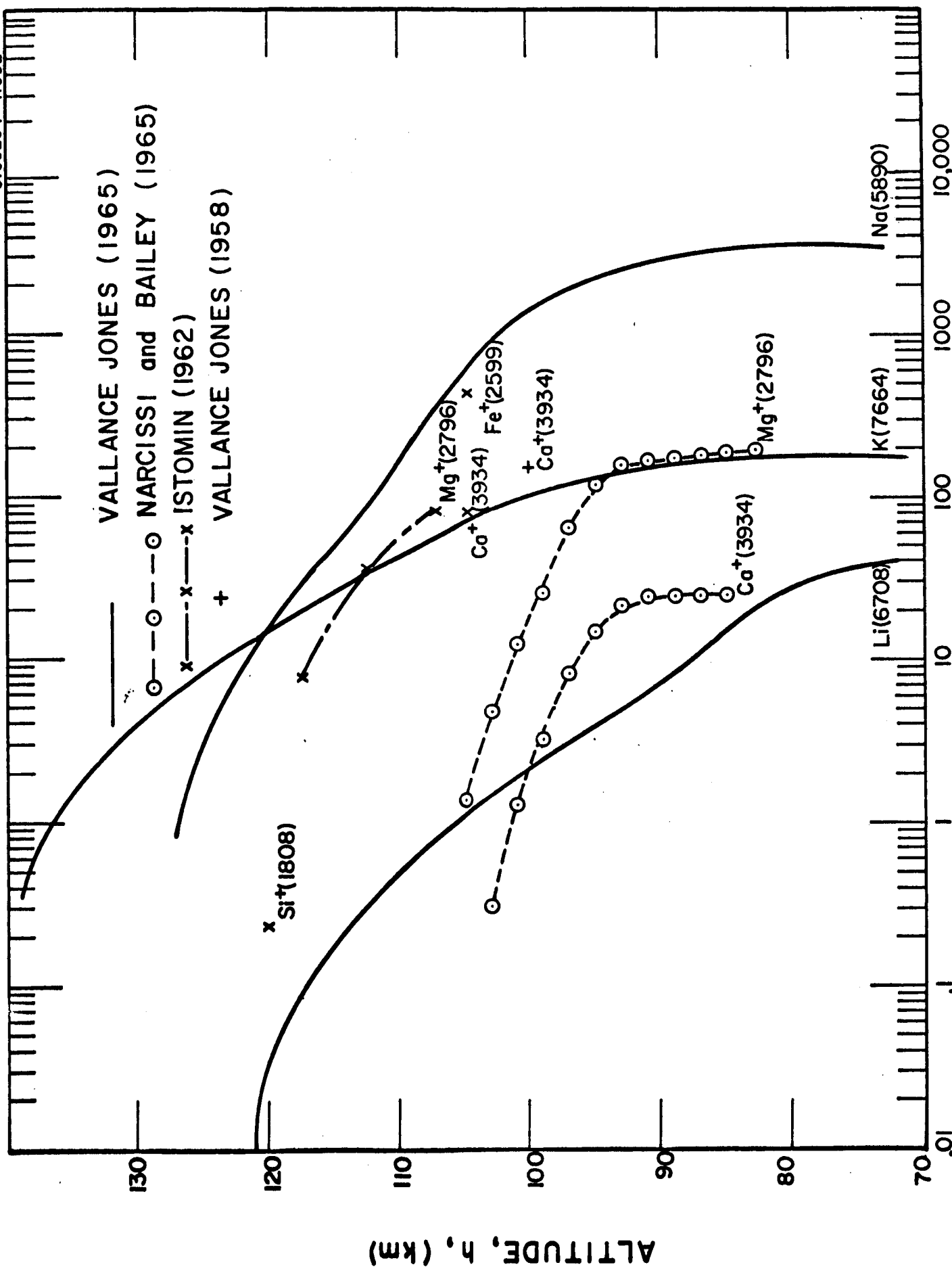
Figure 18. Expected resonance scattering signal levels as a function of altitude.

111

This results in a scattering phase function value, $P(\psi) = 1.125$. Here again, no account has been taken of the contribution due to the additional illumination from earth and atmospheric albedo.[6] The atmospheric column counts were obtained from the 1962 Standard Atmosphere.[7] The results of these calculations are shown in Figure 19 for altitudes of 80, 85, 90, 95, and 100 km. The intensity values are presented in units of Rayleighs/Å (10^6 photons/cm^2 secÅ), so that these backgrounds would be directly applicable to an instrument with a 1Å resolution capability, viewing vertically at the indicated altitudes and a solar zenith angle of 45°.

c. Suggested Experiment

A summary of the previously discussed signal and background results is contained in Table 12 appropriate to an upward viewing instrument and a 45° solar zenith angle. The tabulated signal levels for Ca$^+$ and Mg$^+$ are average values from Figure 18, while the background levels appropriate to rocket viewing altitudes of 80 and 95 km have also been selected. In most instances, it can be seen that the magnitudes of the expected signals (compared to the background levels) indicate that favorable experimental results could be anticipated. Furthermore, the spectral locations and P-values for Ca, Si, Mg, and Fe are also included in the table for reference purposes. Since the P-values for the neutrals are either essentially equivalent to or greater than those of their ionic counterparts, at least equivalent favorable experimental performance can be predicted for these hitherto undetected ambient neutrals if they exist in essentially equivalent amounts.
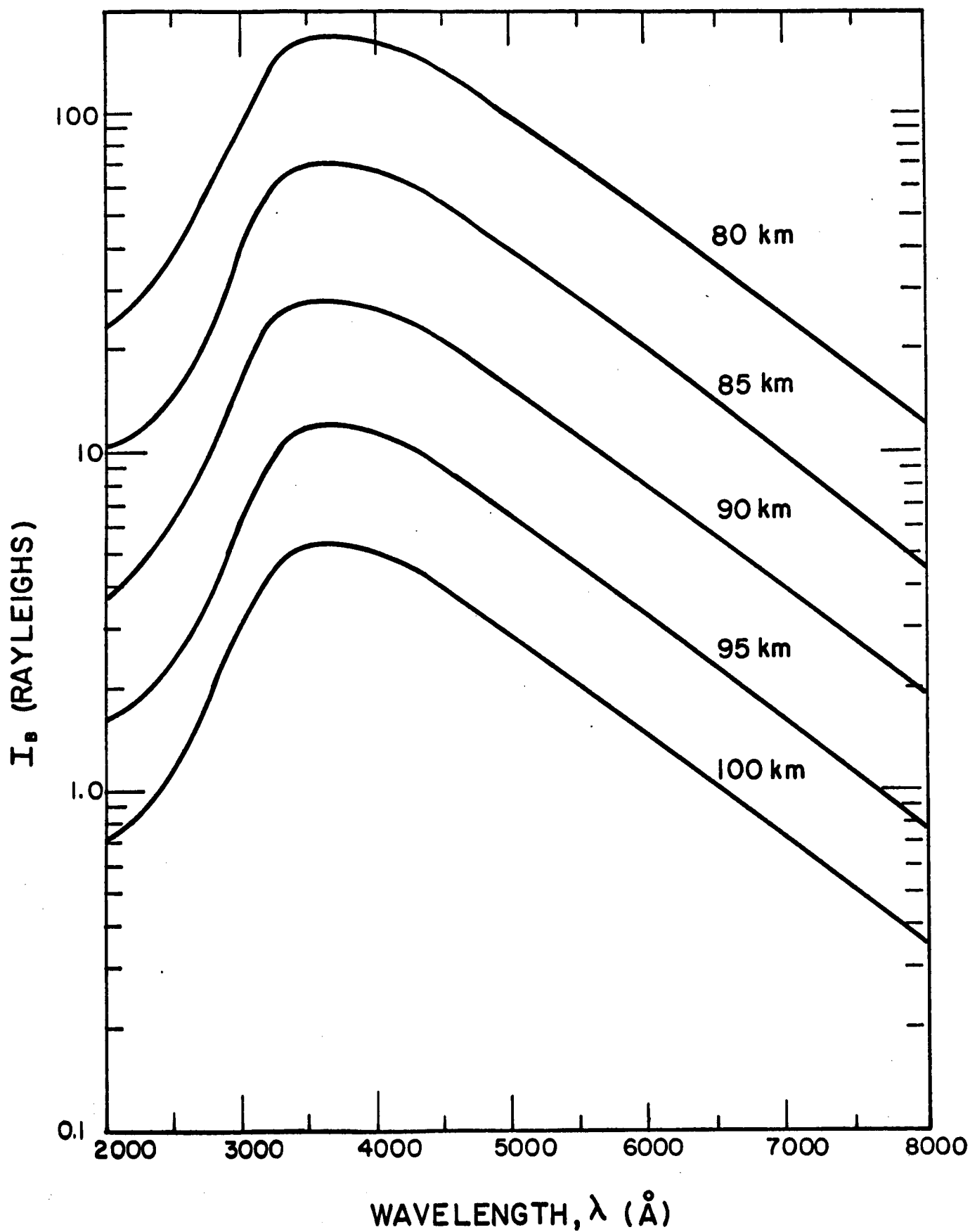
112

Figure 19. Rayleigh scattered background, I_B, for 45° zenith angle solar illumination and a 0^{ρ} zenith look angle.

113

TABLE 12

EXPECTED RESONANCE SCATTERED SIGNAL INTENSITIES AND BACKGROUND LEVELS

Element	λ, Å	$P(\frac{photon}{sec\ atom})$	N_T(observed) (cm^{-2})	T_S(R)	I_B(R/Å)	
					k=80km	k=95km
LiI	6706(d)	1.6×10^1	4×10^6	64	30	2
KI	7665	1.4×10^0	6×10^7	84	20	1
NaI	5890	1.6×10^0	2×10^9	3200	50	4
CaII	3934	3.2×10^{-1}	2.6×10^8	83	140	10
CaI	4227	2.5×10^{-1}	—	—	140	9
SiII	1808	2.7×10^{-4}	8×10^8	0.2	—	—
SiI	2514	1.4×10^{-2}	—	—	30	2
MgII	2796	7.9×10^{-2}	1.8×10^9	140	80	5
MgI	2852	2.6×10^{-1}	—	—	90	6
FeII	2599	6.5×10^{-2}	7×10^9	455	50	3
FeI	3441	1.9×10^{-2}	—	—	170	11

It has thus been shown that the simultaneous measurement of possible meteoric debris species by mass spectrometric and optical resonance scattering techniques will both reduce existing constituent abundance uncertainties and eleminate mass determination ambiguities. Furthermore, if the selected rocket-borne optical instrumentation has a broad spectral operational capability, positive identification and measurement of additional constituents appears possible including the neutral counterparts of previously observed ionic species.

A more detailed future investigation will involve evaluations of the experimental performances of both rocket and satellite borne instrumentations, a variety of solar positions and instrumental look angles including tangentially to the horizon to increase signal intensity, incorporation of earth and atmospheric albedo effects, etc.

REFERENCES

1. Narcisi, R. S. and Bailey, A. D., "Mass Spectrometric Measurement of Positive Ions at Altitudes from 64 to 112 Kilometers," J. Geophys. Res. 17, 3687-3700 (1965).

2. Istomin, V. G., "Ions of Extraterrestrial Origin in the Earth Ionosphere," Space Research III, 209-220 (1963).

3. Vallance Jones, A., Ann. Geophys. 14, 179 (1958).

4. Vallance Jones, A., "Metallic Emissions in the T3ilight and Their Bearing on Atmospheric Dynamics," Planetary Space Sci. 10, 117-127 (1963).

5. Marmo, F. F. and Engelman, A., "The Measurement of Resonance Scattering from Solar-Illuminated Lunar Atmospheric Constituents," Annals of the New York Academy of Sciences (to be published); Presented at Planetology and Space Mission Planning Conference, New York City, N. Y., November 3-4, 1965.

6. McElroy, M. B. and Hunten, D. M., "A Method for Estimating the Earth Albedo for Dayglow Measurements," J. Geophys. Res. 71, 3635-3638 (1966).

7. U. S. Standard Atmosphere, 1962, U. S. Governement Printing Office, Washington, D. C.

III. OTHER PERTINENT INFORMATION

During this Quarter, the following four scientific papers were presented at professional meetings:

(1) Atmospheric Ion-Molecule Reactions by a Photoionization Mass Spectrometric Technique (P. Warneck and F.F. Marmo)

(2) Collision Processes in Planetary Atmospheres (A. Dalgarno)

(3) Atom-Atom Collision Processes in Astrophysics (A. Dalgarno)

(4) Reactions of ^{1}D Oxygen Atoms I (P. Warneck)

For other details see Introduction

Labor Category	Labor Grade	Total Hours
Junior Key Punch Operator	1	8.00
*Junior Technician	2	549.00
*Technician Experimental Machinist	3	74.00
*Senior Technician Senior Experimental Machinist	4	72.50
*Junior Scientist Junior Engineer	5	68.00
*Scientist Engineer	6	21.50
Senior Scientist Senior Engineer	7	156.00
Staff Scientist	8	76.00
Principal Scientist	9	68.00
Group Scientist	10	97.00
ODC (Overhead Direct Charges)		37.50

*and other equivalent categories